

Geo-information Science and Remote Sensing

Thesis Report GIRS-2025-63

SENSING THE FOREST THROUGH THE TREES
A data driven approach to Dutch forest reserve monitoring using AHN

Nik Verweel, BSc.

October 10, 2025



Sensing the forest through the trees
A data driven approach to Dutch forest reserve monitoring using AHN

Nik Verweel, BSc.

Registration number 1012884

Supervisors:

L.C. Vreugdenhil, MSc.
N.E. Kelly, MSc.

A thesis submitted in partial fulfilment of the degree of Master of Science
at Wageningen University and Research,
The Netherlands.

October 10, 2025
Wageningen, The Netherlands

Thesis code number: GRS-80436
Thesis Report: GIRS-2025-63
Wageningen University and Research Centre
Laboratory of Geo-Information Science and Remote Sensing

Abstract

The Dutch forest reserve network was established in 1997 to serve as a source of knowledge on the natural development of Dutch forests, initially conceived as input for exploring new silvicultural systems. Forests assigned to the network would remain free from human intervention, unless strictly necessary, and would function as data-collection sites for 14 forest structure parameters providing insight into forest health and development. Since 1997, 59 forest reserves have been assigned, totalling about 2600 hectares across 11 of the 12 Dutch provinces. After the originally outlined 10-year monitoring cycle collapsed in 2005 due to budget constraints, limited data were collected until monitoring efforts restarted in 2018, when Wageningen Environmental Research resumed fieldwork. This thesis aimed to explore the suitability of remote sensing in the current data collection workflow to potentially enrich data acquisition and aid in the forest reserve program. In particular, the *Actueel Hoogtebestand Nederland* (AHN) was identified as a promising, unique LiDAR dataset, consisting of repeat nationwide aerial LiDAR surveys, with open access and future acquisitions planned. A brief literature review using a single iteration of reference snowballing from three selected review papers identified methodologies of interest for describing or estimating several forest reserve characteristics. Three articles were selected, covering methodologies related to four characteristics, which were first qualitatively assessed through visual inspection of 3D point clouds. Following this, the method for detecting standing dead trees using an intensity-based approach was deemed unfeasible due to high error rates, likely caused by fundamentally different intensity distributions between the AHN and the data used in the original study, stemming from sensor and environmental differences. Methods for individual tree detection, associated height estimation, and tree crown projection were deemed feasible and examined further. Individual tree detection and height estimation yielded poor results when compared against field observations (6.8% detection accuracy), likely due to the inability to detect sub-dominant trees caused by converting the LiDAR point cloud into a two-dimensional Canopy Height Model, though the detection of treetops was observed to yield acceptable results. Despite this limitation, the method may still be valuable for estimating tree top height. Tree crown projection estimation could not be validated against field data, but qualitative analysis combined with strong literature support for the point-cloud based method suggests it can contribute meaningfully to forest reserve monitoring, particularly for canopy gap identification and analysing light-related interactions within the canopy. It may also serve as a replacement for the current crown projection measurements, though this requires confirmation through quantitative assessment once additional field data become available.

Acknowledgements

This thesis would have not reached its current state without the excellent supervision of my supervisors Corné Vreugdenhil and Niamh Kelly. I want to thank Corné for the regular update meetings, the interesting conversations that always distracted us from those meetings, the feedback and the support during the more difficult times. I want to thank Niamh for her valuable insights and ideas, the conversations we've had about the forest reserves, and for always being available to answer any questions I had about forests.

I'd further like to thank Erik Roest and Silke Jacobs for wanting to share their knowledge regarding the forest reserves, always being approachable, helping me acquire data and even letting me tag along during some field work. Lots of valuable insights were generated during the field work in particular, as it allowed me to really put my research into perspective in the real world and remember that I can't do everything from behind my desk!

In addition, I want to say thank you to my mother and Art for the unconditional support during my thesis, the interest, and for offering a home-base I could unwind and stuff myself with (brain)-food.

Thank you to my study advisors Elise and Annemarie for guidance during the thesis progress and urging me to slow down and speed up when necessary.

Thank you to my fellow MGI students in the thesis room, who were always (maybe too often) available for coffees, talks, input, and feedback, with a special thanks to Lotte for all the discussions and conversations in Lumen.

Finally, thank you to my partner Susanna, who kept me motivated throughout the writing, encouraged me to push myself to the best of my abilities, and supported me during the difficult and stressful moments.

For all those who supported me over the years but are no longer with us to accompany me during the last chapter of my studies, I've thought about you a lot during my thesis and I will think about you a lot during my graduation - this work is dedicated to you.

Generative AI Statement

Generative AI was used for limited purposes in this thesis research. ChatGPT was used to check the grammar and flow of writing for paragraphs and sections of text. At no point was the entire thesis uploaded for grammar feedback. At no point was any factual information requested or accepted as truth. ChatGPT was also used as an aid in scripting, particularly with the 'R Wizard' GPT. Additionally, ChatGPT assisted with formatting this LaTeX document. GitHub Copilot was occasionally used for in-line code completion during scripting in the VB Code Integrated Development Environment, the chat or agent functions were not utilised. All prompts to ChatGPT can be found via the following links:

Grammar and miscellaneous prompts - <https://chatgpt.com/share/67d018c8-f48c-8005-9788-f81e6e94455f>
Scripting prompts - <https://chatgpt.com/share/67a09b39-3e9c-8005-ab51-affa8fa0c891>

Table of Contents

1	Introduction	1
1.1	Background	1
1.2	The Dutch forest reserve network	1
1.3	Recent developments	3
1.4	About LiDAR and the potential of AHN	4
1.5	Research objectives	5
2	Data and Methods	6
2.1	Study Area	6
2.1.1	The Dutch forest reserve network	6
2.1.2	Representative reserves	8
2.2	Data	8
2.2.1	Forest reserve data	8
2.2.2	Actueel Hoogtebestand Nederland	9
2.3	Methodology	10
2.3.1	Overview	10
2.3.2	Data collection and preprocessing	10
2.3.3	Literature review	11
2.3.4	Feasibility assessment of found methodologies	12
2.3.5	Analysis of feasible methodology	13
2.3.6	Analysis of unfeasible methodologies	14
2.4	Materials	15
3	Results	16
3.1	Literature review	16
3.2	Feasibility assessment of found methodologies	17
3.2.1	Overview of selected methodologies	17
3.2.2	Individual Tree Detection and height estimation through Canopy Height Model-based Local Maximum Filter	18
3.2.3	Tree crown projection estimation through Multicore Watershed Segmentation and 3D Point Cloud segmentation	20
3.2.4	Standing dead tree (snag) detection through neighbourhood attribute filtering	22
3.3	Analysis of feasible method	22
3.4	Analysis of unfeasible methodologies	25
3.4.1	Tree crown projection estimation	25
3.4.2	Standing dead tree (snag) detection	26
4	Discussion	29
4.1	From literature to methodologies	29
4.2	AHN for Individual Tree Detection	29
4.3	AHN for tree crown segmentation	31
4.4	AHN for snag detection	32
4.5	Final discussion points	32
4.6	On future research	34
5	Conclusion	35
6	Recommendations	37
References		38
Appendices		45
Appendix I		46

Appendix II	47
Appendix III	48
Appendix IV	51
Appendix V	54

List of Figures

Figure 1	Example overview of different monitoring levels for the forest reserve <i>Galgenberg</i> (RSV 3).	2
Figure 2	Flowchart visualising dominant tree and forest type identification.	6
Figure 3	Locations of forest reserves around the Netherlands with their reserve code and forest type.	7
Figure 4	Overview of representative reserves.	8
Figure 5	Flowchart overview of applied process.	10
Figure 6	Comparison between canopy- and stem-down views after ITD for a selection of representative sample plots.	19
Figure 7	Comparison between the MCWS and Li 2012 methods for tree crown projection estimation in a selection of representative sample plots.	21
Figure 8	Distribution of the number of trees identified in field and through ITD.	22
Figure 9	Comparison and distribution of the minimal distance between trees identified in the field and through ITD.	23
Figure 10	Distribution of average tree heights in plots across forest types.	24
Figure 11	Comparison of default and adapted Li 2012 algorithm for artefact reduction	26
Figure 12	Comparison of distributions of intensity index between representative sample sites and the article presented by Wing et al. (2015)	27
Figure 13	Distribution of intensity index in ground-class filtered sample plot S09 in forest reserve <i>Galgenberg</i> (RSV 3)	28

List of Tables

Table 1	Overview of forest reserve characteristics monitored at the three unique monitoring scales. dbh = diameter at breast height. h = height.	3
Table 2	Overview of AHN LAZ data available for the Netherlands and their years of acquisition and quality (Actueel Hoogtebestand Nederland, 2023).	9
Table 3	Derived linear equations for Variable Window Size approach to Individual Tree Detection in SRO3.	13
Table 4	Combinations of parameters in the Li 2012 algorithm tested for visual confirmation.	14
Table 5	Overview of literature review results after snowballing procedure	17
Table 6	Confusion matrix constructed based on visual assessment of individual tree detection	18
Table 7	Confusion matrix constructed based on visual assessment of tree crown projection	20
Table 8	Results of visual comparison of different parameter combinations in the Li 2012 algorithm against the default parameters.	25

List of Acronyms

<i>AHN</i>	Actueel Hoogtebestand Nederland
<i>ALS</i>	Aerial Laser Scanning
<i>BBPR</i>	Branch and Bole Point Ratio
<i>BBvFr</i>	Branch and Bole versus Foliage ratio
<i>CHM</i>	Canopy Height Model
<i>CRS</i>	Coordinate Reference System
<i>DBH</i>	Diameter at Breast Height
<i>DSM</i>	Digital Surface Model
<i>DTM</i>	Digital Terrain model
<i>EU</i>	European Union
<i>FWS</i>	Fixed Window Size
<i>ITD</i>	Individual Tree Detection
<i>LiDAR</i>	Light Detection and Ranging
<i>LMF</i>	Local Maximum Filter
<i>MCWS</i>	Multicore Watershed Segmentation
<i>MLS</i>	Mobile Laser Scanning
<i>NRMSE</i>	Normalised Root Mean Square Error
<i>PGR</i>	Physical Geographic Region
<i>PNV</i>	Potential Natural Vegetation
<i>RMSE</i>	Root Mean Square Error
<i>RS</i>	Remote Sensing / Remotely Sensed
<i>RSV</i>	Forest Reserve Code
<i>SLS</i>	Space-borne Laser Scanning
<i>SRO</i>	Specific Research Objective
<i>TLS</i>	Terrestrial Laser Scanning
<i>UAV</i>	Unmanned Aerial Vehicle
<i>VWS</i>	Variable Window Size
<i>WENR</i>	Wageningen Environmental Research
<i>3DPCS</i>	3D Point Cloud Segmentation

1 Introduction

1.1 Background

Human lives are undeniably highly intertwined with forests. Covering 30.8 percent of the terrestrial planet surface, forests contribute to a wide range of ecosystem, economic and social services (FAO, 2020). From carbon sequestration, an important service in the complex dynamics of climate change (Vizzarri et al., 2021), to sources of recreation, linked with mental health (Clark et al., 2023), forests play a vital role in human lives. Whilst there are still swathes of untouched forests in the Americas, Africa and Asia, this is no longer the case within the European Union (EU), as under three percent of the forests within the EU are classified as primary or old-growth (Potapov et al., 2017). This means that virtually all forests within the EU have seen (extensive) anthropogenic influences (Barredo et al., 2021). Within the Netherlands, there are no primary forests left and only some 11 percent of Dutch forest cover is older than 100 years (FAO and Oldenburger, 2020; Schelhaas et al., 2022), as all forests in the Netherlands stem from human cultivation or have seen anthropogenic influences.

Paired with the planting of forests, the Netherlands has a long history of forest management practices. Some 49 percent of Dutch forest is owned by the Dutch government in one form or another, with *Staatsbosbeheer* (the Dutch National Forest Service) managing 25 percent (Schelhaas et al., 2022). Historically, the prevailing silvicultural system - that is, the applied process of tending, harvesting and regeneration of a forest - was that of clear-cutting, replanting and coppice. Recently, forest management approaches in the Netherlands are generally classified as a "limited intervention" approach, with some areas aimed at "interventions mimicking natural processes" (Hengeveld et al., 2012), though it should be noted that the management decisions and planning vary greatly between, and within, the public and private sectors (De Bruin et al., 2015; Hoogstra-Klein and Burger, 2013).

During the 1990s, as the Dutch political and economical landscape changed to focus more on conservation and recreation, emphasis was placed on the role of forests in the protection of nature. This paradigm shift in forest management was spurred on due to windthrow events in 1972 and 1973 leading to widespread damage to existing forest stands (Mohren and Vodde, 2006). The natural regeneration in the damaged forest areas showed the potential of a silvicultural system based on natural regeneration processes, whereas this was previously believed to lack potential. Despite this show of potential, there was limited knowledge about the natural development of Dutch forests due to the established silvicultural systems and because at the time the majority of forests in the Netherlands were quite young (Mohren and Vodde, 2006). As such, the Minister of Agriculture, Nature and Food Quality of the Netherlands moved to the establishment of a so-called forest reserve network in 1997.

1.2 The Dutch forest reserve network

The Dutch forest reserve network was established to facilitate research on the natural development of Dutch forests. Forest areas could be incorporated into the network at the request of their owners. Initially, the network primarily consisted of forests owned by *Staatsbosbeheer*, but over time, participation expanded to include privately owned forests. Forests incorporated into the forest reserve network are unique in the Netherlands as any and all management interventions by owners are prohibited, as to allow natural forest development to occur (Broekmeyer and Hilgen, 1991; M. Broekmeyer, 1995). In practice, limited interventions are permitted to ensure safety, with specific regulations varying across reserves (E. Roest, personal communication, February 5, 2025). The natural development of the forest reserves serves as the basis for a 10-yearly monitoring cycle, designed to assess key forest parameters indicative of forest health and ecosystem dynamics. Insights gained from the analysis of natural forest development could then be applied and included in forest management practices around the Netherlands (Broekmeyer and Hilgen, 1991; M. Broekmeyer, 1995). Following the inclusion of the most recent reserve in 2000 and an exclusion in 2018, the Dutch forest reserve network currently encompasses 59 forest sites across 11 of the 12 Dutch provinces. The reserves vary in size, from 4 hectares to over 300 hectares, as well as in forest type, management history, and age.

The 10-year monitoring cycle of the reserves has resulted in several forests being surveyed multiple times. However, the majority have only been inventoried once (at the time of their designation as a forest reserve) or twice. Each monitoring cycle involves the collection of a range of forest characteristics through in-field measurements. The monitoring methodology is well documented in an internal field guide and incorporates multiple levels of monitoring (M. Broekmeyer et al., 1997). Measurements are conducted at designated 'core areas' (*kernvlaktes*), along transects, and at circular sample plots. The monitoring levels are systematically assigned: a forest reserve is mapped using a 50×50 -metre grid, with one of these grid cells designated as the centre of the core area, which measures 70×140 metres. In theory, between 10 and 50 grid cells are randomly selected to contain circular sample plots, with the number of plots proportional to the size of the forest reserve, though in practise a greater number of grid cells are selected. Each circular sample plot has a radius of 12.6 metres, centred around the midpoint of the selected grid cell. Additionally, the core area is subdivided into 10×10 -metre subcells, while the transect, positioned at the centre of the core area, extends 100×2 metres and is further divided into 2×2 -metre subsections. Figure 1 illustrates the different monitoring levels for an example forest reserve.

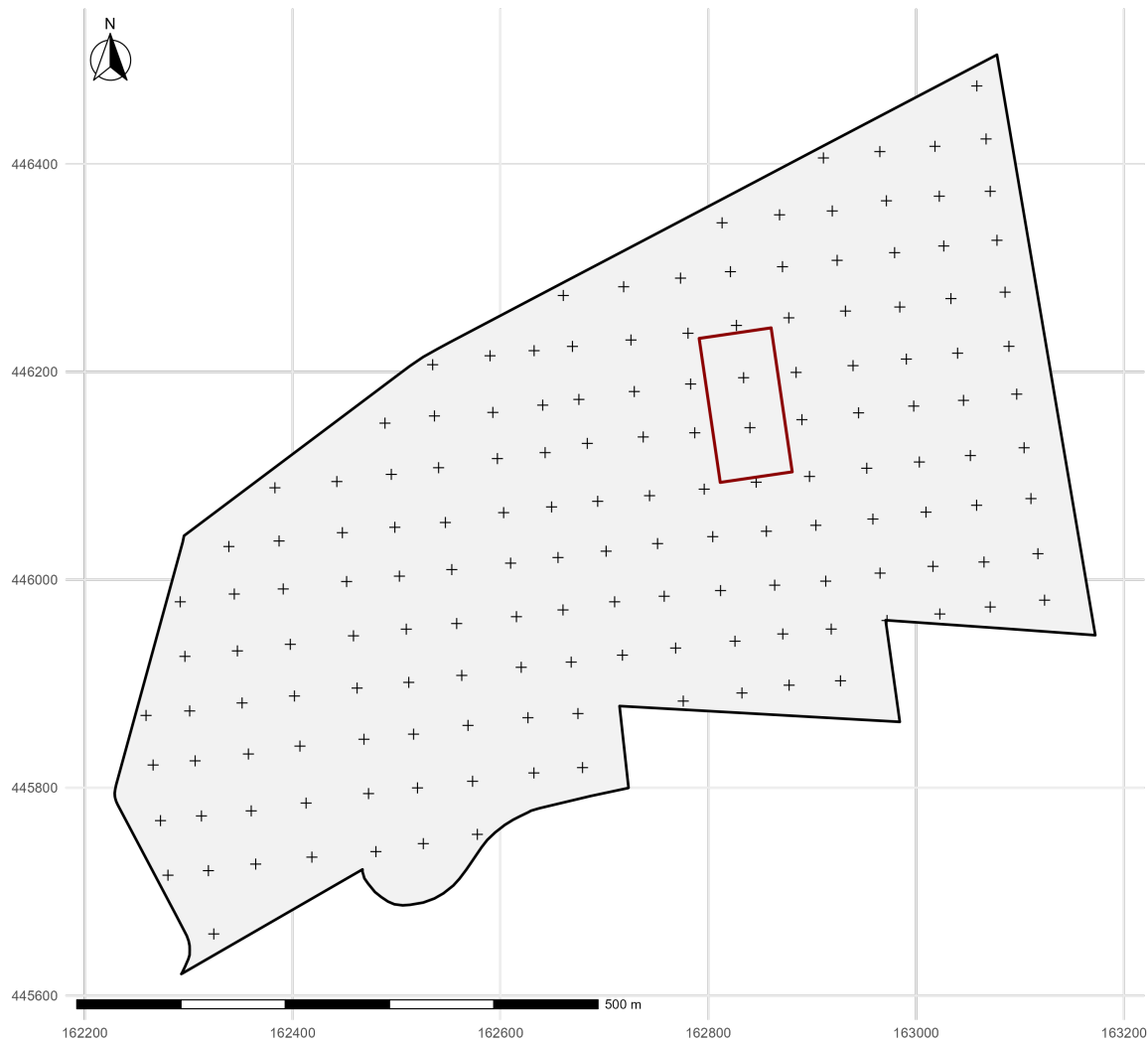


Figure 1: Example overview of different monitoring levels for the forest reserve
Galgenberg (RSV 3).

Core area visualised by the red polygon and the sample plot locations with + markers. Transect not visualised.

The internal field guide by M. Broekmeyer et al. (1997) provides a detailed description of the characteristics monitored and their associated methodologies. Table 1 summarises the various forest reserve characteristics related to forest structure and vegetation, as assessed under the current monitoring programme at the core area, circular sample, or transect level. In addition to the characteristics outlined in 1, aerial imagery was used as a reference for assessing the Potential Natural Vegetation (PNV) of a reserve upon its designation to the network, which was used to describe the anticipated state of mature vegetation in the absence of human intervention (Chiarucci et al., 2010). In theory, this reflects the type of forest the reserve may become given enough time without human intervention. The in-field measurements required to collect data on these characteristics are time-intensive. For instance, at all sample plots, tree positions and species are recorded on a stem map. This involves precisely measuring the angle and distance from the centre point of the sample site for all trees within the 12.6-metre radius. Each tree's Diameter at Breast Height (DBH), measured at 1.3 metres above ground level, is then recorded. Additionally, the height of all trees is either measured directly or estimated. Overall, the time - and thus funding - required to assess all forest characteristics is considerable, particularly when scaling up to larger forest reserves and accounting for the fact that there are 59 reserves in total.

Table 1: Overview of forest reserve characteristics monitored at the three unique monitoring scales. dbh = diameter at breast height. h = height.

Variable	Transect	Core Area	Sample Plots
Plant species distribution	x	x	x
Cover percentage of plants	x	x	x
Shrub presence (dbh<5cm, h<0.5m)	x		
Shrub presence (dbh<5cm, h>0.5m)		x	x
Tree and shrub seedlings		x	x
Tree presence (dbh>5cm)		x	x
Tree position		x	x
Tree crown projection		x	
Tree diameter at breast height		x	x
Tree height		x	x
Tree crown characteristics		x	x
Tree vitality		x	x
Damage to trees		x	x
Decomposition stage of dead trees		x	x

1.3 Recent developments

Changing financial allocations of the government resulted in the budget for the monitoring of the reserves being cut in 2005, causing monitoring at national level to cease. Since the budget cut, new data about some of the reserves has been collected by Wageningen Environmental Research (WENR) on a project basis at provincial level. Since limited restarting of the monitoring programme in 2018, data for multiple forest reserves has been collected again. Furthermore, to support monitoring efforts, a WENR project was started in January 2024 to mark and digitise forest reserve infrastructure, including the locations of core areas and circular sample plots. This project represents a first step toward reinstating nationwide forest reserve monitoring, which aims to once again serve as a valuable source of information for forest management and informed decision-making. However, fieldwork remains costly and labour-intensive, making a rapid expansion of the monitoring program unlikely. Therefore, it is essential to explore approaches to enable the support and reimplementation of monitoring at a national scale.

A key opportunity for the swift upscaling of nationwide forest reserve monitoring lies in the use of remotely sensed (RS) data. RS data is a broad term encompassing various types of data, including active and passive sensors, space-borne and aerial platforms, as well as optical and radar technologies. These diverse data sources enable a range of data-driven approaches to support multiple research objectives. One such remote

sensing technique is Light Detection and Ranging (LiDAR), an active remote sensing method that enables the acquisition of three-dimensional point cloud data. LiDAR data can be collected using various methods, both stationary and mobile. These include Terrestrial Laser Scanning (TLS), Mobile Laser Scanning (MLS), Aerial Laser Scanning (ALS), and Space-borne Laser Scanning (SLS). In addition to this, LiDAR data collected utilising Unmanned Aerial Vehicles (UAVs) is generally considered a separate category. A well-known ALS dataset in the Netherlands is the *Actueel Hoogtebestand Nederland* (AHN, Current Elevation Model of the Netherlands), which contains ALS-derived point clouds for the entire country over a range of years. To date, four datasets (AHN1, AHN2, AHN3, and AHN4) have been fully completed, with the fifth (AHN5) currently being processed. Each AHN version has been acquired during different years since 1997. Commissioned by *Rijkswaterstaat*, this open-access, freely available dataset offers a unique combination of repeated measurements, accessibility, and cost-effectiveness, making it particularly suitable for investigating its potential applications in forest reserve monitoring.

1.4 About LiDAR and the potential of AHN

The variability of LiDAR data is substantial due to the diversity of collection methods and sensor characteristics. A primary distinction in LiDAR technology is between discrete and full-waveform scanners. Discrete LiDAR records individual points at the peaks of returning laser pulses, whereas full-waveform LiDAR captures the entire returning pulse, preserving the complete waveform (Ussyshkin and Theriault, 2011). Compared to full waveform, discrete LiDAR is more widely used and can be acquired through various platforms (Degnan, 2016). Terrestrial Laser Scanning (TLS) collects data from a fixed, terrestrial scanning position at extremely high resolution, producing dense point clouds (>1000 points m^{-2}) over relatively small areas. Mobile Laser Scanning (MLS) enables data collection in a mobile context, such as handheld or backpack-mounted systems. Unmanned Aerial Vehicles (UAVs) facilitate airborne LiDAR scanning, offering high point cloud densities (typically 100–500 points m^{-2}) with flexible, low-altitude operations over larger areas than TLS. Aerial Laser Scanning (ALS) employs helicopter- or aircraft-mounted sensors, enabling large-scale data acquisition but with lower point densities (1–50 points m^{-2}). Space-borne Laser Scanning (SLS) provides global coverage with significantly lower resolution. Some LiDAR sensors are also capable of capturing co-registered optical data in the red, green, and blue (RGB) channels, allowing the generation of colourised point clouds.

LiDAR is widely applied in forest monitoring, with TLS, MLS, and UAV-based LiDAR being particularly useful due to their high point cloud densities (Camarretta et al., 2019; Dassot et al., 2011; Ko and Remmel, 2017). Numerous studies have explored the applications of different LiDAR sensors and platforms in forestry (Beland et al., 2019). TLS-derived point clouds, due to their high point density, have proven useful for estimating DBH (Compeán-Aguirre et al., 2024), tree branch angles (Peng et al., 2024), tree volume (Moskal and Zheng, 2011), tree height, and crown base height (Yrttimaa et al., 2020). UAV LiDAR offers high point densities and has been applied in estimating crown diameter (Sankey et al., 2017), tree height (K. Liu et al., 2018), tree volume (Corte et al., 2020), and individual tree detection (Sung et al., 2024). Preliminary research suggests that ALS LiDAR is also suitable for forest monitoring, with applications in aboveground biomass estimation (Ene et al., 2016), canopy height metric determination (Goldbergs, 2023), individual tree segmentation (Wielgosz et al., 2024), and modelling tree curves and volume (Muhojoki et al., 2024).

However, the AHN datasets were not collected for forestry purposes, but rather to support the Dutch water boards in hydrological models. It is therefore no surprise that research on the specific application of AHN data for forestry and forest-related topics remains limited. Previous research indicates that the AHN2 dataset is suitable for mapping tree canopy projections, particularly in non-urban areas (Meijer et al., 2015). Additionally, several theses have been written at Wageningen University, exploring the potential of AHN data for forest applications. For instance, research into the use of AHN for monitoring succession processes in forest structure has shown that various methodologies can be used for segmenting AHN forest point clouds into vegetation layers with promising results for upper vegetation layers, but discouraging results for shrub layers (de Pagter, 2024). A comparative analysis of Individual Tree Detection (ITD) algorithms using AHN data also showed favourable outcomes for coniferous forests, although lower accuracies were observed for deciduous forests (Koop, 2024). Furthermore, a combination of Canopy Height Model (CHM) change-detection methods using AHN has been shown to be effective for the detection of canopy gaps in

forested areas (Koelewijn, 2023). Despite these studies, the use of AHN for monitoring the outlined forest reserve characteristics to support the forest reserve programme remains largely unexplored, and thus the question remains what role, if any, AHN can play specifically in the current forest reserve programme.

1.5 Research objectives

As established in the previous subsections, the monitoring of Dutch forest reserves could benefit from novel approaches. The AHN datasets have been identified as a promising resource for developing a data-driven approach to achieve this. While remote sensing has been widely applied to forest-related research worldwide, the specific use of AHN data within a forest management context remains largely unexplored. In particular, novel applications of AHN data have been identified as a research gap within the Dutch forest management sector. Therefore, this thesis aims to explore the suitability of the Dutch national ALS dataset (AHN) for monitoring forest reserve characteristics, thereby supporting the national forest reserve programme. To achieve this aim, the following Specific Research Objectives (SROs) have been defined:

- SRO1: Identify and evaluate potential methodologies that utilise ALS-derived LiDAR point cloud data for analysing the outlined forest reserve characteristics.
- SRO2: Assess the feasibility of applying the identified methodologies to AHN data.
- SRO3: Evaluate the suitability of AHN-applied methodologies through comparison with field-collected data where available.

The outcome of SRO1 will be a structured overview of identified methodologies, their applicability to specific forest reserve characteristics, and relevant literature. SRO2 will provide a qualitative distinction through visual assessment between methodologies that can be effectively applied to nationwide AHN data and those that cannot. Finally, SRO3 will present a quantitative evaluation, comparing the performance of applicable methodologies against field-collected data where possible.

2 Data and Methods

2.1 Study Area

2.1.1 The Dutch forest reserve network

Considering the research objectives of this thesis, the study area comprises all 59 Dutch forest reserves. As previously discussed, these reserves were deliberately selected to represent the full range of forest types present in the Netherlands, resulting in substantial diversity between them.

Each reserve, identified by a unique forest reserve code and name (e.g. RSV 3, *Galgenberg*), contains trees of varying species and ages, and is located within a specific Physical Geographic Region (PGR). The PGR reflects the forest's geographical characteristics, based on the *Landschapsleutel* by Maas et al. (2018). Most forest reserves (approximately 50%) are situated on inland sand soils, followed by marine clay ($\pm 20\%$) and coastal dune areas ($\pm 10\%$). Others are located in colline, peatland, or riverine regions. This diversity is further illustrated by the range of Potential Natural Vegetation (PNV) types and Natura 2000 woodland habitat types found within the reserves. Notably, the PNV types *Fago-Quercetum* ($\pm 25\%$) and *Fraxino-Ulmetum* ($\pm 10\%$) are particularly well represented (Bijlsma and Clerkx, 2019b). While the PNV describes the expected vegetation in the absence of human interference, this does not mean that the forest reserves currently resemble this forest type and as such offers limited insight into the reserves' current vegetation. As such, a different distinction in forest types must be made.

For the purposes of analysis in this thesis, forest reserves and sample sites were categorised into three forest types: 'coniferous', 'deciduous', and 'mixed'. This classification is commonly used in scientific literature, as model performance often varies depending on forest type (Lisiewicz et al., 2022; Stereńczak et al., 2020). As no such classification was readily available for the Dutch forest reserves, it was derived manually. The *NLForestReserve2018* database (described in Section 2.2) was used as input data to determine forest types, as it contains an inventory of all identified trees within the circular sample plots and core areas of each reserve, including species information. Forest types were assigned based on species frequency from the most recent year of data collection available in the database, with the method illustrated in Figure 2. For each reserve, the occurrence of tree species per sample plot and core area was calculated. In cases with fewer than three unique species, all identified species were used for classification. Where more than three species were recorded, the three most frequent species were selected. If all selected species were either coniferous or deciduous, the reserve was classified accordingly; if both were present, it was classified as 'mixed'. In cases where no tree data were available (reserves 36, 37, 40, 42, 54, and 58), the forest type was recorded as 'NA'.

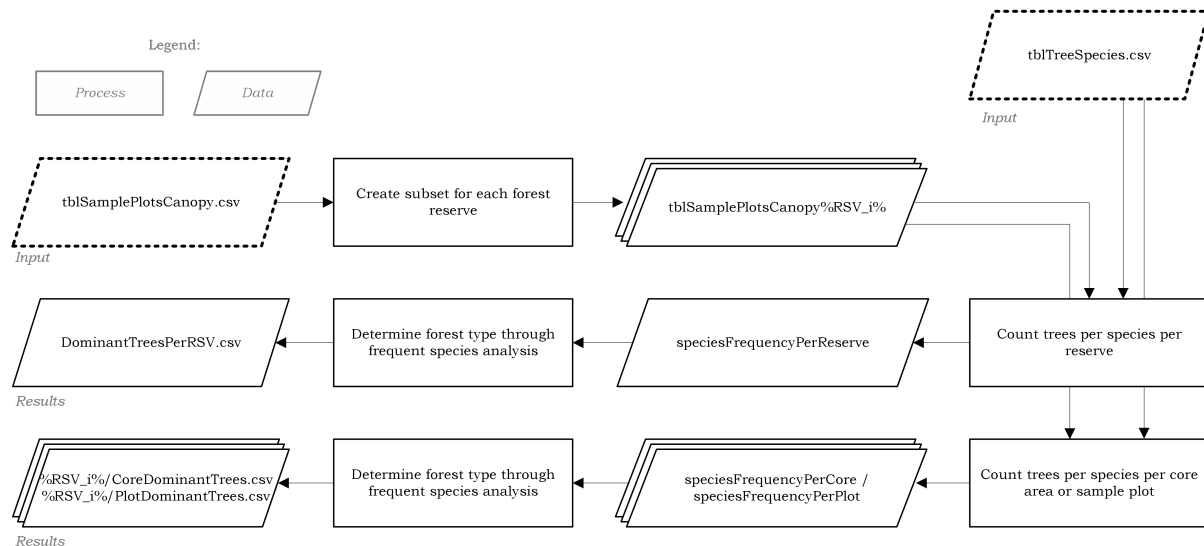


Figure 2: Flowchart visualising dominant tree and forest type identification.

Among the classified reserves, two were categorised as coniferous, 23 as deciduous, and 29 as mixed. The tools and scripts used for this classification are described in Section 2.4. Of the two coniferous reserves, most sample plots were classified as mixed (92 out of 100 plots), as they often contained only two tree species whereas the method requires at least three. From the 29 mixed reserves, 518 of the 674 plots were also classified as mixed, with 135 classified as deciduous and 21 as coniferous. Finally, of the 23 deciduous reserves, the majority of plots were classified as deciduous (501 out of 533), while the remaining plots were classified as mixed; no coniferous plots were identified.

In total, the Dutch forest reserves cover 2,598.2 hectares across the country. A complete list of reserves, including their codes, names, sizes, and forest types, is provided in Appendix I and visualised in Figure 3. An interactive map with additional information—such as dominant species per reserve, links to the AHN 3D Point Cloud Viewer, and a search function—is available as a digital appendix online [here](#) (Verweel, 2025a).

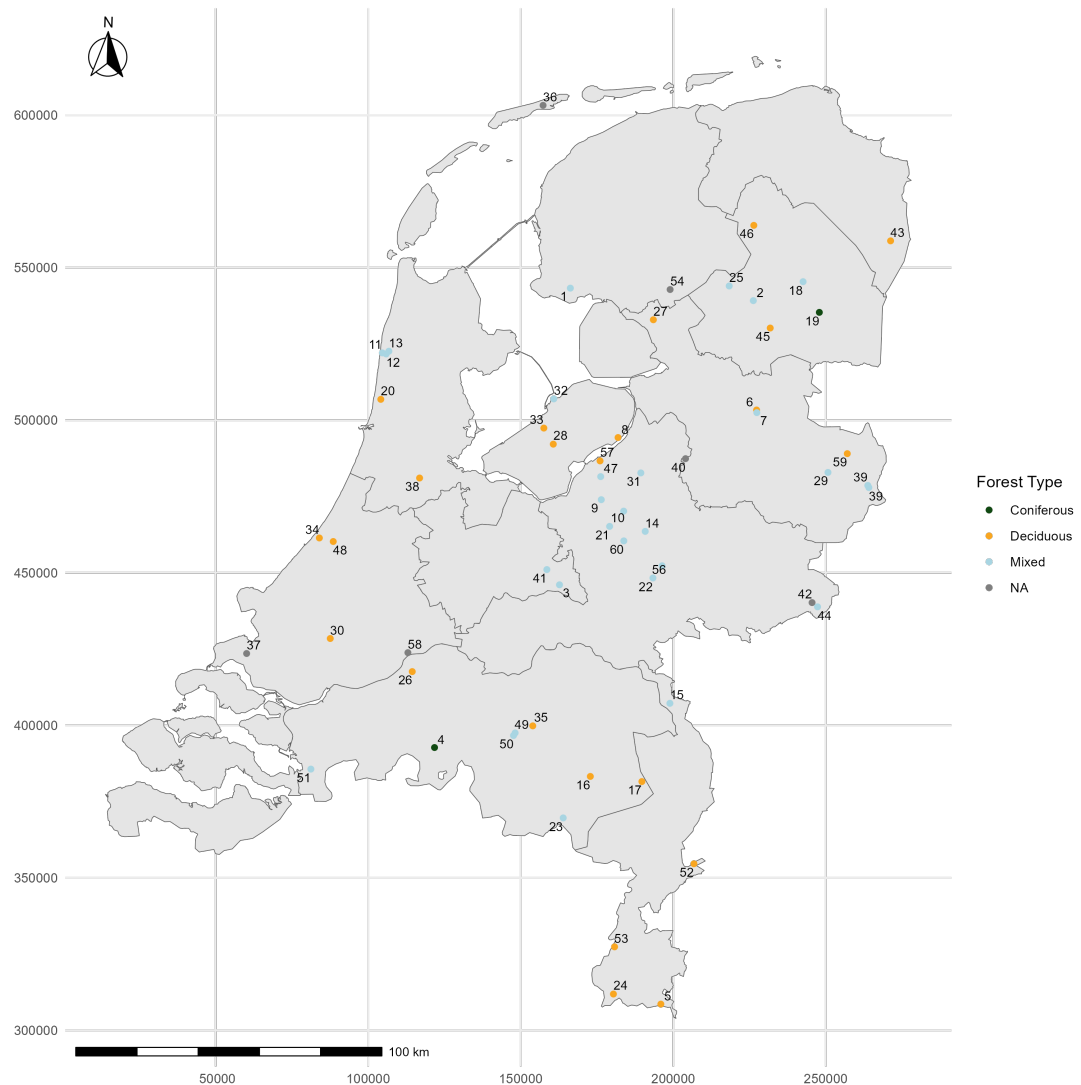


Figure 3: Locations of forest reserves around the Netherlands with their reserve code and forest type.

2.1.2 Representative reserves

To assess the feasibility of applying the identified methodologies to AHN data for SRO2, three representative reserves were selected to ensure the inclusion of coniferous, deciduous, and mixed forest types. Model feasibility may vary between these forest classes due to structural differences, with coniferous trees generally exhibiting a more conical form compared to the broader, irregular canopies of deciduous trees.

Based on the classification of the forest reserves into the three distinct forest types, informed selections were made. Forest reserve *Galgenberg* (RSV 3) was selected as the representative mixed forest, with dominant species *Quercus robur*, *Betula pendula*, and *Pinus sylvestris*. Forest reserve *Sang* (RSV 16) was chosen to represent deciduous forests, characterised by dominant species *Quercus robur*, *Alnus glutinosa*, and *Betula pubescens*. Finally, forest reserve *Oosteresch* (RSV 19) was selected as the representative coniferous forest, with dominant species *Pinus sylvestris*, *Pseudotsuga menziesii*, and *Larix kaempferi*. The selected reserves are illustrated in Figure 4.

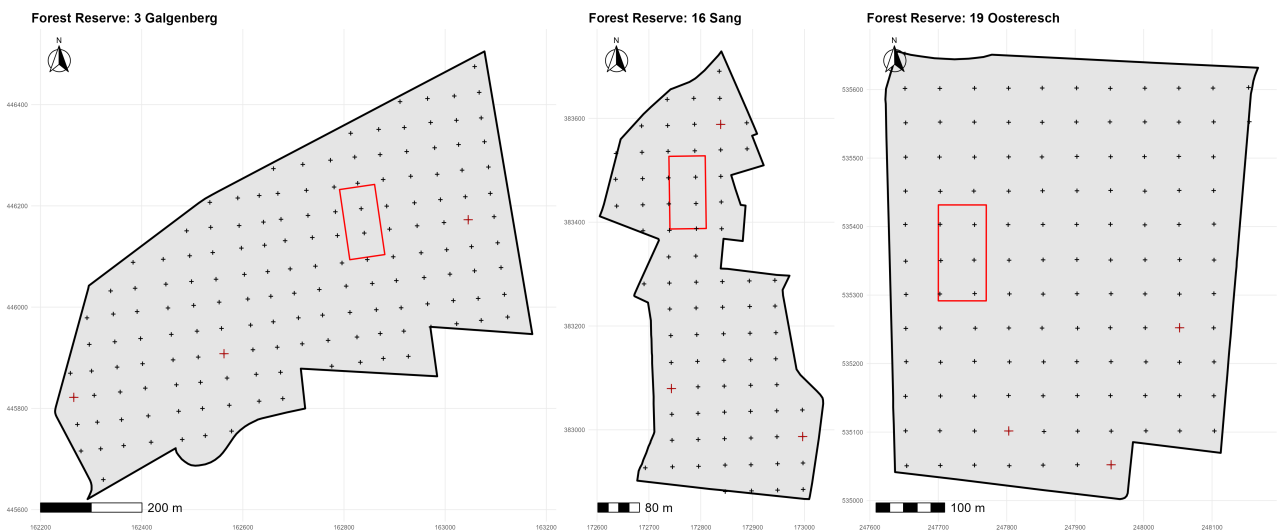


Figure 4: Overview of representative reserves.

Core areas visualised by red polygons, sample plots locations shown with +, and representative sample sites with a dark red +.

For each forest reserve, three circular sample plots were selected for the feasibility assessment, corresponding to the forest type of the reserve in which they are located. For forest reserve *Galgenberg* (RSV 3), sample plots A04, G05, and S09 were chosen, reflecting the dominant species present within the reserve. Using the same approach, sample plots C05, E15, and H03 were selected for forest reserve *Sang* (RSV 16), and plots D02, G01, and J05 for forest reserve *Oosteresch* (RSV 19).

2.2 Data

2.2.1 Forest reserve data

Central to this thesis is data concerning the Dutch Forest Reserve network, which is available in multiple formats. The primary source is a Microsoft Access database, accompanied by ESRI ArcGIS Shapefiles, both hosted by the Data Archiving and Networked Services (DANS; Bijlsma and Clerkx, 2019a). The Microsoft Access database, *NLForestReserve2018*, contains historical fieldwork measurements for all forest reserves up to the last recorded measurements in 2018, and is documented in an accompanying report by Bijlsma and Clerkx (2019b). The database includes general information on the forest reserves, their core areas, and sample plots in the tables *tblReserveGeneral*, *tblCoreAreaGeneral*, and *tblSamplePlotsGeneral*, respectively. Additional information concerning the canopy of the core areas and sample plots, as well as regeneration data, is found in the tables *tblCoreAreaCanopy*, *tblSamplePlotsCanopy*, and *tblSamplePlotsRegeneration*. Lastly, the database provides details on tree species, tree condition codes, and error status codes in the tables *tblTreeSpecies*, *tblTreeCondition*, and *tblErrorStatusCode*.

The accompanying ESRI ArcGIS Shapefiles include spatial representations of each reserve's boundary, core area (as either polygons or vertices), sample plots, and soil types. These are contained in the files *ReserveBoundary.shp*, *ReserveCoreAreaPolygon.shp*, *ReserveCoreAreaVertices.shp*, *ReserveSamplePlots.shp*, and *ReserveSoil.shp*.

As the aforementioned dataset includes only minimal recent data, up to 2018, there is limited temporal overlap with AHN data. Therefore, additional data were requested from WENR concerning recent fieldwork conducted in the Netherlands. The received data and reports are in draft form and currently under embargo, and therefore cannot be shared or included in the online appendix. These data cover fieldwork at a number of sample plots for reserves *Pijpebrandje* (RSV 9) and *Leesten* (RSV 14) in 2018, as well as *Norgerholt* (RSV 46) in 2021. The data are structured almost identically to those in the *NLForestReserve2018* database, as their purpose is to enable direct comparison with previously collected measurements. Accordingly, the data collection methods used in 2018 and 2021 closely resemble those applied between 1998 and 2005, as detailed in the field work manual by M. Broekmeyer et al. (1997). One notable exception is that during the course of this research, it became clear that the tree crown projection variable was not measured at during the recent fieldwork (E. Roest, personal communication, August 18, 2025).

2.2.2 Actueel Hoogtebestand Nederland

The *Actueel Hoogtebestand Nederland* (AHN) provides detailed elevation data of the Netherlands through a series of datasets. These data are periodically acquired using airborne laser scanning (ALS) LiDAR and are published as compressed point clouds (.LAZ files), classified according to LAS 1.4 specifications ([ASPRS], 2019). In addition, Digital Surface Model (DSM) and Digital Terrain Model (DTM) rasters (.TIF files) are made available at various resolutions. AHN data are released in numbered versions, each corresponding to specific acquisition periods: AHN1 was collected between 1996–2003, AHN2 between 2007–2012, AHN3 between 2014–2019, AHN4 between 2020–2022, AHN5 between 2023–2024, and AHN6 is currently being collected and scheduled to be finished in 2027 (Actueel Hoogtebestand Nederland, 2024). Over time, the sensors and acquisition methods have evolved, resulting in varying levels of detail and accuracy across versions. Table 2 summarises the reported theoretical accuracy demands for the .LAZ files. As AHN5 has not achieved full national coverage, with data collection instead pivoting to AHN6, AHN4 currently offers the highest quality, nationwide data coverage with temporal overlap with the supplied additional data. As such, AHN4 data are used in this thesis.

Table 2: Overview of AHN LAZ data available for the Netherlands and their years of acquisition and quality (Actueel Hoogtebestand Nederland, 2023).

AHN Version	Years of acquisition	Pulse density	Systemic Error (cm)	Stochastic Error (cm)
AHN1	1996–2003	$1/16 \text{ m}^{-2}$ to 1 m^{-2}	5	15
AHN2	2007–2012	6 m^{-2} to 10 m^{-2}	5	5
AHN3	2014–2019	6 m^{-2} to 10 m^{-2}	5	5
AHN4	2020–2022	10 m^{-2} to 14 m^{-2}	5	5
AHN5	2023–2025	$>10 \text{ m}^{-2}$	Unknown	Unknown
AHN6	2025–2027	Unknown	Unknown	Unknown

The AHN data used in this study were accessed via the GeoTiles service (van Natijne et al., 2020). AHN4 data are structured into tiles measuring 6.25 km by 5 km, with each tile typically ranging between 4–6 GB in size (.LAZ format). GeoTiles subdivides each AHN4 tile into 25 smaller tiles of 1.25 km by 1 km, incorporating slight overlap and additional RGB data sourced from *Beeldmateriaal*, the Dutch aerial imagery service (Beeldmateriaal Nederland, 2023). These GeoTiles .LAZ files are considerably smaller, averaging 400-500 MB per file. In most cases, a single tile is sufficient to cover an entire forest reserve; however, multiple tiles may be necessary if the reserve boundary intersects several tiles. The GeoTiles can be downloaded automatically from the server, facilitating efficient data retrieval.

2.3 Methodology

2.3.1 Overview

The overall methodology of this thesis is summarized graphically in Figure 5. Prior to approaching the previously outlined specific research objectives, certain data required preprocessing. This section describes the methodology applied during the data preprocessing and the methodologies applied to obtain results for the specific research objectives.

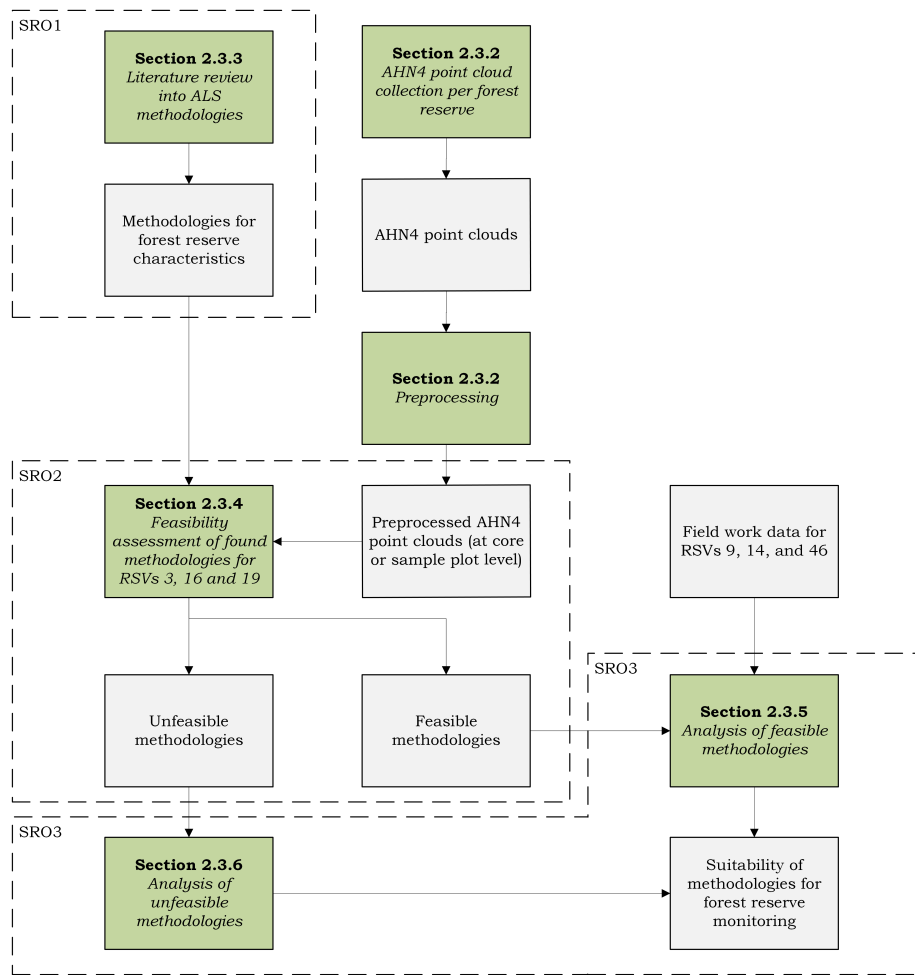


Figure 5: Flowchart overview of applied process.

2.3.2 Data collection and preprocessing

The *NLForestReserve2018* database and associated ESRI ArcGIS Shapefiles were manually downloaded via DANS (Bijlsma and Clerkx, 2019a). All subsequent preprocessing steps were performed using R scripts, as described in Section 2.4. The Coordinate Reference System (CRS) of the forest reserve shapefiles was reprojected to "Amersfoort / RD New + NAP height" (EPSG:7415; Committee and Solutions, 2008) to match the CRS of the AHN4 GeoTiles point clouds. The data were cleaned by removing forest reserve 55, which was excluded from the project in 2018, along with any reserves with a code exceeding 60. For each reserve, the relevant AHN4 GeoTiles were identified and subsequently downloaded in .LAZ format. To reduce storage requirements, the AHN4 point clouds were clipped. This process involved buffering all sample plots and core areas by 5 metres to prevent edge effects, using `st_buffer` from the `sf` R package (Pebesma, 2018), followed by clipping the point clouds using the `readLASCatalog`, `clip_roi`, and `clip_circle` functions from the `lidR` R package (Roussel and Auty, 2025). The clipped point clouds were saved in .LAZ format for further use, and the original AHN4 .LAZ files were deleted to conserve storage space. During preprocessing, two faulty spatial indices for geotiles 33BZ1_16 and 12AZ2_22 were identified resulting in artefacts in the clipped point clouds. Subsequently, the decision was made to perform the clipping without spatial indices - a computationally slower approach - to guarantee the quality of the clipped point clouds.

2.3.3 Literature review

The literature review aimed to identify a range of methodologies for determining one or more of the previously outlined forest characteristics. To ensure reproducibility, a structured approach was applied based on the snowballing methodology — also known as citation chaining or citation searching — following the framework established by Wohlin (2014) and further described by Radboud University Library (n.d.). This approach begins with one or more seed articles, from which references (backward snowballing) or citations (forward snowballing) are examined based on predefined inclusion criteria. If an article meets the criteria, its references or citations are subsequently assessed. In Wohlin's framework (Wohlin, 2014), this process continues iteratively until no new relevant articles are identified. Due to time constraints and the fact that this literature review is not the sole research objective of this thesis, the snowballing procedure was limited to a single iteration following the selection of seed articles.

Scopus served as the primary database for this review. The initial search for seed articles was queried with "review AND (aerial OR airborne) AND lidar AND forest," reflecting the focus on methodologies applied to aerial LiDAR data in forested environments. Including the term "review" ensured that the search encompassed a broad range of relevant references. Essentially, this constituted a review of existing reviews to establish a comprehensive overview of available methodologies. Given the scope of the literature review, only the first 10 search results - sorted by publication date - were evaluated for potential inclusion as seed articles. Evaluating only the first 10 ensures the scope remains limited whilst encapsulating the most recent developments in the domain.

Seed articles and their references were assessed based on the following inclusion criteria: (1) The article must discuss LiDAR data, though not exclusively so. LiDAR should be explicitly mentioned to ensure relevance, but the inclusion of additional data sources did not prevent selection, as comparative studies may provide valuable methodological insights. (2) The article must include ALS, platform-agnostic data, or datasets with a point density below 30 points m⁻², ensuring compatibility with AHN data. Notably, studies focusing on UAV-based LiDAR platforms were excluded. Additionally, as 'ALS' is not a standardized acronym and may refer to 'Aerial LiDAR System,' 'Airborne Laser Scanner,' or a combination of those terms, all such variations were considered equivalent. (3) The article must refer to forestry or explicitly reference trees to ensure relevance to the study area. (4) The article must have been published within the past 15 years (i.e., 2010 or later at time of writing) to ensure coverage of recent methodologies in this rapidly evolving field.

To further refine the scope, a maximum of three seed papers were selected. As more than three potential seed papers were identified, a justified selection process was applied further described in Section 3.1. Following seed article identification, the backward snowballing method was used to identify relevant earlier works. All references of the seed articles were assessed based on their title, abstract, and keywords against the selection criteria. An overview document was created to track what selection criteria the articles met or did not meet. Articles not meeting all four criteria were discarded, and articles meeting all four criteria were noted and examined further for the identification of methodologies.

Articles that met the initial selection criteria were further examined to identify methodologies applicable to the analysis of one or more forest reserve characteristics. To ensure methodological relevance, a second set of selection criteria was applied: (1) The article must describe a methodology that specifically addresses at least one of the defined forest reserve characteristics. (2) That methodology must be applicable using only AHN4 data as the source of remote sensing information. Articles that failed to meet both criteria were discarded. The remaining articles and their applicable forest reserve characteristics were compiled into a table, representing the final results of SRO1.

2.3.4 Feasibility assessment of found methodologies

Following the results of SRO1, in the case of multiple methodologies for the same forest reserve characteristic, the presented accuracy metrics were compared, and the most promising method for each forest reserve characteristic was assessed for its feasibility in application to AHN data. The selected methodologies were applied to the representative sample sites described in Section 2.1.2, following the procedures in the corresponding publications as closely as possible, although adjustments were occasionally necessary. Brief summaries of the applied methodologies are provided below, in the order in which they appear in Section 3.2.

For Individual Tree Detection and height estimation, the methodology presented by Sparks et al. (2022) was applied exactly as described. For each representative sample plot, a Canopy Height Model (CHM) was computed at a spatial resolution of 50 cm. A circular search window with a radius of 1.5 metres was then used for the Local Maximum Filter (LMF) without any parameter optimisation, implemented using the `locate_trees` function from the `lidR` R package. This process resulted in the identification of treetop locations and their corresponding heights.

For crown projection mapping, the methodology described by Bazezew et al. (2018) was replicated using open-source software alternatives. First, a pit-free CHM was computed for each sample plot at a spatial resolution of 50 cm, with height intervals of 0, 2, 5, 10, and 15 metres, as described by Khosravipour et al. (2014). This was achieved using the `rasterize_canopy` function in `lidR`, with the argument `algorithm = pitfree()`. The resulting pit-free CHM was aggregated to a 1 m spatial resolution. Unlike the original approach by Bazezew et al. (2018), CHM multiresolution segmentation was not performed using eCognition due to licensing restrictions and this thesis' focus on open-source applicability. Instead, Multicore Watershed Segmentation (MCWS) was performed using the `mcws` function from the `ForestTools` R package (Plowright, 2017), a common raster-based approach for crown delineation (Kleinsmann et al., 2023; Penglase et al., 2023; So et al., 2025). The function required the input of previously identified treetops, which were provided by the ITD approach described in Sparks et al. (2022). As MCWS and multiresolution segmentation differ significantly in methodology, an additional algorithm was applied that better replicates the multiresolution concept, this time operating directly on the point cloud, allowing the comparison of two methods and guaranteeing the application of the most suitable method. The method developed by Li et al. (2012) was implemented using the `segment_trees` function from the `lidR` package, with the `algorithm` argument set to `li2012()`. Following segmentation using the `li2012` algorithm, crown projections were visualised using the `crown_metrics` function from the same package.

The standing dead tree (snag) detection algorithm was applied as described by Wing et al. (2015). The clipped point clouds of each representative sample plot was height-normalised using the `normalize_height` function from the `lidR` package with the `tin` (Triangulated Irregular Network) algorithm. Subsequently, the overstory threshold - a set height threshold for what part of the point cloud is considered overstory - was determined. In the study by Wing et al. (2015), this threshold ranged between 1.5 and 2 metres depending on the site; here, the upper bound of 2 metres was used due to the observed relative tallness of the trees in the study area. The height-normalised point cloud was then filtered to retain only first and second return points. Next, a point intensity index was calculated by scaling the intensity values between 0 and 255 using min-max normalisation and added as an additional attribute to each point. Following this, five plot-level variables were computed as outlined by Wing et al. (2015): point density, maximum intensity index, fraction of canopy cover, mean canopy height, and the Branch and Bole versus Foliage ratio (BBvFr). These variables were used to compute filtering thresholds using the linear equations provided in the original publication. Based on these thresholds, point density ratio selection was applied and the branch and bole point ratio (BBPR) matrix was constructed. This matrix contains conditional assessments of BBPR and point densities, which are used in the algorithm to distinguish between different snag types. Finally, the snag detection model was executed using the `segment_snags` function from the `lidR` package with the argument `algorithm = wing2015()`.

The feasibility assessment of the outlined methods was based on a twofold approach: visual and computational. The visual assessment involved a detailed examination of the outputs of each methodology to identify potential weaknesses or shortcomings and to construct a form of confusion matrix. This matrix allowed the comparison of correct versus incorrect measurements, serving as the basis for determining a method's feasibility. Given the diverse range of forest characteristics assessed—spanning nominal, interval, and ratio measurement scales—it was not possible to adopt a single confusion matrix format. Therefore, confusion matrices are presented per characteristic in the relevant subsections of Section 3.2. The visual assessment safeguards the minimum level of accuracy required for meaningful comparison with field-collected data in SRO3. Computationally, the execution of the relevant function(s) to determine the variable of interest was limited to a maximum of 200 seconds per sample plot, as measured using the `system.time` function from R Core. This threshold ensures that the methods remain scalable to additional forest sample plots and reserves in SRO3.

2.3.5 Analysis of feasible methodology

In order to test the feasible methodology found in Section 3.2 against the provided field work data described in Section 2.2.1, the field work data was preprocessed to ensure relevancy of the data and easy comparison against the results from SRO2. Preprocessing involved the dropping of unnecessary data columns and rows, obtaining the most recent tree height datapoint, and subsequently splitting the Excel files into CSV files with tree data for each sample site. As the Excel files received were similar in layout, but not exactly so, this required some manual input which is documented in the `preprocessFieldData()` function found in the functions script in the digital appendix described in Section 2.4. Following the preprocessing of the data, locations of individual trees in each sample site were converted into the RD New coordinate system from its original format of degrees and metres distance from the sample site centre using simple geometric transformation. This process can be examined in the `addLocationData()` function in the scripts.

Following field data preprocessing, parameter optimisation was carried out for the ITD algorithm described by Sparks et al. (2022) in an attempt to improve the results. Instead of applying a Fixed Window Size (FWS) approach, as in SRO2, a Variable Window Size (VWS) method was used based on the previously defined forest type of each sample plot. Literature generally suggests that VWS approaches yield better results than FWS approaches (Dalponte & Coomes, 2016; Eysn et al., 2015; Roussel et al., 2020). Based on the sample sites examined in SRO2, a set of linear equations was derived to estimate the relationship between tree height and canopy radius for mixed, coniferous, and deciduous forests. This analysis was performed in R and documented in the `vwsTraining.R` script provided in the digital appendix. The resulting set of linear equations is presented in Table 3.

Table 3: Derived linear equations for Variable Window Size approach to Individual Tree Detection in SRO3.

Forest type	Equation ($r = \text{radius (m)}$, $h = \text{height (m)}$)
Mixed	$r = -0.856 + 0.178h$
Deciduous	$r = 1.786 + 0.056h$
Coniferous	$r = -0.843 + 0.145h$

With the derived linear equations, the VWS approach was applied during ITD through application of the forest-specific equation, setting a minimum radius of 2.5 m to prevent over-classification and a minimum tree height of 4 m for the same reason. Following the execution of the ITD algorithm utilising VWS on the forest reserves for which field data were available, comparison metrics were calculated.

Metrics were computed at both individual-tree and plot levels, and grouped by forest type (mixed, deciduous, and coniferous) to explore patterns across forest types. At the individual-tree level, the distance between each field-observed tree and its closest ITD-derived tree was determined using `sf`'s `st_nearest_feature` function, providing insight into whether the ITD algorithm identified trees in close proximity to those observed in the field. In addition to distance, the height difference between each nearest ITD-derived tree and its corresponding field-observed tree ($Z_{itd} - Z_{field}$) was calculated to assess tree height over- or under-

estimation. At the plot level, the number of field-observed and ITD-derived trees was tallied to determine whether the ITD algorithm over- or underestimated tree counts in a given plot. Furthermore, the average tree heights for both field-observed and ITD-derived trees were calculated, along with the averages of the individual-tree-level distance and height difference metrics. Statistical testing was performed on variables of interest using the Wilcoxon signed-rank test, as the data were not normally distributed, with $\alpha = 0.05$ as test threshold. Field observations were treated as expected outcomes, and ITD-derived values were treated as predictions.

2.3.6 Analysis of unfeasible methodologies

Further analysis was conducted on methodologies deemed unfeasible to clarify the reasons for their lack of feasibility, thereby supporting robust conclusions regarding their current and future applicability within the forest reserve monitoring framework. The steps and methods of visualisation used for this analysis are documented in the `unfeasibleMethodsAnalysis.R` script in the online appendix.

An additional analysis of the algorithm by Li et al. (2012) for crown segmentation was undertaken to identify potential causes of the artefacts and errors observed in the crowns. To this end, the segmented point clouds were visually examined prior to conversion into crown projections to explore possible sources of error. The algorithm includes numeric thresholds, d_t and Z_u , which can be adjusted to better suit user requirements. These thresholds define the spacing and height criteria used to identify individual trees. In the R implementation, the d_t threshold is further divided into $dt1$ and $dt2$. Table 4 lists the combinations of $dt1$, $dt2$, Z_u , and h_{min} values explored, where the algorithm's default values are 1.5, 2, 15, and 2, respectively. The results were visually compared side by side in linked 3D viewing windows, allowing simultaneous manipulation of multiple point clouds. This approach facilitated the identification of parameter combinations that yielded the best results with the fewest artefacts.

Table 4: Combinations of parameters in the Li 2012 algorithm tested for visual confirmation.

Algorithm default values highlighted in the first row.

$dt1$	$dt2$	Z_u	h_{min}
1.5	2	15	2
1.5	2	15	4
1.5	2	10	2
1.5	2	20	2
1.5	2	30	2
1.5	3	15	2
2	3	15	2
1	2	15	2
1	1.5	15	2
1.5	1.75	25	2
1.6	1.85	20	5
1.7	2	20	4

The snag detection algorithm, applied according to the method described by Wing et al. (2015), resulted in overwhelming levels of over-classification in SRO2. Following this, various point cloud characteristics were examined as potential causes of the over-classification, including the laser system used for data acquisition, flight height, sensor scan angle, percentages of single and multiple returns, and point density. In addition, the distributions of intensity values were analysed.

Following this initial examination, the sample plot point clouds were first filtered to exclude classified ground points before calculating the intensity index, with the aim of reducing the influence of high-intensity ground points during the min-max normalisation procedure. Although Wing et al. (2015) do not explicitly mention masking ground-classified points in their methodology, they repeatedly refer to "overstory" points, defined

as points above a specified height threshold. While this distinction had already been made in SRO2, it was hypothesised that explicitly removing ground-classified points might alter the initial intensity index distribution and yield more realistic results.

Subsequently, the ground-filtered point clouds were randomly resampled to better match the point density reported in the article using lidR's `decimate_points` function, with a target density of $6.8 \text{ points m}^{-2}$ — the average point density of the data used in the study by Wing et al. (2015). After ground filtering and point cloud decimation, the snag detection algorithm, as described in Section 2.3.4, was applied to the point clouds, and the outcomes were evaluated by calculating the percentage of the point cloud classified as snag, alongside visual inspections in a 3D viewer.

2.4 Materials

Given the digital nature of this thesis, no physical materials were used aside from computing hardware. All work was conducted on an *ASUS Vivobook Pro 16X*, equipped with 16GB RAM, an Intel Core i7 CPU, and an NVIDIA GeForce RTX 3050 Laptop GPU.

For SRO1, the Scopus document database was utilised to apply the snowballing procedure for literature selection. Scripts used in SRO2 and SRO3 were written in the R programming language (version 4.4.3; R Core Team, 2023). A variety of R packages were utilised, with `terra` (version 1.7-65; Hijmans, 2023), `sf` (version 1.0-15; Pebesma, 2018), and `lidR` (version 4.0.4; Roussel and Auty, 2025) playing key roles in data processing. For visualisation, the packages `rgl` (version 1.2.8; Murdoch and Adler, 2023) and `ggplot2` (version 3.5.1; Wickham, 2016) were used. Additional packages were utilised for minor tasks, these can be identified in the scripts available in the digital appendix.

A digital appendix accompanies this thesis, which is available online, containing all scripts, visualisations, and datasets produced and referenced in this thesis. It can be accessed via [this link](#) (Verweel, 2025b). The scripts contain all code required to execute the method as outlined in the previous sections, as well as the scripts required to create the visualisations presented and the presented web map. Data created during this these are also available in the online appendix to allow easy verification. A README further explains the use of the online appendix.

3 Results

3.1 Literature review

The initial search for seed articles in Scopus, using the query described in Section 2.3.3, returned 122 results. Contrary to the outlined methodology, the first 11 articles were evaluated for consideration as seed articles. This deviation from the methodology is explained due to the fact that the 10th result was inaccessible, and as such could not be considered. Effectively, only 10 articles were considered, in line with the outlined methodology. Five of the 10 assessed articles met the predefined selection criteria, inaccessible article not included, and were considered as seed article. An overview of the considered seed articles is found in Appendix II.

From the considered seed articles, the articles by Sánchez-Chero et al. (2024), Rodrigues et al. (2024) and Goodbody et al. (2024) were selected as seed articles to which the backwards snowballing methodology was applied. This decision was made based on the topics covered by the different articles.

The article by Sánchez-Chero et al. (2024) was selected as a seed article as, although it focuses on forest microclimates, the reviewed methodologies are potentially applicable to one or more forest reserve characteristics of interest. For example, the mapping of tree canopy and tree height are specifically mentioned in the article's abstract. The second seed article, by Rodrigues et al. (2024), was chosen due to its focus on forest inventories, which often assess similar characteristics to those monitored in the forest reserves. The third seed article, by Goodbody et al. (2024), was selected based on its explicit focus on ALS data, as indicated in the article's title, suggesting that a significant portion of the article's references would be relevant to this thesis.

Conversely, the article by Khan et al. (2024) was not selected as seed article as it primarily addresses above-ground biomass estimation, which does not necessarily include any relevant forest reserve characteristics. Furthermore, the article's scope includes a broader application of remote sensing including satellite and aerial imagery. The article by Ocón et al. (2024) was not selected as it focussed primarily on urban forests which are distinct from forest reserves. Consequently, the article's references were considered unlikely to provide useful contributions to this thesis.

All references of the three selected seed articles were assessed for their relevance against the selection criteria. In this process, 248 unique articles were assessed, of which 82 matched all selection criteria and subsequently examined further for methodologies. A complete overview of assessed articles during the snowballing procedure can be found in the digital appendix accompanying this thesis, introduced in Section 2.4.

Following the snowballing process, the set of 82 articles was narrowed down to eight through the application of the additional selection criteria. A total of 37 articles were rejected because they did not clearly describe a methodology, 11 were rejected because they could not be applied to (only) AHN data, and a further 26 were rejected for failing on both criteria. A detailed overview of this second round of assessment is also available in the digital appendix. Table 5 presents the eight selected articles, including their authors and the specific forest reserve characteristics for which their methodologies are applicable.

The found methodologies cover six of the 14 outlined forest reserve characteristics. In particular, the forest reserve characteristics related to trees are well represented: Tree presence, position, crown projection, DBH, vitality (snag detection) and height can be approached with the found methodologies. Plant species distribution, cover percentage of plants, shrub presence, tree crown characteristics, tree decomposition stage, tree damage, tree and shrub seedling identification are not covered with the found methodologies.

Table 5: Overview of literature review results after snowballing procedure

Article	Title	Applicable to forest characteristics
Sparks et al. (2022)	"Cross-Comparison of Individual Tree Detection Methods Using Low and High Pulse Density Airborne Laser Scanning Data"	Tree presence and location (ITD), tree height
Puliti et al. (2019)	"A comparison of UAV laser scanning, photogrammetry and airborne laser scanning for precision inventory of small-forest properties"	Tree height, tree DBH (basal area)
Pearse et al. (2018)	"Comparison of models describing forest inventory attributes using standard and voxel-based lidar predictors across a range of pulse densities"	Tree height, tree DBH (basal area)
Gril et al. (2023)	"Using airborne LiDAR to map forest microclimate temperature buffering or amplification"	Tree height
Kissling et al. (2022)	"Laserfarm – A high-throughput workflow for generating geospatial data products of ecosystem structure from airborne laser scanning point clouds"	Tree height, tree crown projection
Bazezew et al. (2018)	"Integrating Airborne LiDAR and Terrestrial Laser Scanner forest parameters for accurate above-ground biomass/carbon estimation in Ayer Hitam tropical forest, Malaysia"	Tree crown projection
Wing et al. (2015)	"Individual snag detection using neighbourhood attribute filtered airborne lidar data"	Standing dead tree (snag) detection
Joyce et al. (2018)	"Detection of coarse woody debris using airborne light detection and ranging (LiDAR)"	Lying dead tree detection

3.2 Feasibility assessment of found methodologies

3.2.1 Overview of selected methodologies

As certain forest characteristics could be derived using multiple methods described in various publications, the most promising approach for each was selected for further feasibility assessment. For tree presence and location, commonly referred to as Individual Tree Detection (ITD), the study by Sparks et al. (2022) was the only relevant source identified and was therefore adopted. The study evaluated a wide range of methods, and as such the approach with the highest accuracy metrics was selected. Specifically, this was a Canopy Height Model (CHM)-based method employing a Local Maximum Filter (LMF).

For tree height estimation, several methodologies were considered. The model proposed by Sparks et al. (2022) was selected due to its superior reported accuracy metrics, which generally outperformed those reported by Puliti et al. (2019), Pearse et al. (2018), Gril et al. (2023), and Kissling et al. (2022). Specifically, an r^2 of 0.99 and a root mean square error (RMSE) of 0.97m were achieved. In comparison, Puliti et al. (2019) reported an r^2 of 0.64 and RMSE of 0.91m, while Pearse et al. (2018) obtained an r^2 of 0.76 and RMSE of 6.4%. Gril et al. (2023) did not provide specific accuracy figures, as tree height was calculated as an intermediate step in a broader methodology. The study by Kissling et al. (2022) employed a considerably coarser spatial resolution (10m raster) as part of a broader Python-based workflow, and was therefore not selected due to its likely lower precision.

Tree crown projection was assessed using the methodology of Bazezew et al. (2018), which reported a segmentation accuracy of 73% and a detection accuracy of 57%. Although Kissling et al. (2022) also addressed this topic, no comparable accuracy metrics were provided, and their method was therefore not considered further.

For dead tree detection, the study by Wing et al. (2015) was preferred over Joyce et al. (2018). The latter did not employ an automated approach and relied on manual inspection of point clouds against field data, achieving 23% accuracy. By contrast, Wing et al. (2015) reported detection rates ranging from 43% to 100%, depending on the DBH, with an overall detection rate of 56% for snags with a DBH \geq 25cm.

The methods presented by Pearse et al. (2018) and Puliti et al. (2019) both show promising results for estimating tree diameter at breast height (DBH) through the calculation of plot basal area, with reported r^2 values of 0.67 and 0.33 respectively, and normalised RMSE (NRMSE) values of 19.6% and 9.67%. However, both methodologies require the development of models trained on field-collected data, which falls outside the scope of this thesis. Consequently, these methods were considered unfeasible within the context of this research.

3.2.2 Individual Tree Detection and height estimation through Canopy Height Model-based Local Maximum Filter

The results for ITD and height estimation using the methodology of Sparks et al. (2022) indicate feasibility for application to AHN data. Computationally, the functions required an average of 2.43 seconds per sample plot, suggesting the method is scalable for broader use in SRO3. Visual assessment was conducted using a 3D point cloud viewer for each sample plot. Detected treetops were visualised in three-dimensional space and buffered with a one-metre radius to account for wind sway. Treetops were plotted at both the top and bottom of the Z-axis, enabling a comparison between detected treetops and tree stems. To facilitate this, ground points were removed from the point cloud during the visualisation procedure. Figure 6 presents selected visualisations of representative reserves from top and bottom perspectives, with the remaining visualisations available in Appendix III.

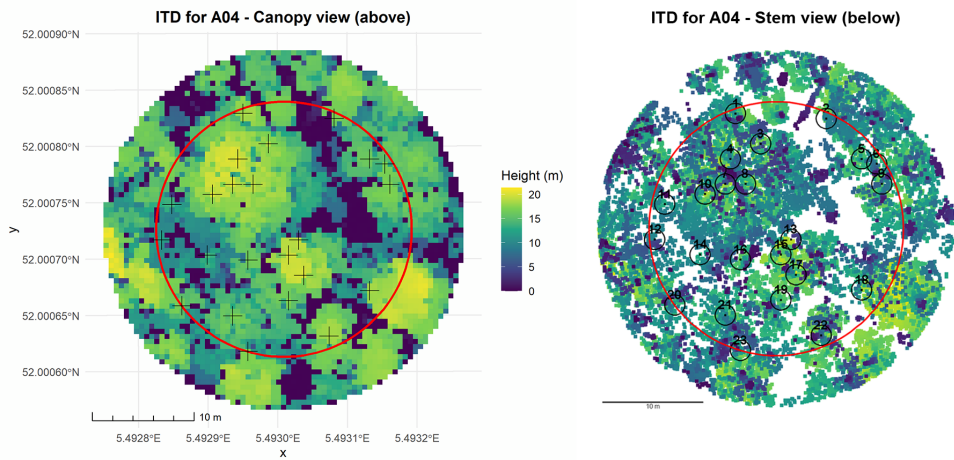
The visual assessment revealed some limitations in mixed and deciduous forests, with performance lowest in the latter. This is evident from Figure 6a and Figure 6b, where the identified treetops infrequently align with the tree stems. Detection in coniferous forests, however, was most accurate and shows strong potential, as is evident in Figure 6c where the majority of identified treetops align with tree stems. Table 6 provides the corresponding confusion matrix for individual tree detection, where the number of true positives (TP) refers to visually confirmed tree stems located within a one-metre radius of the modelled tree tops. The number of false positives (FP) refers to a modelled tree location being further than one-metre away from a visually identifiable tree. Finally, the number of false negatives (FN) refers to visually identified treetops that failed to be detected by the model.

Table 6: Confusion matrix constructed based on visual assessment of individual tree detection

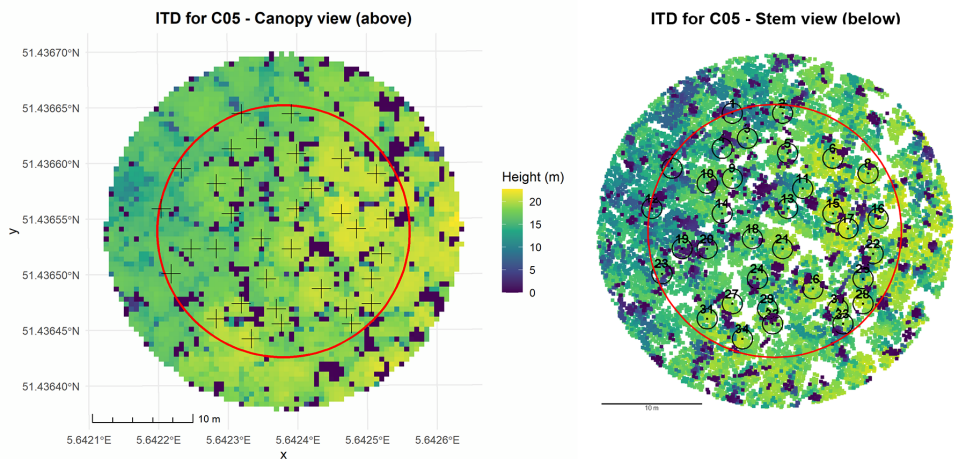
	True positives (TP)	False positives (FP)	False negatives (FN)
RSV 3: Mixed forest	43	32	4
RSV 16: Deciduous forest	48	48	9
RSV 19: Coniferous forest	41	21	5

Estimated tree heights based on the tree top detection fell within the ranges of 15–22m for mixed, 15–23m for deciduous, and 19–36m for coniferous plots.

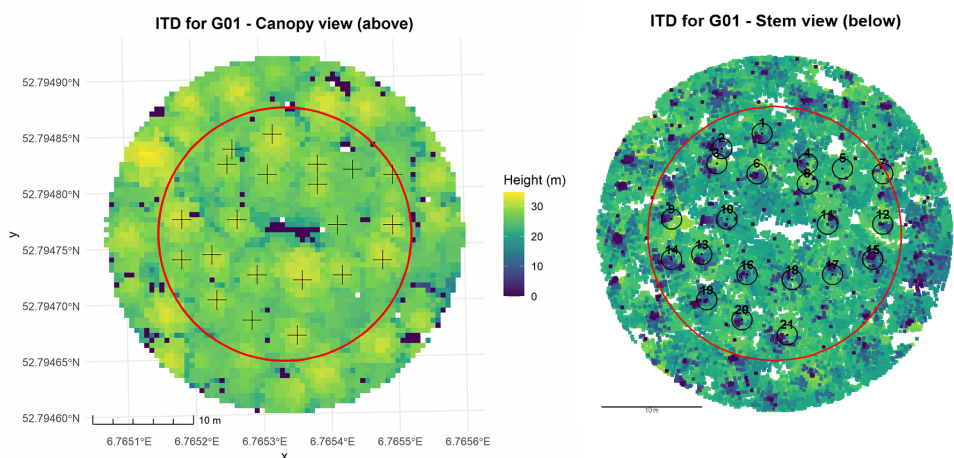
Given the strong performance in coniferous forests and the potential parameter optimisation, the method is considered feasible for application to AHN data. The computational limit of 200 seconds was not reached during Individual Tree Detection.



(a) Comparison between top and bottom view after ITD for sample plot A04 in forest reserve Galgenberg (RSV 3)



(b) Comparison between top and bottom view after ITD for sample plot C05 in forest reserve Sang (RSV 16)



(c) Comparison between top and bottom view after ITD for sample plot G01 in forest reserve Oosteresch (RSV 19)

Figure 6: Comparison between canopy- and stem-down views after ITD for a selection of representative sample plots.

3.2.3 Tree crown projection estimation through Multicore Watershed Segmentation and 3D Point Cloud segmentation

Open-source alternatives to the multiresolution CHM segmentation described by Bazezew et al. (2018) were identified in the form of a Multicore Watershed Segmentation (MCWS) algorithm applied to a pit-free CHM, and a 3D Point Cloud Segmentation (3DPCS) algorithm as presented by Li et al. (2012). Of these, the 3DPCS method was considered feasible for application to AHN data. The function implementing the 3DPCS algorithm required an average of 2.66 seconds per sample plot, indicating its potential scalability for broader use in SRO3. A visual assessment of the results produced by both the MCWS and 3DPCS algorithms was conducted using a 3D point cloud viewer. The point cloud for each sample plot was visualised alongside a 2D overlay of the identified tree crown shapefiles, allowing 3D manipulation of the scene with crown boundaries clearly superimposed. Selected 2D representations of this visualisation are shown in Figure 7, with the full set available in Appendix IV.

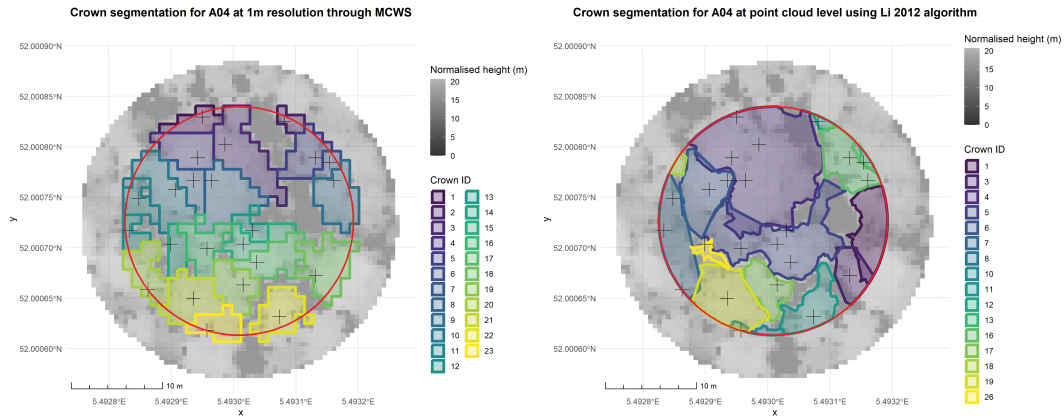
Based on the visual assessment, a confusion matrix was constructed for the representative reserves, shown in Table 7. The table presents the number of correctly identified tree crowns (n_c) and incorrectly identified crowns (n_i) for both methods. Here, n_c refers to model-identified tree crowns matching a visually identified crown within a 2-metre tolerance. In contrast, n_i denotes crowns that were either incorrectly sized (i.e., a partial crown or one model-identified crown covering multiple visually identified ones) or positioned where no crown was visually observed. Finally, n_r denotes the number of crowns that were visually identified as a reference.

Table 7: Confusion matrix constructed based on visual assessment of tree crown projection

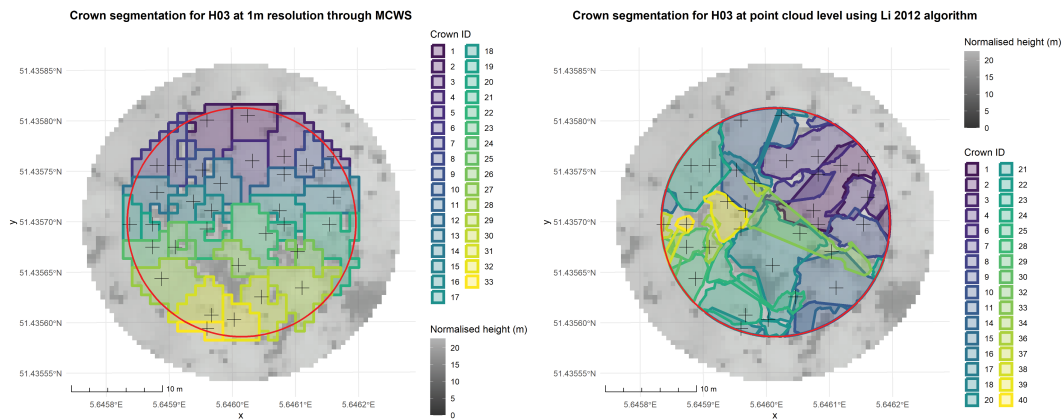
	MCWS		Li et al., 2012		Reference (n_r)
	Correct (n_c)	Incorrect (n_i)	Correct (n_c)	Incorrect (n_i)	
RSV 3: Mixed	34	39	37	17	47
RSV 16: Deciduous	39	56	46	21	64
RSV 19: Coniferous	31	29	47	16	62

The results presented in Table 7 indicate that the 3DPCS model consistently outperforms the MCWS model across all forest types. The MCWS model generally produces a higher number of incorrect identifications (n_i) than correct ones (n_c), which is largely attributable to its tendency to identify multiple partial crowns in place of one complete crown, as illustrated in Figure 7a. This limitation is directly linked to the quality of the initial individual tree detection (ITD), since the MCWS model attempts to delineate a crown for each tree identified in the ITD step. Consequently, errors introduced during ITD propagate through to crown segmentation. By contrast, the 3DPCS model performs its own ITD based on the point cloud and derives crown metrics independently. Although this approach resulted in fewer errors, some overfilling of the canopy with crown shapes was observed, as shown in Figure 7b.

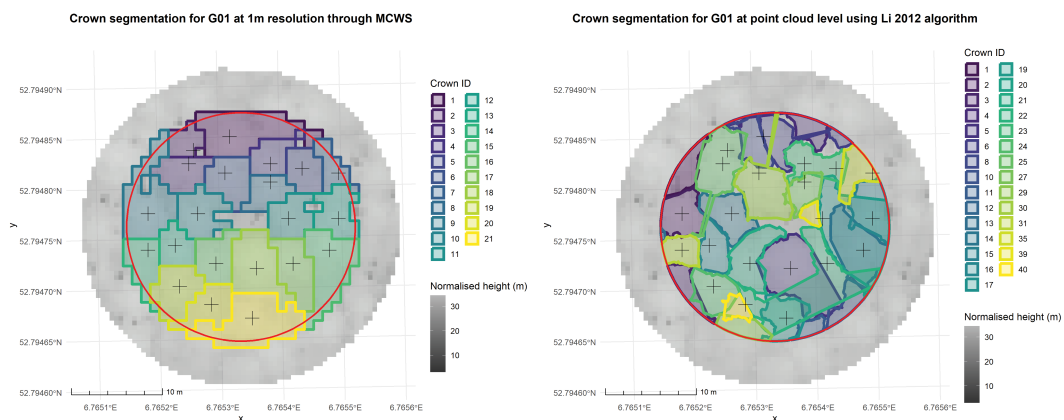
Given the relatively strong performance of the 3DPCS model across all three forest types, it is considered a feasible method for application to AHN data. Additionally, the model's computational demand remained within the 200-second time limit throughout all tests. However, as there is no recent fieldwork data to compare it against, it cannot be considered feasible for SRO3, and as such will be further analysed as an unfeasible method.



(a) Comparison between the MCWS and Li 2012 methods for tree crown projection estimation in sample plot A04 in forest reserve *Galgenberg* (RSV 3)



(b) Comparison between the MCWS and Li 2012 methods for tree crown projection estimation in sample plot H03 in forest reserve *Sang* (RSV 16)



(c) Comparison between the MCWS and Li 2012 methods for tree crown projection estimation in sample plot G01 in forest reserve *Oosteresch* (RSV 19)

Figure 7: Comparison between the MCWS and Li 2012 methods for tree crown projection estimation in a selection of representative sample plots.

3.2.4 Standing dead tree (snag) detection through neighbourhood attribute filtering

The results of the snag detection model developed by Wing et al. (2015) were found to be unsuitable for application to AHN data within the scope of this study. A confusion matrix was not constructed, as the method classified over 90% of all overstory points as belonging to a snag. While the specific snag classes (i.e., general, small, live crown edge, or high canopy cover) varied between ‘general’ and ‘small’, on average some 90 to 95 percent of the points within the representative sample plot point clouds were identified as snags — an outcome that is unrealistic.

Efforts to fine-tune the model, particularly by adjusting the BBPR matrix, did not lead to improved performance. Although the method was computationally efficient, with an average processing time of 0.46 seconds per sample plot, its classification results were overwhelmingly inaccurate. Therefore, this approach was deemed unsuitable for further application in SRO3.

3.3 Analysis of feasible method

Following the results from SRO2, the only method found feasible for comparison against field-work data was the ITD and tree-height method proposed by Sparks et al. (2022). Among the sample plots for which field observation data were acquired, the number of coniferous (P_{con}), deciduous (P_{dec}), and mixed (P_{mix}) plots were 5, 42, and 50, respectively.

Figure 8 presents the comparison of distributions between the number of trees observed in the field and the number of trees estimated by the ITD methodology per forest type. Overall, the ITD approach underperformed when compared to field-observed tree counts. In coniferous and mixed forests, the ITD algorithm saw a high omission error rate when compared to the field observations, whereas in deciduous forests it over-detected them.

Distribution of field-observed and ITD-derived tree counts per forest type

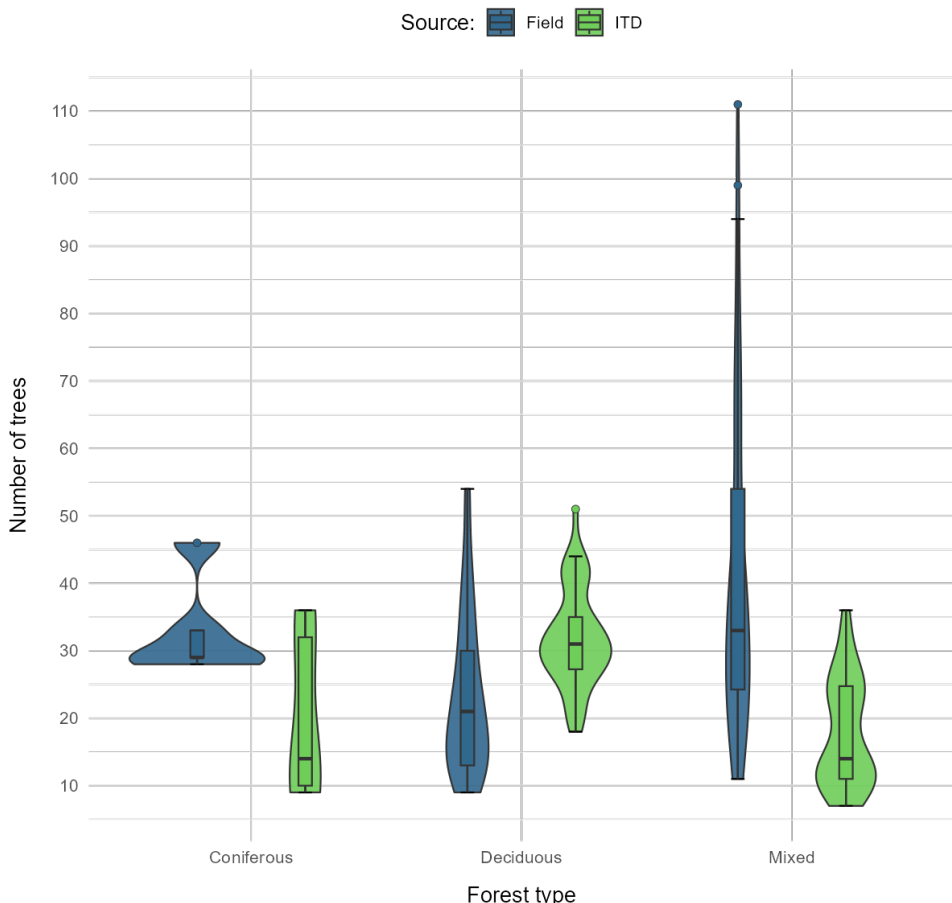


Figure 8: Distribution of the number of trees identified in field and through ITD.

Using Wilcoxon's signed-rank test, a statistically significant difference between the field-observed and ITD-derived number of trees was detected for deciduous ($p = 3.1 \times 10^{-10}$) and mixed ($p = 1.7 \times 10^{-10}$) forest types, but not for coniferous forests ($p = 0.06$), though this is likely a result of the low number of coniferous plots. Further analysis showed that only 20% of coniferous plots contained an ITD-derived tree count within a 5% margin of the field-observed count, while for deciduous and mixed plots these percentages were 7% and 0%, respectively. The Root Mean Squared Error (RMSE) and Normalised Root Mean Squared Error (NRMSE) for coniferous forests were 14.47 and 43.8%. For deciduous and mixed forests, these values were 13.50 and 57.9%, and 31.91 and 77.5%, respectively.

Figure 9 presents the comparison and distributions of the distances between field-observed trees and their closest ITD-derived tree. The boxplots indicate a relatively high number of outliers in deciduous and mixed forests. The violin plots illustrate the overall distribution of distances, generally showing a higher frequency around or below the 2 m mark. The mean distances for coniferous, deciduous, and mixed forests were 2.44 m, 1.96 m, and 2.51 m, respectively.

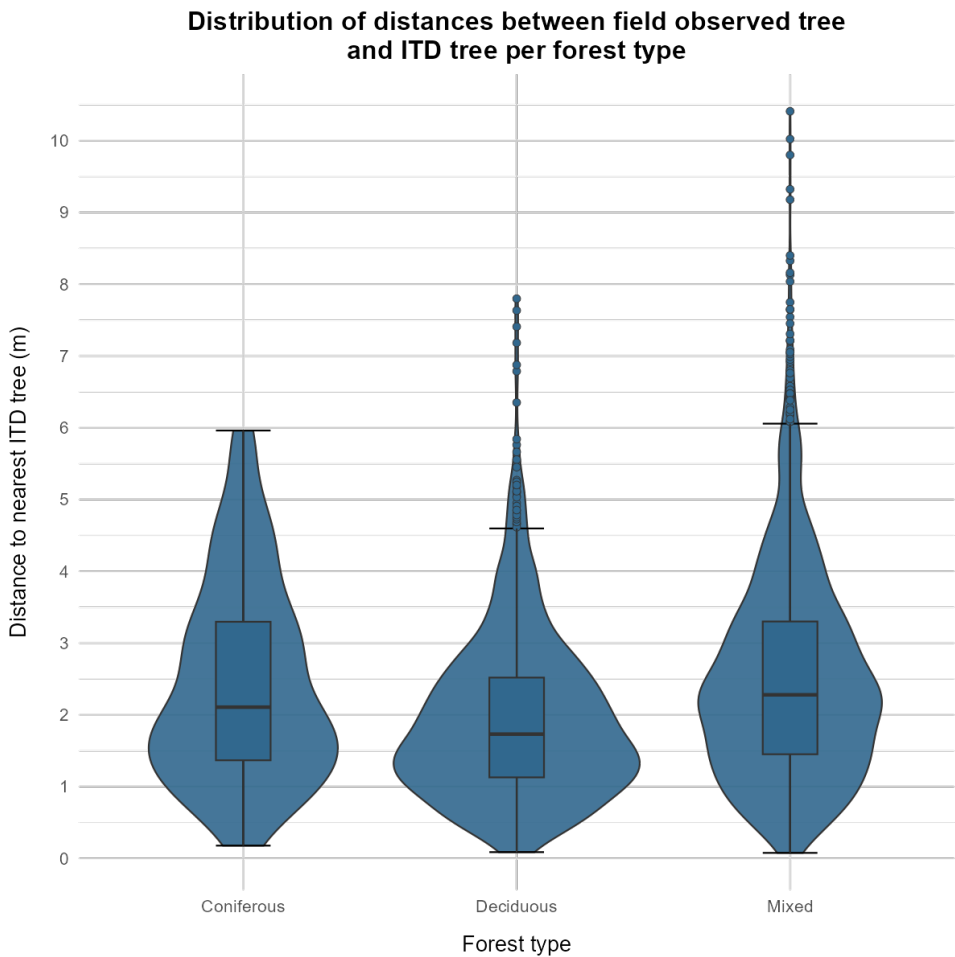


Figure 9: Comparison and distribution of the minimal distance between trees identified in the field and through ITD.

Of the total 3,203 field-observed trees across all plots, 491 (15.3%) had an ITD-derived tree within a 1 m radius. Deciduous forest plots showed a higher rate of ITD-derived trees within 1 m proximity, with 193 out of 980 trees (19.7%). Coniferous and mixed forests exhibited lower rates, with 20 out of 165 trees (12.1%) and 278 out of 2,058 trees (13.5%), respectively. However, proximity alone is insufficient to confirm a correct identification by the ITD algorithm, as the height difference between the field-observed and ITD-derived tree should also be within a reasonable margin to indicate they are likely describing the same tree. Given the challenges of accurately measuring tree heights from the ground in a forest environment (De Petris et al., 2022), a relatively wide margin of 3 m of potential error in the field observations was applied. In total, 248 field-observed trees had an ITD-derived tree within a radius of 1 m whose height fell within the

assumed height error margin of ± 3 m. This corresponds to an overall detection accuracy of 6.8%. Trees in coniferous and deciduous plots showed higher detection accuracies of 7.3% and 9.1% respectively, whereas mixed plots reduced the overall accuracy, with only 5.7% of trees detected.

Noticeably, a relatively large number of field-observed trees exhibited substantial height differences compared to their closest ITD-derived tree. Of the 491 field-observed trees with an ITD-derived tree within a 1 m radius, 139 had a height difference greater than 10 m, with extremes reaching up to 140 m. Extremes were identified as errors in the fieldwork data collection sheet, as in the case of tree numbers 11 and 18 in sample plot C11 in forest reserve *Norgerholt* (RSV 46), where the tree heights were recorded as 152 m and 165 m. These are likely data-entry errors, and more realistic values would be 15.2 m and 16.5 m, respectively. Furthermore, closer inspection of the data revealed that field-observed trees with height differences exceeding 10 m relative to nearby ITD points were frequently noted as dead standing trees in the fieldwork forms.

Figure 10 shows the distribution of average tree heights per forest type, with averages calculated at the plot level. The figure highlights that, in general, the ITD method tends to identify (whether correctly or not) taller trees, whereas field observations tend to record lower tree heights. This difference is particularly evident in coniferous and mixed forests. However, Wilcoxon's signed-rank test did not indicate statistical significance for coniferous forests ($p = 0.13$), whereas significant differences were found for deciduous ($p = 7.9 \times 10^{-10}$) and mixed forests ($p = 7.8 \times 10^{-10}$).

Distribution of field vs ITD average tree height per plot by forest type

n = total number of trees

Source: Field (blue) ITD (green)

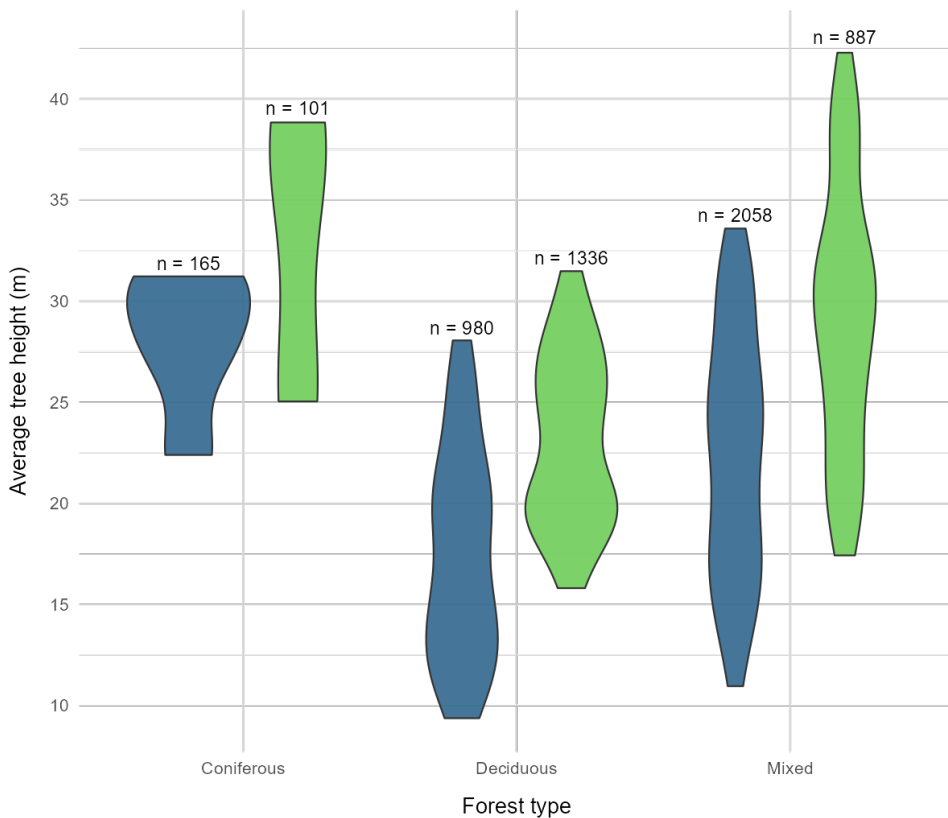


Figure 10: Distribution of average tree heights in plots across forest types.

3.4 Analysis of unfeasible methodologies

3.4.1 Tree crown projection estimation

As crown projection measurements were not performed during the recent fieldwork, no up-to-date data are available to directly compare the 3DPCS model with field observations. Nevertheless, further analysis of the method is warranted due to visible artefacts, as shown in Figure 18c and Figure 19b in Appendix IV, where certain crowns exhibit unexpected shapes with linear outcroppings.

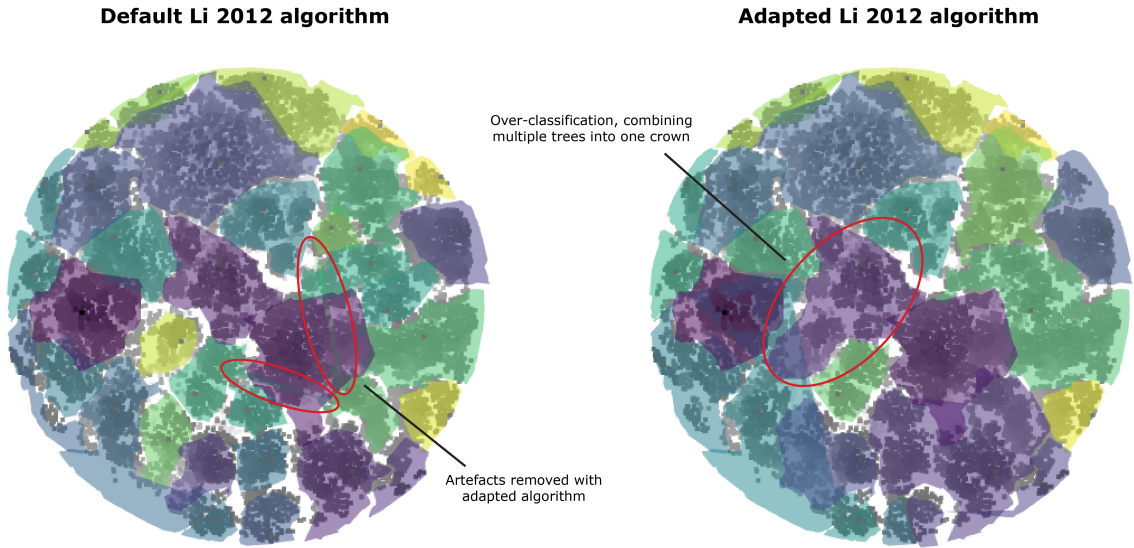
As the model is run on buffered point clouds with a radius of 17.6 m and subsequently clipped to the actual sample plot radius of 12.6 m, edge effects in the point cloud analysis can be ruled out as a likely cause of the artefacts. Table 8 presents the visually confirmed results from the comparison between the default 3DPCS algorithm by Li et al. (2012) and the adapted algorithm resulting from parameter testing.

No direct cause for the artefacts observed in the original algorithm could be visually identified. No strong relationship with any of the tested parameters was evident, although some parameter combinations reduced the number of artefacts while increasing the degree of over-classification. Furthermore, no relationship between point height and the occurrence of artefacts could be visually determined.

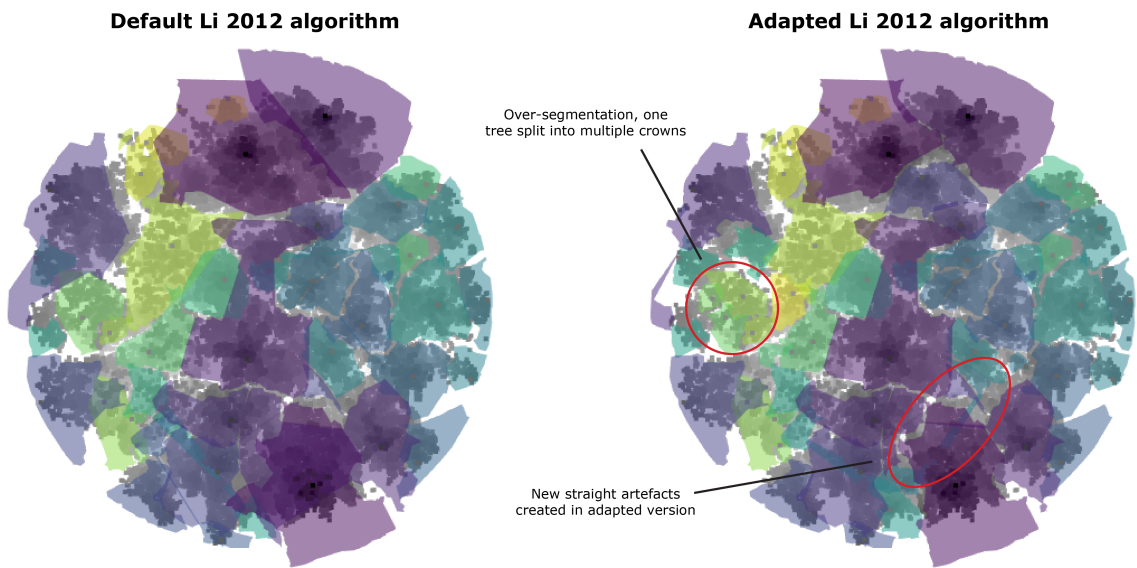
Table 8: Results of visual comparison of different parameter combinations in the Li 2012 algorithm against the default parameters.

$dt1$	$dt2$	Z_u	h_{min}	Visual results
1.5	2.00	15	4	No notable differences
1.5	2.00	10	2	No notable differences
1.5	2.00	20	2	No notable differences
1.5	2.00	30	2	No notable differences
1.5	3.00	15	2	Over-classification
2.0	3.00	15	2	Over-classification
1.0	2.00	15	2	No notable differences
1.0	1.50	15	2	Over-segmentation
1.5	1.75	25	2	Minimal over-segmentation
1.6	1.85	20	5	Minimal over-segmentation
1.7	2.00	20	4	No notable differences

For the majority of parameter combinations tested, no notable improvements were observed during visual inspection. Parameter sets that tended to cause over-classification ($dt1 = 1.5$, $dt2 = 3$, $Z_u = 15$, $h_{min} = 2$) also reduced the number of artefacts, as shown in Figure 11a. In contrast, parameter sets leading to over-segmentation of the point cloud ($dt1 = 1.5$, $dt2 = 1.75$, $Z_u = 25$, $h_{min} = 2$) generally resulted in the formation of additional artefacts, a typical example of which is presented in Figure 11b.



(a) Comparison of default and adapted Li 2012 algorithm for sample plot S09 in forest reserve *Galgenberg* (RSV 3)



(b) Comparison of default and adapted Li 2012 algorithm for sample plot J05 in forest reserve *Oosteresch* (RSV 19)

Figure 11: Comparison of default and adapted Li 2012 algorithm for artefact reduction

3.4.2 Standing dead tree (snag) detection

The examination of the point cloud characteristics revealed several differences between the data used in the study by Wing et al. (2015) and the AHN4 data. The study's data were acquired using a Leica ALS50 Phase II laser system, whereas the exact system used for AHN4 is not publicly disclosed, other than being a system developed by RIEGL. One notable difference is that the Leica system stored intensity values as 8-bit data (Geosystems, 2014), whereas the RIEGL system used for AHN4 employed 16-bit storage (GmbH, 2017), although this was addressed through min–max normalisation. Similarly, the flight altitude during AHN4 data acquisition is not publicly known and thus cannot be compared with the 900 m altitude reported in the original study.

In the original study, the sensor scan angle during acquisition was fixed at $\pm 14^\circ$ from nadir, whereas inspection of the AHN4 point clouds for representative sample sites showed that the scan angle varied both between and within reserves. For forest reserve *Galgenberg* (RSV 3), the scan angle ranged from 19° to 25° within sample plot A04, but from -9° to -11° within sample plot S09. Similar variability was observed

in other plots in reserves *Sang* (RSV 16) and *Oosteresch* (RSV 19). Across all sample plots, scan angles ranged from $\pm 5^\circ$ to $\pm 25^\circ$ from nadir.

Further differences were observed in the proportion of single and multiple returns. The original study reported a high proportion of single returns (81.4% and 78.2% in the two study sites), whereas the representative AHN4 samples had only 15.4% single-return points across nine plots. Consequently, AHN4 had a much higher proportion of multiple returns (84.6%), compared with the 9.2% and 10.1% reported in the study. Interestingly, the percentages reported in the original study do not sum to 100%, leaving some ambiguity in the exact distribution. In addition, the original study reported an average point-cloud density of 6.8 points m^{-2} (standard deviation 5.8 points m^{-2}), whereas the representative AHN4 sites had a substantially higher average density of 42.8 points m^{-2} (standard deviation 10.2 points m^{-2}).

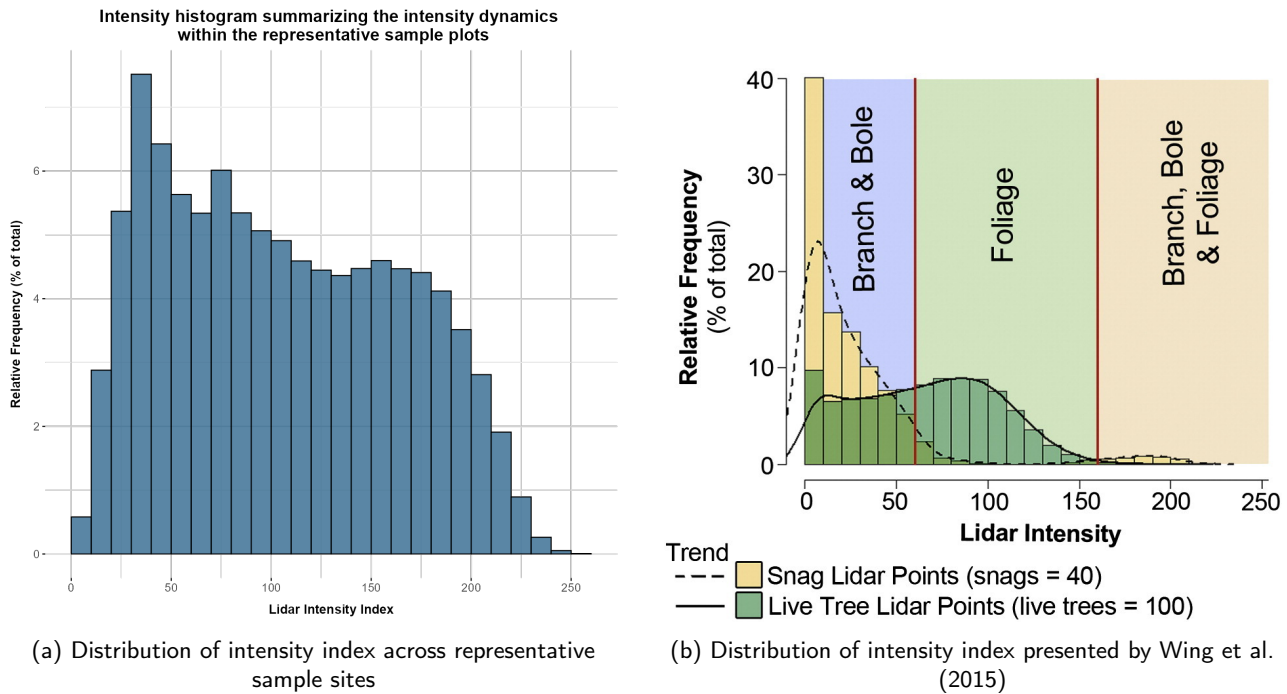


Figure 12: Comparison of distributions of intensity index between representative sample sites and the article presented by Wing et al. (2015)

Figure 12 shows a notable difference between the distributions of intensity indices in the original study and in the AHN4 data for the representative sample sites. Although the relative frequencies cannot be compared directly, as Wing et al. (2015) present two histograms in a single figure and do not provide the number of points used to derive the histogram, differences in the distribution of the intensity index are evident. In particular, the low (<20) and high (>150) intensity index values differ substantially between the study and the AHN4 data. The distribution shown in the study (Fig. 12b) decreases more rapidly, with most points having an intensity value of 150 or less, whereas in the AHN4 data (Fig. 12a) these high-intensity values account for approximately 34% of all points. Conversely, points with lower intensity values are more prevalent in the study's data, as indicated by the peaks in the 0–10 bin range. By contrast, the AHN4 data peak at an intensity value of around 40. This general trend does not appear to be dependent on the forest type, as examining the intensity index distributions for the individual forest types shows similar distributions (Appendix V). Notably, all individual forest types peak in the same intensity, around 40, and all see a relatively low frequency in the lower intensity range of <40 .

Following this observation, results for plot A04 in forest reserve *Galgenberg* (RSV 3) revealed an interesting pattern. While intensity index values below 20 did not display a clear trend, values above 150 were predominantly associated with ground points. The same pattern was observed when plotting all representative sample point clouds. Indeed, when applying min–max normalisation to determine the intensity index after filtering the point cloud to exclude ground points, the resulting distribution more closely resembled that

reported by Wing et al. (2015), at least in the higher intensity range, as shown in Figure 13. Nevertheless, a visible difference remained in the lower intensity range, with the ground-filtered intensity distribution showing a noticeably lower frequency of values between 0–10 compared with the distribution reported in the study.

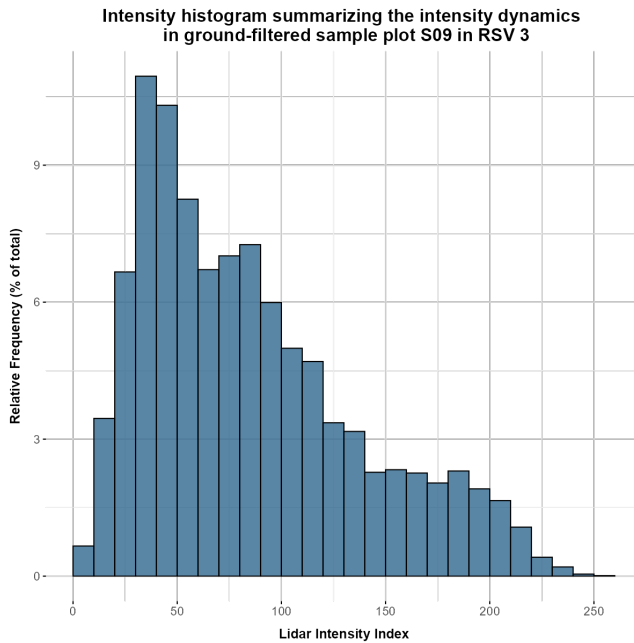


Figure 13: Distribution of intensity index in ground-class filtered sample plot S09 in forest reserve *Galgenberg* (RSV 3)

Despite the change in intensity distribution, the model continued to over-classify points as snags, with an average of 85.1% of all non-ground points in the representative samples being classified as snags. This remains an unrealistic overestimation, effectively classifying the vast majority of all trees within a sample plot as snags. Notably, the percentage was slightly higher in plots from forest reserve *Oosteresch* (RSV 19), where the average across the three plots reached 93.0%.

Following point cloud decimation, the average point density of the representative sample plots was 7.1 points m^{-2} , with a standard deviation of 0.1 points m^{-2} , closely resembling the density as outlined in the study by Wing et al. (2015). The distributions of intensity indices in the ground-filtered, decimated point clouds did not differ significantly from those in the ground-filtered clouds prior to decimation. Consequently, this adaptation did not mitigate the over-classification. In fact, relative over-classification appeared to increase compared to the intact point clouds, with the proportion of points classified as snags rising to an average of 89.7%. Again, the plots in RSV 19 showed a slightly higher rate of over-classification, at 95.5%.

4 Discussion

4.1 From literature to methodologies

The results of the brief literature review undertaken for SRO1 highlight that there is a substantial body of knowledge on remote sensing applications in forestry. The initial search query for seed articles, targeted specifically at review papers, yielded well over 100 results. From just three seed articles, more than 240 unique references were identified within one snowballing iteration, covering applications of remote sensing, case studies, or new methodologies. These papers considered a wide range of locations, forest types, tree species, and sensors for their optimal use, and this brief review only touches upon the vast literature available. In short, there is an extremely large body of knowledge to draw upon. Whilst generally advantageous, such volumes of information can also be contradictory, and the knowledge fragmented.

Arguably, this thesis attempted too broad a scope, as a comprehensive literature review could itself form an entire thesis. By limiting the scope of the literature review in SRO1, certain important sources of information may have been overlooked. For example, the method presented by Li et al. (2012), although close to the lower boundary of the imposed time cut-off, is a highly cited article with an average of 94 citations per year in recent years (2020–2025). In 2025 alone, the method was applied in studies of mangrove forests (Duan et al., 2025), urban areas (Siljander et al., 2025), pine forests (Yu et al., 2025), and savannah (Muumbi et al., 2025), among others. One could argue that the time cut-off should not have been applied, and instead greater emphasis should have been placed on selecting articles more relevant to the forest types found in the Netherlands. For instance, the review by Goodbody et al. (2024) yielded several useful references, but these were primarily focussed on boreal forests, as the review itself centred on Canada, where such forests predominate. As such, it is recommended that future approaches disregard the age criterion applied in this thesis, as older methodologies may still hold relevance today.

In addition, the exclusive use of reverse snowballing may have resulted in the omission of newly developed methodologies. Although the selected seed articles were relatively recent (all published in 2024), any methodologies introduced subsequently fell outside the scope of this review. A potential solution would have been to apply a single iteration of both forward and reverse snowballing. This approach is therefore recommended for future studies adopting a similar methodology to that presented in this thesis.

Despite these shortcomings, the literature review produced results of interest and demonstrated that methods exist which could, in principle, be applied to AHN data, though their practical utility within the forest reserve monitoring programme may vary, as discussed further in this chapter. It should also be noted that, although many methods are described in the literature, translating these written methodologies into tangible, applicable workflows can be highly time-consuming. Several articles considered in this thesis provided vague methodological details, omitting crucial information about input data—an issue particularly evident in the methodology of Wing et al. (2015). This hinders knowledge transfer, especially when no online appendices or scripts are provided, and makes it difficult to assess the reliability of results, since poor outcomes could reflect either methodological weaknesses or errors in translation from article to implementation. The other methods examined in this thesis were simpler and therefore allowed a more straightforward transition from published description to applied scripts.

4.2 AHN for Individual Tree Detection

The ITD model proposed by Sparks et al. (2022) showed promising results in the original article's results, but during SRO2 and SRO3 it became clear that results were less accurate when applied to AHN4 data. Initial testing of the methodology in SRO2, utilising a Fixed Window Size approach, yielded promising results in coniferous forests, but performed poorly in mixed and deciduous forests. While generally yielding good results at detecting tree tops, this does not reliably correspond to the stem location.

The original study focusses mainly on coniferous forest stands, generally known for having trees with roughly conical crown shapes, wherein a fixed moving window has been shown to produce good ITD results, though

this is often in combination with a smoothing window (Douss & Farah, 2022; Lisiewicz et al., 2022; Mohan et al., 2017). This is reflected in the results of SRO2, where accuracy in coniferous plots exceeded that in mixed and deciduous plots. However, when studying the results of SRO3, in which a Variable Window Size was approached, this trend was not observed. While trees in coniferous forest plots still see a higher detection accuracy than mixed plots, they had lower accuracies compared to deciduous plots.

Studying Figure 8 and Figure 10, an interesting dynamic between the number of detected trees per forest plot and the average height of trees within the forest plot is visible. In both coniferous and mixed forests, the number of trees detected using the model is substantially lower than the number of trees identified in the field, whereas the average height of those trees is substantially higher. This suggests that a large proportion of younger, smaller trees were not being detected by the ITD algorithm. When considering the method by Sparks et al. (2022) conceptually, this makes logical sense, as the AHN4 point clouds are in fact only considered for their top layer. By reducing the 3D information into a 2D plane in the form of a CHM, younger and smaller trees are absent. Indeed, it is observed that the method is suitable for the detection of treetops of the tallest trees within a plot. This too, is noted by Sparks et al. (2022), as they state that "For applications where dominant trees are the focus, it could be argued that the selection of a specific ITD method is somewhat arbitrary", and they further note that "future benchmarking studies for ITD methods should consider more diverse methods such as bottom-up approaches that detect more subdominant trees". In general, it has been noted that taller trees are easier to identify and their locations to be determined accurately (Gebreslasie et al., 2011; Kaartinen et al., 2012).

Interestingly, the article by Sparks et al. (2022) also considers the 3DPCS algorithm by Li et al. (2012), used in this thesis for crown segmentation, in their comparison of ITD methodologies. Sparks et al. (2022) report an underperformance of the 3DPCS approach compared to the CHM-based approach, whereas during the limited visual assessments of the 3DPCS algorithm in action during the crown segmentation, the segmentation of trees appeared to perform adequately. A further exploration of a point-cloud based approach could prove beneficial.

A potential shortcoming in the used approach for ITD, as briefly mentioned before, is the CHM. Indeed, flattening the 3D data into 2D means information is lost when creating a CHM, but this information-loss can be mitigated by implementing pit-free CHMs, which creates multiple CHMs at different height intervals (Khosravipour et al., 2014). This approach was also part of the crown-segmentation method by Bazezew et al. (2018), and has shown improved results in crown-segmentation and ITD over the so-called 'raw' CHMs in multiple articles (Erfanifard et al., 2018; Pucino et al., 2025; Zhou et al., 2024).

In the context of this study, more attention to the forest type could have been paid. The vast majority of Dutch forest reserves is mixed or deciduous forest, and as such forest-type specific methods should be prioritised. Despite an attempt to develop the Sparks et al. (2022) method into a broader-applied method through the move from a Fixed Window Size to a Variable Window Size approach, a potential weakness is found in the determined relationships between tree height and canopy. The derived linear equations are a rough estimation, but greater effort could be devoted to exploring more accurate relationships between these two parameters, as further research suggests that this relationship is generally better described using quadratic models (Asigbaase et al., 2023; Chen et al., 2006; Popescu et al., 2002).

Despite this room for improvement, the application of this method on AHN data for ITD currently seems unsuitable in the forest reserve network context. The results obtained are far removed from an accurate method, and are well below the results reported by Sparks et al. (2022). Other articles utilising ALS data for individual tree detection similarly yielded better results than obtained in this thesis (Jarron et al., 2020; Wang et al., 2016).

Some likely reasons this method has underperformed have already been mentioned, but a final likely factor is stand density and crown complexity. The Dutch forest reserves, having seen no human intervention for an extended period of time, likely have a higher stand density and forest complexity compared to managed

forests in which thinning is applied (Ashton & Kelty, 2018). Multiple sources report that the accuracy of ITD decreases in high-density forest stands, or in forest stands with high crown complexity (Falkowski et al., 2008; Vauhkonen et al., 2011; Wang et al., 2016). This relationship likely plays a role in the relatively poor ITD performance in this thesis.

Whilst deemed unsuitable for ITD, the method could play a valuable role in extracting the height of dominant trees in the forest reserves or in detecting canopy gaps. In the original study, a very high correlation between modelled and actual tree heights was reported, with an r^2 of 0.99. Although no direct comparison between modelled and field-observed tree heights was made, the identified values appeared realistic and often coincided with the highest point of the dominant trees. Conceptually, this method is well suited for this purpose, as the Local Maximum Filter approach consistently identifies the height of the highest raster cell or point-cloud point. This could serve as an additional data source to link CHM-derived heights to field-observed trees, improving tree height accuracy. Likewise, canopy gaps are conceptually relatively easy to detect using the CHMs generated in this process, as they appear as areas with significantly lower heights compared to surrounding pixels. This method has demonstrated strong accuracy in previous research by Bonnet et al. (2015) and could therefore be valuable for monitoring Dutch forest reserves, though a dedicated methodology assessment within these reserves would first be required.

4.3 AHN for tree crown segmentation

While the original crown segmentation model proposed by Bazezew et al. (2018) was adapted to an open-source application, the method utilising AHN data was found to have suitability within the forest reserve framework, depending on its use case. The MCWS algorithm did not perform well, due to its over-segmentation of tree crowns resulting from shortcomings in the ITD methodology. As the MCWS algorithm uses treetops identified by an ITD method as input, errors in the ITD propagate into the crown segmentation. This represents a potential drawback in the use of a MCWS approach to crown segmentation (Y. Liu et al., 2024).

Given the poor performance of ITD, and thus MCWS, a second algorithm was considered, namely a point-cloud based method developed by Li et al. (2012). This method, in contrast to MCWS, does not rely on previously determined treetops and instead performs its own tree segmentation, utilising information from the 3D point cloud. Results from SRO2 indicate that this method is promising, and generally performs well at identifying tree crowns, though some artefacts were observed. While the root cause of the artefacts could not be identified, the exploration highlighted the potential for parameter optimisation of the algorithm. Although not attempted in this thesis, future work could explore different parameter sets for each forest type, enabling the model to select the most suitable configuration and potentially yielding more accurate results.

The Li et al. (2012) algorithm provides a reasonable estimation of crown projections, and even identifies overlapping crowns. In the context of the forest reserve monitoring programme, this would likely be beneficial as an additional source of information for gap-detection analysis and the analysis of light penetration to undergrowth layers. For gap-detection analysis, some additional parameter optimisation might be beneficial, as the results showed that the algorithm occasionally over-estimated the size of certain crowns. Notably, the crown projections of trees are generally simplified during field work (Clerkx et al., 2002), and the more exact shapes of the crowns identified through this model could provide a valuable source of information. Despite being unable to concretely quantify the accuracy of the method due to unavailability of data, there is strong literature support for this method, with positive results shown in a range of contexts, although accuracy may be influenced by variables such as forest type and slope (Jing et al., 2012; Marcello et al., 2024).

To ensure the practical relevance of this method within the forest reserve monitoring programme, a comparison to field observation data should be made as soon as this data is available. Tree crowns identified utilising the algorithm could then be compared on location, area, geometry roundness and the goodness of matching (Clinton et al., 2010; Zhang, 1996), allowing a more robust conclusion.

4.4 AHN for snag detection

The snag detection algorithm outlined by Wing et al. (2015) is unsuitable for application to AHN data in the forest reserve context presented in this thesis. The results from SRO2 highlight an incompatibility with AHN data, leading to substantial over-classification of points, with more than 90% classified as snag points. A systematic exploration of the method, despite not leading to accuracy improvements, identified the most likely cause of the poor results.

The difference in point cloud density was excluded as a reason for poor performance, as point cloud decimation failed to improve results. Instead, a mismatch in intensity patterns between the AHN data and the data utilised in the original study was identified. The coniferous, deciduous, and mixed plots considered in this thesis showed similar intensity distributions to each other after min–max normalisation, but these distributions differed markedly from that reported by Wing et al. (2015). After filtering ground points to reduce the frequency of higher intensity values, results still did not improve. Fundamentally, the distribution of intensity values is misaligned with the original study, which undermines the method, as it is distribution-based.

The reasons behind the difference in distributions are likely multi-faceted. A first consideration is the difference in sensors and the lack of transparency regarding the sensor used for AHN4 data. Intensity values are affected by a range of variables, including the wavelength of the LiDAR pulse, the scan angle, and the reflectivity of the object struck (Wing et al., 2012; Wu et al., 2021). Inherently, this means that the range of intensity values depends not just on the sensor but also on the acquisition environment. An additional consideration is that min–max normalisation is sensitive to extremes in the data. This combination is a likely determinant of the different distributions. Further reasoning for the differences in AHN4 intensity data likely relates to acquisition dates. Wing et al. (2015) collected data during the leaf-on season in July, whereas AHN4 data was typically collected in the winter months during the leaf-off season. Furthermore, the study area in the original research had experienced a forest fire nine years prior to data collection. Differences in season, weather events, and soil type may also contribute to variation in intensity distributions, given the sensitivity of intensity to moisture presence (Garroway et al., 2011). Given the numerous variables influenced by the flight season, particularly those affecting intensity, it is logical that the results differed from those reported in the original study.

The above reasons show that, despite the positive results reported by Wing et al. (2015), the method is not applicable in the forest reserve context. This does not imply that the methodology has no value or is inherently flawed, as multiple studies report high accuracy values for snag detection when applying similar intensity-based approaches (Bright et al., 2013; Casas et al., 2016; Stitt et al., 2022), notably often in post-forest fire study areas. Regardless of these results, the method offers limited usability within the forest reserve network. Frequent changes to AHN sensors and the lack of transparency about these sensors would lead to unpredictable results. Moreover, intensity values may not even be provided in future AHN datasets, as the AHN6 acquisition is currently set to exclude intensity values.

4.5 Final discussion points

In general, the results highlight the complexities of applying established methods to new areas. It is unlikely that a method described in an article can be applied directly or without modification, and in the context of the forest monitoring programme, considerations must be made regarding the time and effort required to adapt methods to different forest types and environments.

In this thesis, the potential of remote sensing for forest reserve monitoring was assessed only briefly, with a marginal subset of the available methods. For example, there are numerous methods that use photogrammetry (Goodbody et al., 2019), or a combination of LiDAR and photogrammetry (Fassnacht et al., 2023). These approaches may be particularly relevant in the future as AHN6 data will combine LiDAR with aerial imagery to provide point clouds with RGB values. Furthermore, many methods based on machine learning or deep learning (Estrada et al., 2023; Hamedianfar et al., 2022) were not applied here, as they require well-trained models and high-quality training data.

Specifically in the context of the forest reserves, a key consideration must be addressed before focussing on future research. In this thesis, approaches were selected that were all based on detecting individual trees and estimating parameters of these trees. However, methodologies for area-based approaches are also available (Roussel et al., 2020), which allow more generalised information about the forest as a whole, rather than at the level of individual trees or sample plots. Given that the information acquired in the sample sites is used to draw conclusions about the forest reserves in their entirety, an area-based approach may be particularly well suited.

Now may be the time to consider the data acquisition pipeline as a whole, broadening the perspective to ensure that efficient methods are used at appropriate scales. ALS, which provides a top-down view of relatively large areas, may not be best suited for drawing conclusions regarding individual trees, particularly so in forest with high stand density or complexity, but it can provide valuable insights into overall forest structure, including biomass, basal area, and canopy organisation using area-based methods (Maltamo et al., 2014; White et al., 2016). During current data collection, it would also be beneficial to consider whether training machine- or deep-learning models with high-quality data is feasible, as this could enable partial automation of future analyses. Such applications are wide-ranging, from automated species detection (Zhong et al., 2024) to machine-learning-based basal-area models (S. Brown et al., 2022).

A further point of consideration, both in this thesis and for future research, concerns what is accepted as "truth". In this study, particularly in SRO3, data collected during field work was assumed to represent the true values and was used as the basis for accuracy metrics. It should not be overlooked that, as in any process involving humans, errors may occur; this was indeed the case during field work, as shown by the example of the 165 m tall tree recorded in SRO3. Field work is often complex, and while rigorous protocols generally minimise subjectivity, mistakes remain possible. This is especially important to bear in mind if models are developed or additional methods are assessed for suitability. Similarly, in SRO2, the quantitative analyses of methods relied on human interpretation of 3D point clouds, which inherently allows some subjectivity. Ideally, this qualitative analysis would be more tightly controlled through a robust protocol, a point worth considering for future studies.

Finally, relevant both to this thesis and to potential future research is the temporal variability in the collected field data. Field data were collected throughout the year, varying not only between reserves but sometimes also within the same reserve. For example, fieldwork in reserve *Leesten* (RSV 14) was conducted during September–November 2018 and again in August–September 2019. In contrast, *Pijpebrandje* (RSV 9) was surveyed in August–September 2018, whereas *Norgerholt* (RSV 46) saw field collections in May–June 2021. Within this thesis, this temporal variation may have introduced minor inconsistencies when comparing field data with AHN-derived metrics. Notably, *Pijpebrandje* and *Norgerholt* were surveyed during the leaf-on season, whereas AHN data are acquired during leaf-off conditions. *Leesten*, on the other hand, was surveyed during the transition between both periods. Despite these differences, errors in SRO3 are expected to be minimal, as only ITD locations were compared to field data. Although the presence or absence of leaves may affect tree height or crown shape marginally, the effects are likely negligible on the detection of treetops, as these are based on the local maxima. However, this factor should be carefully considered in future studies, particularly when validating crown segmentation results against field data. Seasonal differences in leaf cover may influence crown morphology and thus affect comparisons between modelled and field-observed crowns. Nevertheless, since field-recorded crown shapes are typically simplified to an ellipsoidal form, much of the fine structural detail is already lost, suggesting that any resulting error remains limited. These considerations can generally be regarded as moot in coniferous plots and forests, as coniferous species are predominantly evergreen and do not experience a leaf-off period. A notable exception to this is the genus *Larix* (larches), which are deciduous conifers and do occur within the Dutch forest reserves. Of greater importance is the partial lack of temporal overlap between the AHN data and the field observations. In this thesis, AHN4 was selected as it represented the highest-quality, nationwide dataset available with temporal overlap with the field data, though this overlap existed only for reserve *Norgerholt*. For the other two reserves, AHN3 would have provided better temporal alignment. This lack of temporal overlap may have introduced errors in SRO3, as trees may have fallen or grown (though this is less likely within the one- to two-year interval)

between data collections, potentially influencing ITD results. In hindsight, a more suitable approach might have been to combine different AHN versions depending on the timing of the field data collections, which should be considered in future research.

4.6 On future research

In this section, future research has been mentioned frequently. Before providing concrete recommendations in Section 6, this subsection summarises potential areas of research that warrant consideration, together with additional insights gained during the literature review.

Given the relatively poor results of the methods presented in this thesis and the identified underlying mechanisms, future research may be better directed towards area-based approaches. Retrieving parameters from individual trees using out-of-the-box models in combination with AHN data is inherently challenging due to the point density of the LiDAR cloud and the nature of leaf-off season data acquisition. Nonetheless, some exceptions have been demonstrated, particularly in tree height detection, crown segmentation, and potential gap detection. Furthermore, the training of specific models—whether machine learning or deep learning—may yield valuable insights at the tree level. Thus, individual tree-based approaches should not be dismissed entirely. Promising methods have already been discussed, but additional methods identified during the literature review could also be valuable for future exploration. In particular, a deep-learning based approach to ITD presented by Windrim and Bryson (2020) may lead to more reliable identification of individual trees, while the deep-learning based tree species detection method introduced by Marinelli et al. (2022) could greatly enhance the monitoring of forest reserves. If successful, such methods could theoretically integrate tree detection, species identification, height estimation, and canopy metrics. However, whether these methods perform reliably across varying environments remains an open question, as reported accuracies do not always translate to strong performance in practice, as demonstrated in this thesis. Alternatively, area-based methods may offer greater potential. Their relevance is not yet clearly established with respect to the currently monitored forest reserve characteristics, but observations from these characteristics could inform their application. For instance, if tree-related parameters are generalised at the plot level to estimate biomass volume, area-based methods such as those presented by Ayrey and Hayes (2018) or Kotivuori et al. (2016) may be appropriate.

Notably, the literature revealed a lack of research focused on the understory or lower vegetation layers. Existing studies, such as Korpela et al. (2012), have not produced encouraging results. This suggests that, among the currently monitored variables, those related to shrub and herbaceous vegetation are unlikely to be accurately derived using ALS data.

5 Conclusion

This thesis was aimed at supporting the Dutch national forest reserve programme through an exploration of the suitability of AHN data for the monitoring of different forest reserve characteristics. An initial, brief literature review revealed extensive knowledge of the application of remote sensing, including ALS, for diverse forestry applications. During the literature review, potential methodologies for six of the 14 currently monitored forest reserve characteristics were identified, though it is highly likely that an extended literature review would identify further methods for the remaining characteristics. Following this identification, a selection was made of methodologies for further assessment based on their reported accuracy metrics. From this selection, the method by Sparks et al. (2022) was selected for Individual Tree Detection (ITD) and associated tree height. The method by Bazezew et al. (2018) was identified for the estimation of tree crown projection, but it was adapted to utilise a point-cloud based approach proposed by Li et al. (2012). Finally, the method by Wing et al. (2015) was identified for the detection of standing dead trees. Following method identification, the suitability and applicability to AHN4 data was assessed through an initial qualitative performance assessment followed by, where applicable, a quantitative assessment.

The method for ITD was initially deemed feasible for application to AHN4 data during qualitative assessment, as trees in coniferous sample plots were identified with acceptable accuracy. For deciduous and mixed forests, the results were considerably weaker, but room for improvement of the method utilising a Variable Window Size (VWS) led to the method being deemed feasible. Following adaptation of the method to utilise a VWS, based on linear relationships between tree height and crown radius for the different forest types, the results were compared against field-collected data. This comparison highlighted that the method does not function well in this specific context, with a correct tree detection rate of only 6.8%. These poor results are attributed mainly to the method of ITD, as a flat representation of 3D space is utilised in the form of a Canopy Height Model (CHM). This leads to a loss of information for trees below the upper canopy, resulting in sub-dominant trees not being identified. In addition, while the detection of tree tops is generally acceptable, the tree top location does not directly correlate with the tree stem location, likely contributing to the poor accuracy ratings as field-based tree identification is stem-based. Some potential improvements to the methods were suggested, but fundamentally this approach struggles with detecting smaller trees in the complex environments of forest reserves. As such, the method is deemed unsuitable for application to AHN data in the context of the Dutch forest reserve network, though it could play a valuable role in tree height measurements or gap detection.

The assessed MCWS algorithm for crown segmentation was deemed unfeasible, but the point-cloud based algorithm by Li et al. (2012) generally performed well in qualitative assessment, despite some visible artefacts. Unable to compare the results against field-observations, attempts were made to remove artefacts from the method, but this introduced other issues such as over-classification. There is likely still room to improve this method by utilising a forest-type specific approach, where parameter optimisation is applied depending on the forest type. Based on the qualitative findings and literature support, the method is deemed feasible for AHN application and can serve as a valuable information source for identifying canopy gaps and canopy cover - especially the upper canopy layer - though linking crowns to individual tree stems, as in the current monitoring programme, may prove difficult given the poor ITD results.

Standing dead tree detection using the intensity-based method proposed by Wing et al. (2015) is not feasible with AHN data. Initial qualitative assessment showed extensive over-classification of points as snags, which made a quantitative assessment unnecessary. Instead, focus was placed on determining the cause of the over-classification and attempts at parameter optimisation. Despite these efforts, results did not improve. The causes behind the over-classification were identified as a fundamental mismatch in intensity data, likely as a result of environmental variables and differences between LiDAR scanners. This highlights a fundamental flaw in intensity-based approaches, as intensity is always a relative measure, meaning it is highly susceptible to changes between sensors, locations, environments, and even weather. This makes it unsuitable for application in the forest reserve context, as different AHN sensors and varying data acquisition conditions will make time-series analyses complex and unreliable.

With these findings, several suggestions for future research were outlined. A wider, more thorough literature review focusing not only on ALS but also on photogrammetric data could be highly beneficial in preparing for AHN6. Further literature work could also investigate the forest reserve characteristics not covered in this thesis. In addition, methods utilising an area-based approach might be explored to provide additional insights into the forest reserves, though insights into sub-canopy layers will likely prove fundamentally difficult to achieve given the nature of ALS data. In addition, current in-field data collection moments are an excellent opportunity to consider the development and training of machine learning or deep learning models that have been identified. Finally, considerations into area-based approaches might be made, though the practical applicability of these methods will depend on the desired knowledge output of the monitoring programme.

To conclude, the application possibilities for AHN data in monitoring the Dutch forest reserves currently remain limited, though only a subset of variables and methods has been tested. Opportunities lie in moving toward an area-based approach, and future research may reveal whether this benefits the monitoring process. Limited conclusions can be drawn regarding the tested methods themselves, as the study areas and other variables varied. Forest environments remain complex, and adapting models to specific forest areas is time-consuming and sometimes convoluted. AHN-based analyses may well have a place in the forest reserve monitoring, though highly unlikely as a replacement for field observations. Instead, combining AHN-based analyses and field work could yield additional information for reserve-wide monitoring. Further research into alternative methods may also prove insightful into practical approaches to replace some parts of field work.

A crucial consideration must be made regarding the overall approach of using remote sensing for forest reserve monitoring. The differences between individual-tree and area-based methods are substantial. Rather than focusing solely on replacing currently monitored characteristics, it is suggested that emphasis should be placed on identifying the information each characteristic provides and on developing new workflows that utilise remote sensing—potentially including AHN—to strengthen these analyses.

6 Recommendations

The potential for future research is broad in this context. AHN data has seen limited usage in the forestry context so far, and its potential applications could be highly beneficial for the broader sector. Focus should be placed on developing robust, well-functioning models and on modelling specific relationships between variables typical of forests in the Netherlands. With new data collection currently occurring — not just in the forest reserves but across the Netherlands as a whole during the 8th cycle of the Dutch Forest Inventory - there lies a unique opportunity for this type of development.

New technologies such as machine learning, but in particular deep learning, should be explored for their potential. The advent of AHN6, combining ALS and high-resolution aerial imagery, allows the application of new methods such as CNN-based automated tree species detection. Considerations must, however, be made regarding adaptability to the Dutch environment. It is recommended to conduct thorough reviews of individual methods, rather than broad but superficial reviews. First and foremost, a thorough and robust literature review should identify key methodologies and new developments, with a strong focus on methods that have been successfully applied in environments similar to Dutch forests. These methods may be divided into individual tree-based and area-based approaches.

Following this, these methods must be tested. Testing should utilise AHN4, AHN5, and potentially AHN6 data if available, as well as the new field data currently being collected. The key consideration of all future research should be identifying relationships between variables and methods that are specific to Dutch forests. Without this focus, contributions to the monitoring programme are likely to remain limited, as generalised models or models based on other forest types will likely yield unsatisfactory results.

Concretely, within the context of the forest reserve monitoring programme, it is advisable to take a step back and reconsider the overall approach. A key question should be whether an individual-tree-based methodology is truly desirable, or whether area-based approaches could offer greater benefits. It is recommended that the currently monitored characteristics be generalised to the desired information outputs at the forest scale. This would enable a more targeted and robust literature review, encompassing previously identified methods such as machine- and deep learning, and allowing their full potential to be applied to AHN6 data. In contrast to this thesis, a more extensive literature review with clearly defined testing constraints - focused particularly on forests similar to those in the Netherlands - is recommended. Theoretically, this should reduce the effort required to adapt identified methods to AHN data. If machine- or deep-learning-based methods, or other model-dependent approaches, are identified, they should not be dismissed. Ongoing field work provides a valuable opportunity to develop and calibrate such methods specifically for Dutch forest conditions. Subsequently, methods should be tested, not necessarily with the intention of replacing field work - though this may be feasible for some - but rather to gain additional insights and strengthen existing data collection efforts. Finally, given the apparent scarcity of research on understory, subdominant, and shrub-layer detection, future work may benefit from focusing primarily on information derived from dominant trees.

References

- Actueel Hoogtebestand Nederland. (2023, March 27). *Kwaliteitsbeschrijving*. Retrieved April 14, 2025, from <https://www.ahn.nl/kwaliteitsbeschrijving>
- Actueel Hoogtebestand Nederland. (2024, August). Dataroom. <https://www.ahn.nl/dataroom>
- Ashton, M. S., & Kelty, M. J. (2018). *The Practice of Silviculture : Applied Forest Ecology* (10th ed.). Wiley. <https://research.ebsco.com/c/kp5dft/search/details/inlin3pkv?db=nlebk>
- Asigbaase, M., Dawoe, E., Abugre, S., Kyereh, B., & Nsor, C. A. (2023). Allometric relationships between stem diameter, height and crown area of associated trees of cocoa agroforests of Ghana. *Scientific Reports*, 13(1). <https://doi.org/10.1038/s41598-023-42219-6>
- [ASPRS], T. (2019, July 9). *Las specification 1.4 - r15*. Retrieved April 14, 2025, from https://www.asprs.org/wp-content/uploads/2019/07/LAS_1_4_r15.pdf
- Ayrey, E., & Hayes, D. J. (2018). The use of Three-Dimensional Convolutional Neural Networks to interpret LIDAR for forest inventory. *Remote Sensing*, 10(4), 649. <https://doi.org/10.3390/rs10040649>
- Barredo, Brailescu, Teller, Sabatini, Mauri, & Janouskova. (2021). *Mapping and assessment of primary and old-growth forests in europe*. European Commission: Joint Research Centre. <https://doi.org/10.2760/797591>
- Bazezew, M. N., Hussin, Y. A., & Kloosterman, E. (2018). Integrating airborne lidar and terrestrial laser scanner forest parameters for accurate above-ground biomass/carbon estimation in ayer hitam tropical forest, malaysia. *International Journal of Applied Earth Observation and Geoinformation*, 73, 638–652. <https://doi.org/10.1016/j.jag.2018.07.026>
- Beeldmateriaal Nederland. (2023, March 14). *Beeldmateriaal nederland*. Retrieved April 14, 2025, from <https://www.beeldmateriaal.nl/>
- Beland, M., Parker, G., Sparrow, B., Harding, D., Chasmer, L., Phinn, S., Antonarakis, A., & Strahler, A. (2019). On promoting the use of lidar systems in forest ecosystem research. *Forest Ecology and Management*, 450, 117484. <https://doi.org/10.1016/j.foreco.2019.117484>
- Bijlsma, R., & Clerkx, A. (2019a). *Dutch forest reserves database and network*. <https://doi.org/10.17026/dans-2bd-kskz>
- Bijlsma, R., & Clerkx, A. (2019b, January 1). *The dutch forest reserves network : Documentation of monitoring design and databases*. <https://doi.org/10.18174/472664>
- Bonnet, S., Gaulton, R., Lehaire, F., & Lejeune, P. (2015). Canopy Gap Mapping from Airborne Laser Scanning: An Assessment of the Positional and Geometrical Accuracy. *Remote Sensing*, 7(9), 11267–11294. <https://doi.org/10.3390/rs70911267>
- Bright, B. C., Hudak, A. T., McGaughey, R., Andersen, H.-E., & Negrón, J. (2013). Predicting live and dead tree basal area of bark beetle affected forests from discrete-return lidar. *Canadian Journal of Remote Sensing*, 39(sup1), S99–S111. <https://doi.org/10.5589/m13-027>
- Broekmeyer & Hilgen. (1991, April). *Basisrapport bosreservaten*. Informatie- en Kenniscentrum Natuur, Bos, Landschap en Fauna. Retrieved November 8, 2024, from <https://edepot.wur.nl/422517>
- Broekmeyer, M. (1995, January 1). *Bosreservaten in nederland* (IBN-133). Wageningen, Instituut voor Bos- en Natuuronderzoek. Retrieved November 8, 2024, from <http://edepot.wur.nl/422514>
- Broekmeyer, M., Clerkx, S., van Hees, A., & Koop, H. (1997, April). *Veldwerkhandleiding bosreservaten* (IBN-DLO).
- Brown, I. A., Ghaly, M., Greiser, C., Lam, N., & Lehmann, P. (2024). Seasonal optimisation of drone-based photogrammetry in a heterogeneous boreal landscape. *Applied Vegetation Science*, 27(3). <https://doi.org/10.1111/avsc.12797>
- Brown, S., Narine, L. L., & Gilbert, J. (2022). Using airborne LIDAR, multispectral imagery, and field inventory data to estimate basal area, volume, and aboveground biomass in heterogeneous mixed species forests: a case study in southern Alabama. *Remote Sensing*, 14(11), 2708. <https://doi.org/10.3390/rs14112708>
- Camarretta, N., Harrison, P. A., Bailey, T., Potts, B., Lucieer, A., Davidson, N., & Hunt, M. (2019). Monitoring forest structure to guide adaptive management of forest restoration: A review of remote sensing approaches. *New Forests*, 51(4), 573–596. <https://doi.org/10.1007/s11056-019-09754-5>

- Casas, Á., García, M., Siegel, R. B., Koltunov, A., Ramírez, C., & Ustin, S. (2016). Burned forest characterization at single-tree level with airborne laser scanning for assessing wildlife habitat. *Remote Sensing of Environment*, 175, 231–241. <https://doi.org/10.1016/j.rse.2015.12.044>
- Chen, Q., Baldocchi, D., Gong, P., & Kelly, M. (2006). Isolating individual trees in a savanna woodland using small footprint LIDAR data. *Photogrammetric Engineering Remote Sensing*, 72(8), 923–932. <https://doi.org/10.14358/pers.72.8.923>
- Chiarucci, A., Araújo, M. B., Decocq, G., Beierkuhnlein, C., & Fernández-Palacios, J. M. (2010). The concept of potential natural vegetation: An epitaph? *Journal of Vegetation Science*, 21(6), 1172–1178. <https://doi.org/10.1111/j.1654-1103.2010.01218.x>
- Clark, H., Vanclay, J., & Brymer, E. (2023). Forest features and mental health and wellbeing: A scoping review. *Journal of Environmental Psychology*, 89, 102040. <https://doi.org/10.1016/j.jenvp.2023.102040>
- Clerkx, A., Sanders, M., & Bijlsma, R. (2002). *Bosdynamiek in bosreservaat Het Leesten* (tech. rep. No. Alterra-rapport 556). Wageningen, nl, Alterra, Research Instituut voor de Groene Ruimte. <https://edepot.wur.nl/17244>
- Clinton, N., Holt, A., Scarborough, J., Yan, L., & Gong, P. (2010). Accuracy assessment measures for object-based image segmentation goodness. *Photogrammetric Engineering Remote Sensing*, 76(3), 289–299. <https://doi.org/10.14358/pers.76.3.289>
- Committee, I. G., & Solutions, G. (2008). Amersfoort / RD New + NAP height. https://epsg.org/crs_7415/Amersfoort-RD-New-NAP-height.html?sessionkey=l1g6dr2y2s
- Compeán-Aguirre, J. L., López-Serrano, P. M., Silván-Cárdenas, J. L., Martínez-García-Moreno, C. A., Vega-Nieva, D. J., Corral-Rivas, J. J., & Pompa-García, M. (2024). Evaluation of two-dimensional dbh estimation algorithms using tls. *Forests*, 15(11), 1964. <https://doi.org/10.3390/f15111964>
- Corte, A. P. D., Souza, D. V., Rex, F. E., Sanquette, C. R., Mohan, M., Silva, C. A., Zambrano, A. M. A., Prata, G., De Almeida, D. R. A., Trautenmüller, J. W., Klauberg, C., De Moraes, A., Sanquette, M. N., Wilkinson, B., & Broadbent, E. N. (2020). Forest inventory with high-density uav-lidar: Machine learning approaches for predicting individual tree attributes. *Computers and Electronics in Agriculture*, 179, 105815. <https://doi.org/10.1016/j.compag.2020.105815>
- Dalponte, M., & Coomes, D. A. (2016). Tree-centric mapping of forest carbon density from airborne laser scanning and hyperspectral data. *Methods in Ecology and Evolution*, 7(10), 1236–1245. <https://doi.org/10.1111/2041-210x.12575>
- Dassot, M., Constant, T., & Fournier, M. (2011). The use of terrestrial lidar technology in forest science: Application fields, benefits and challenges. *Annals of Forest Science*, 68(5), 959–974. <https://doi.org/10.1007/s13595-011-0102-2>
- De Bruin, J., Hoogstra-Klein, M., Mohren, G., & Arts, B. (2015). Complexity of forest management: Exploring perceptions of dutch forest managers. *Forests*, 6(9), 3237–3255. <https://doi.org/10.3390/f6093237>
- de Pagter, T. (2024). *Ahn for monitoring succession processes in forest structure: Developing a procedure for the segmentation of ahn forest point clouds into vegetation layers*. Wageningen University & Research.
- De Petris, S., Sarvia, F., & Borgogno-Mondino, E. (2022). About tree height measurement: Theoretical and practical issues for uncertainty quantification and mapping. *Forests*, 13(7), 969. <https://doi.org/10.3390/f13070969>
- Degnan, J. (2016). Scanning, multibeam, single photon lidars for rapid, large scale, high resolution, topographic and bathymetric mapping. *Remote Sensing*, 8(11), 958. <https://doi.org/10.3390/rs8110958>
- Douss, R., & Farah, I. R. (2022). Extraction of individual trees based on Canopy Height Model to monitor the state of the forest. *Trees Forests and People*, 8, 100257. <https://doi.org/10.1016/j.tfp.2022.100257>
- Duan, M., Sanchez-Azofeifa, A., Abdulmajeed, M., Turner, D., Buckingham, K., Odari, A., Mtawana, J., Kipkoech, S., & Kasraee, N. (2025). Aboveground carbon estimation in a mangrove ecosystem using uav-based remote sensing and machine learning. *Ecological Indicators*, 178, 113950. <https://doi.org/10.1016/j.ecolind.2025.113950>
- Ene, L. T., Næsset, E., Gobakken, T., Bollandsås, O. M., Mauya, E. W., & Zahabu, E. (2016). Large-scale estimation of change in aboveground biomass in miombo woodlands using airborne laser

- scanning and national forest inventory data. *Remote Sensing of Environment*, 188, 106–117. <https://doi.org/10.1016/j.rse.2016.10.046>
- Erfanifard, Y., Stereńczak, K., Kraszewski, B., & Kamińska, A. (2018). Development of a robust canopy height model derived from ALS point clouds for predicting individual crown attributes at the species level. *International Journal of Remote Sensing*, 39(23), 9206–9227. <https://doi.org/10.1080/01431161.2018.1508916>
- Estrada, J. S., Fuentes, A., Reszka, P., & Cheein, F. A. (2023). Machine learning assisted remote forestry health assessment: a comprehensive state of the art review. *Frontiers in Plant Science*, 14. <https://doi.org/10.3389/fpls.2023.1139232>
- Eysn, L., Hollaus, M., Lindberg, E., Berger, F., Monnet, J., Dalponte, M., Kobal, M., Pellegrini, M., Lingua, E., Mongus, D., & Pfeifer, N. (2015). A benchmark of lidar-based single tree detection methods using heterogeneous forest data from the alpine space. *Forests*, 6(5), 1721–1747. <https://doi.org/10.3390/f6051721>
- Falkowski, M. J., Smith, A. M., Gessler, P. E., Hudak, A. T., Vierling, L. A., & Evans, J. S. (2008). The influence of conifer forest canopy cover on the accuracy of two individual tree measurement algorithms using lidar data. *Canadian Journal of Remote Sensing*, 34(sup2), S338–S350. <https://doi.org/10.5589/m08-055>
- FAO. (2020, January 1). *Global forest resources assessment 2020 - key findings*. Rome. <https://doi.org/10.4060/ca8753en>
- FAO & Oldenburger. (2020). *Global forest resources assessment 2020: Report netherlands*. Rome.
- Fassnacht, F. E., White, J. C., Wulder, M. A., & Næsset, E. (2023). Remote sensing in forestry: current challenges, considerations and directions. *Forestry An International Journal of Forest Research*, 97(1), 11–37. <https://doi.org/10.1093/forestry/cpad024>
- Garroway, K., Hopkinson, C., & Jamieson, R. (2011). Surface moisture and vegetation influences on lidar intensity data in an agricultural watershed. *Canadian Journal of Remote Sensing*, 37(3), 275–284. <https://doi.org/10.5589/m11-036>
- Gebreslasie, M. T., Ahmed, F. B., Van Aardt, J. A. N., & Blakeway, F. (2011). Individual tree detection based on variable and fixed window size local maxima filtering applied to IKONOS imagery for even-agedEucalyptusplantation forests. *International Journal of Remote Sensing*, 32(15), 4141–4154. <https://doi.org/10.1080/01431161003777205>
- Geosystems, L. (2014, July). *Leica ALS50-II Airborne Laser Scanner* (tech. rep. No. 070414_ALS50 – II – Description).
- GmbH, R. L. M. S. (2017, December). *LAS Extrabytes Implementation in RIEGL Software* (tech. rep.).
- Goldbergs, G. (2023). Comparison of canopy height metrics from airborne laser scanner and aerial/satellite stereo imagery to assess the growing stock of hemiboreal forests. *Remote Sensing*, 15(6), 1688. <https://doi.org/10.3390/rs15061688>
- Goodbody, T. R. H., Coops, N. C., & White, J. C. (2019). Digital Aerial Photogrammetry for Updating Area-Based Forest Inventories: A review of opportunities, challenges, and future directions. *Current Forestry Reports*, 5(2), 55–75. <https://doi.org/10.1007/s40725-019-00087-2>
- Goodbody, T. R., Coops, N. C., Irwin, L. A., Armour, C. C., Saunders, S. C., Dykstra, P., Butson, C., & Perkins, G. C. (2024). Integration of airborne laser scanning data into forest ecosystem management in canada: Current status and future directions. *The Forestry Chronicle*, 100(2), 240–260. <https://doi.org/10.5558/tfc2024-014>
- Gril, E., Laslier, M., Gallet-Moron, E., Durrieu, S., Spicher, F., Roux, V. L., Brasseur, B., Haesen, S., Van Meerbeek, K., Decocq, G., Marrec, R., & Lenoir, J. (2023). Using airborne lidar to map forest microclimate temperature buffering or amplification. *Remote Sensing of Environment*, 298, 113820. <https://doi.org/10.1016/j.rse.2023.113820>
- Hamedianfar, A., Mohamedou, C., Kangas, A., & Vauhkonen, J. (2022). Deep learning for forest inventory and planning: a critical review on the remote sensing approaches so far and prospects for further applications. *Forestry An International Journal of Forest Research*, 95(4), 451–465. <https://doi.org/10.1093/forestry/cpac002>

- Hengeveld, G. M., Nabuurs, G., Didion, M., Van Den Wyngaert, I., Clerkx, A., & Schelhaas, M. (2012). A forest management map of european forests. *Ecology and Society*, 17(4). <https://www.jstor.org/stable/26269226>
- Hijmans, R. J. (2023). *Terra: Spatial data analysis* [R package version 1.7-65]. <https://CRAN.R-project.org/package=terra>
- Hoogstra-Klein, M. A., & Burger, M. (2013). Rational versus adaptive forest management planning: Exploratory research on the strategic planning practices of dutch forest management organizations. *European Journal of Forest Research*, 132(5-6), 707–716. <https://doi.org/10.1007/s10342-013-0707-0>
- Jarron, L. R., Coops, N. C., MacKenzie, W. H., Tompalski, P., & Dykstra, P. (2020). Detection of sub-canopy forest structure using airborne LiDAR. *Remote Sensing of Environment*, 244, 111770. <https://doi.org/10.1016/j.rse.2020.111770>
- Jing, L., Hu, B., Li, J., & Noland, T. (2012). Automated Delineation of Individual Tree Crowns from Lidar Data by Multi-Scale Analysis and Segmentation. *Photogrammetric Engineering Remote Sensing*, 78(12), 1275–1284. <https://doi.org/10.14358/pers.78.11.1275>
- Joyce, M. J., Erb, J. D., Sampson, B. A., & Moen, R. A. (2018). Detection of coarse woody debris using airborne light detection and ranging (lidar). *Forest Ecology and Management*, 433, 678–689. <https://doi.org/10.1016/j.foreco.2018.11.049>
- Kaartinen, H., Hyppä, J., Yu, X., Vastaranta, M., Hyppä, H., Kukko, A., Holopainen, M., Heipke, C., Hirschmugl, M., Morsdorf, F., Næsset, E., Pitkänen, J., Popescu, S., Solberg, S., Wolf, B. M., & Wu, J. (2012). An international comparison of individual tree detection and extraction using airborne laser scanning. *Remote Sensing*, 4(4), 950–974. <https://doi.org/10.3390/rs4040950>
- Khan, M. N., Tan, Y., Gul, A. A., Abbas, S., & Wang, J. (2024). Forest aboveground biomass estimation and inventory: Evaluating remote sensing-based approaches. *Forests*, 15(6), 1055. <https://doi.org/10.3390/f15061055>
- Khosravipour, A., Skidmore, A. K., Isenburg, M., Wang, T., & Hussin, Y. A. (2014). Generating Pit-free Canopy Height Models from Airborne Lidar. *Photogrammetric Engineering Remote Sensing*, 80(9), 863–872. <https://doi.org/10.14358/pers.80.9.863>
- Kissling, W. D., Shi, Y., Koma, Z., Meijer, C., Ku, O., Nattino, F., Seijmonsbergen, A. C., & Grootes, M. W. (2022). Laserfarm – a high-throughput workflow for generating geospatial data products of ecosystem structure from airborne laser scanning point clouds. *Ecological Informatics*, 72, 101836. <https://doi.org/10.1016/j.ecoinf.2022.101836>
- Kleinsmann, J., Verbesselt, J., & Kooistra, L. (2023). Monitoring individual tree phenology in a Multi-Species forest using high resolution UAV images. *Remote Sensing*, 15(14), 3599. <https://doi.org/10.3390/rs15143599>
- Ko, C., & Remmel, T. K. (2017, January 1). *Airborne lidar applications in forest landscapes*. https://doi.org/10.1007/978-1-4939-7331-6_4
- Koelewijn, N. (2023). *Influence of forest management on canopy gap dynamics: Uncovering the potential of the ahn to map, characterize and compare canopy gap dynamics*. Wageningen University & Research.
- Koop, T. (2024). *Counting trees in dutch forests: Using ahn lidar data for national forest inventory*. Wageningen University & Research.
- Korpela, I., Hovi, A., & Morsdorf, F. (2012). Understory trees in airborne LiDAR data — Selective mapping due to transmission losses and echo-triggering mechanisms. *Remote Sensing of Environment*, 119, 92–104. <https://doi.org/10.1016/j.rse.2011.12.011>
- Kotivuori, E., Korhonen, L., & Packalen, P. (2016). Nationwide airborne laser scanning based models for volume, biomass and dominant height in Finland. *Silva Fennica*, 50(4). <https://doi.org/10.14214/sf.1567>
- Kuang, W., Ho, H. W., Zhou, Y., Suandi, S. A., & Ismail, F. (2024). A comprehensive review on tree detection methods using point cloud and aerial imagery from unmanned aerial vehicles. *Computers and Electronics in Agriculture*, 227, 109476. <https://doi.org/10.1016/j.compag.2024.109476>
- Li, W., Guo, Q., Jakubowski, M. K., & Kelly, M. (2012). A New Method for Segmenting Individual Trees from the Lidar Point Cloud. *Photogrammetric Engineering Remote Sensing*, 78(1), 75–84. <https://doi.org/10.14358/pers.78.1.75>

- Lisiewicz, M., Kamińska, A., & Stereńczak, K. (2022). Recognition of specified errors of Individual Tree Detection methods based on Canopy Height Model. *Remote Sensing Applications Society and Environment*, 25, 100690. <https://doi.org/10.1016/j.rsase.2021.100690>
- Liu, K., Shen, X., Cao, L., Wang, G., & Cao, F. (2018). Estimating forest structural attributes using uav-lidar data in ginkgo plantations. *ISPRS Journal of Photogrammetry and Remote Sensing*, 146, 465–482. <https://doi.org/10.1016/j.isprsjprs.2018.11.001>
- Liu, Y., Chen, D., Fu, S., Mathiopoulos, P. T., Sui, M., Na, J., & Peethambaran, J. (2024). Segmentation of individual tree points by combining Marker-Controlled watershed segmentation and spectral clustering optimization. *Remote Sensing*, 16(4), 610. <https://doi.org/10.3390/rs16040610>
- Maas, van Delft, & Makaske. (2018). *De landschappelijke bodemkaart van nederland*. Retrieved April 3, 2025, from <http://landschapsleutel.wur.nl>
- Maltamo, M., Næsset, E., & Vauhkonen, J. (2014, January). *Forestry applications of airborne laser scanning*. <https://doi.org/10.1007/978-94-017-8663-8>
- Marcello, J., Spínola, M., Albors, L., Marqués, F., Rodríguez-Esparragón, D., & Eugenio, F. (2024). Performance of individual tree segmentation algorithms in forest ecosystems using uav lidar data. *Drones*, 8(12), 772. <https://doi.org/10.3390/drones8120772>
- Marinelli, D., Paris, C., & Bruzzone, L. (2022). An approach based on deep learning for tree species classification in LIDAR data acquired in mixed forest. *IEEE Geoscience and Remote Sensing Letters*, 19, 1–5. <https://doi.org/10.1109/lgrs.2022.3181680>
- Meijer, M., Rip, F., Van Benthem, R., Clement, J., & Van Der Sande, C. (2015, January). *Boomkronen afleiden uit het actueel hoogtebestand nederland* (Alterra-rapport 2671). Wageningen, nl, Alterra Wageningen UR. Retrieved November 21, 2024, from <http://edepot.wur.nl/362099>
- Mohan, M., Silva, C., Klauberg, C., Jat, P., Catts, G., Cardil, A., Hudak, A., & Dia, M. (2017). Individual Tree Detection from Unmanned Aerial Vehicle (UAV) Derived Canopy Height Model in an Open Canopy Mixed Conifer Forest. *Forests*, 8(9), 340. <https://doi.org/10.3390/f8090340>
- Mohren, G., & Vodde, F. (2006). *Forests and forestry in the netherlands*. <http://library.wur.nl/WebQuery/wurpubs/351494>
- Moskal, L. M., & Zheng, G. (2011). Retrieving forest inventory variables with terrestrial laser scanning (tls) in urban heterogeneous forest. *Remote Sensing*, 4(1), 1–20. <https://doi.org/10.3390/rs4010001>
- Muhojoki, J., Tavi, D., Hyppä, E., Lehtomäki, M., Faitli, T., Kaartinen, H., Kukko, A., Hakala, T., & Hyppä, J. (2024). Benchmarking under- and above-canopy laser scanning solutions for deriving stem curve and volume in easy and difficult boreal forest conditions. *Remote Sensing*, 16(10), 1721. <https://doi.org/10.3390/rs16101721>
- Murdoch, D., & Adler, D. (2023). *Rgl: 3d visualization using opengl* [R package version 1.2.8]. <https://CRAN.R-project.org/package=rgl>
- Muumbe, T. P., Raumonen, P., Baade, J., Coetsee, C., Singh, J., & Schmullius, C. (2025). A Comparison of Tree Segmentation Methods for Savanna Tree Extraction from TLS Point Clouds. *Land*, 14(9), 1761. <https://doi.org/10.3390/land14091761>
- Ocón, J. P., Stavros, E. N., Steinberg, S. J., Robertson, J., & Gillespie, T. W. (2024). Remote sensing approaches to identify trees to species-level in the urban forest: A review. *Progress in Physical Geography Earth and Environment*, 48(3), 438–453. <https://doi.org/10.1177/03091333241252520>
- Pearse, G. D., Watt, M. S., Dash, J. P., Stone, C., & Caccamo, G. (2018). Comparison of models describing forest inventory attributes using standard and voxel-based lidar predictors across a range of pulse densities. *International Journal of Applied Earth Observation and Geoinformation*, 78, 341–351. <https://doi.org/10.1016/j.jag.2018.10.008>
- Pebesma, E. (2018). Simple Features for R: Standardized Support for Spatial Vector Data. *The R Journal*, 10(1), 439–446. <https://doi.org/10.32614/RJ-2018-009>
- Peng, X., Calders, K., Terryn, L., & Verbeeck, H. (2024). Evaluating tree branch angle measurements of european beech using terrestrial laser scanning. *Forest Ecosystems*, 100279. <https://doi.org/10.1016/j.fecs.2024.100279>
- Penglase, K., Lewis, T., & Srivastava, S. K. (2023). A new approach to estimate fuel budget and wild-fire hazard assessment in commercial plantations using Drone-Based photogrammetry and image analysis. *Remote Sensing*, 15(10), 2621. <https://doi.org/10.3390/rs15102621>

- Plowright, A. (2017, January). ForestTools: Tools for analyzing remote sensing forest data. <https://doi.org/10.32614/cran.package.foresttools>
- Popescu, S. C., Wynne, R. H., & Nelson, R. F. (2002). Estimating plot-level tree heights with lidar: local filtering with a canopy-height based variable window size. *Computers and Electronics in Agriculture*, 37(1-3), 71–95. [https://doi.org/10.1016/s0168-1699\(02\)00121-7](https://doi.org/10.1016/s0168-1699(02)00121-7)
- Potapov, P., Hansen, M. C., Laestadius, L., Turubanova, S., Yaroshenko, A., Thies, C., Smith, W., Zhuravleva, I., Komarova, A., Minnemeyer, S., & Esipova, E. (2017). The last frontiers of wilderness: Tracking loss of intact forest landscapes from 2000 to 2013. *Science Advances*, 3(1). <https://doi.org/10.1126/sciadv.1600821>
- Pucino, N., McVicar, T., Levick, S., & Van Dijk, A. (2025). The accuracy of image-based individual tree crown detection and delineation across vegetation types. *The international archives of the photogrammetry, remote sensing and spatial information sciences/International archives of the photogrammetry, remote sensing and spatial information sciences*, XLVIII-G-2025, 1223–1227. <https://doi.org/10.5194/isprs-archives-xlviii-g-2025-1223-2025>
- Puliti, S., Dash, J. P., Watt, M. S., Breidenbach, J., & Pearse, G. D. (2019). A comparison of uav laser scanning, photogrammetry and airborne laser scanning for precision inventory of small-forest properties. *Forestry An International Journal of Forest Research*, 93(1), 150–162. <https://doi.org/10.1093/forestry/cpz057>
- R Core Team. (2023). *R: A language and environment for statistical computing*. R Foundation for Statistical Computing. Vienna, Austria. <https://www.R-project.org/>
- Radboud University Library. (n.d.). *Libguides: Literature search: Citation search*. Retrieved February 3, 2025, from <https://libguides.ru.nl/literaturesearch/snowball>
- Rodrigues, W. G., Vieira, G. S., Cabacinha, C. D., Bulcão-Neto, R. F., & Soares, F. (2024). Applications of artificial intelligence and lidar in forest inventories: A systematic literature review. *Computers & Electrical Engineering*, 120, 109793. <https://doi.org/10.1016/j.compeleceng.2024.109793>
- Roussel, J.-R., & Auty, D. (2025). *Airborne lidar data manipulation and visualization for forestry applications* [R package version 4.0.4]. <https://cran.r-project.org/package=lidR>
- Roussel, J.-R., Auty, D., Coops, N. C., Tompalski, P., Goodbody, T. R., Meador, A. S., Bourdon, J.-F., De Boissieu, F., & Achim, A. (2020). lidR: An R package for analysis of Airborne Laser Scanning (ALS) data. *Remote Sensing of Environment*, 251, 112061. <https://doi.org/10.1016/j.rse.2020.112061>
- Roy, A. D., Karpowicz, D. A., Hendy, I., Rog, S. M., Watt, M. S., Reef, R., Broadbent, E. N., Asbridge, E. F., Gebrie, A., Ali, T., & Mohan, M. (2024). Current status of remote sensing for studying the impacts of hurricanes on mangrove forests in the coastal united states. *Remote Sensing*, 16(19), 3596. <https://doi.org/10.3390/rs16193596>
- Sánchez-Chero, M., Sánchez-Chero, J., Flores-Mendoza, L., Janampa, F., & Cesare, M. (2024). Review of microclimate mapping methods in forestry. *Revista de la Facultad de Agronomía*, 42(1), e254204. [https://doi.org/10.47280/revfacagron\(luz\).v42.n1.iv](https://doi.org/10.47280/revfacagron(luz).v42.n1.iv)
- Sankey, T., Donager, J., McVay, J., & Sankey, J. B. (2017). Uav lidar and hyperspectral fusion for forest monitoring in the southwestern usa. *Remote Sensing of Environment*, 195, 30–43. <https://doi.org/10.1016/j.rse.2017.04.007>
- Schelhaas, M., Teeuwen, S., Oldenburger, J., Beerken, G., Velema, G., Kremers, J., Lerink, B., Paulo, M., Schoonderwoerd, H., Daamen, W., Dolstra, F., Lusink, M., Van Tongeren, K., Scholten, T., Pruijsten, I., Voncken, F., & x, A. (2022, January 1). *Zevende nederlandse bosinventarisatie : Methoden en resultaten*. <https://doi.org/10.18174/571720>
- Siljander, M., Männistö, S., Kuoppamäki, K., Taka, M., & Ruth, O. (2025). Urban green space classification using Object-Based Image Analysis (OBIA) and LIDAR fusion: accuracy evaluation and landscape metrics assessment. *Urban forestry urban greening*, 128997. <https://doi.org/10.1016/j.ufug.2025.128997>
- So, K., Chau, J., Rudd, S., Robinson, D. T., Chen, J., Cyr, D., & Gonsamo, A. (2025). Direct Estimation of Forest Aboveground Biomass from UAV LiDAR and RGB Observations in Forest Stands with Various Tree Densities. *Remote Sensing*, 17(12), 2091. <https://doi.org/10.3390/rs17122091>

- Sparks, A. M., Corrao, M. V., & Smith, A. M. S. (2022). Cross-comparison of individual tree detection methods using low and high pulse density airborne laser scanning data. *Remote Sensing*, 14(14), 3480. <https://doi.org/10.3390/rs14143480>
- Stereńczak, K., Kraszewski, B., Mielcarek, M., Piasecka, Ż., Lisiewicz, M., & Heurich, M. (2020). Mapping individual trees with airborne laser scanning data in an European lowland forest using a self-calibration algorithm. *International Journal of Applied Earth Observation and Geoinformation*, 93, 102191. <https://doi.org/10.1016/j.jag.2020.102191>
- Stitt, J. M., Hudak, A. T., Silva, C. A., Vierling, L. A., & Vierling, K. T. (2022). Evaluating the Use of Lidar to Discern Snag Characteristics Important for Wildlife. *Remote Sensing*, 14(3), 720. <https://doi.org/10.3390/rs14030720>
- Sung, U., Eum, J., & Chung, K. (2024). Evaluation of tree object segmentation performance for individual tree recognition using remote sensing techniques based on urban forest green structures. *Land*, 13(11), 1856. <https://doi.org/10.3390/land13111856>
- Ussyshkin, V., & Theriault, L. (2011). Airborne lidar: Advances in discrete return technology for 3d vegetation mapping. *Remote Sensing*, 3(3), 416–434. <https://doi.org/10.3390/rs3030416>
- van Natijne et al. (2020, October 12). *Geotiles: Readymade geodata with a focus on the netherlands*. Retrieved April 14, 2025, from <https://geotiles.citg.tudelft.nl/>
- Vauhkonen, J., Ene, L., Gupta, S., Heinzel, J., Holmgren, J., Pitkanen, J., Solberg, S., Wang, Y., Weinacker, H., Hauglin, K. M., Lien, V., Packalen, P., Gobakken, T., Koch, B., Naesset, E., Tokola, T., & Maltamo, M. (2011). Comparative testing of single-tree detection algorithms under different types of forest. *Forestry An International Journal of Forest Research*, 85(1), 27–40. <https://doi.org/10.1093/forestry/cpr051>
- Verweel, N. (2025a). Dutch Forest Reserve Webmap. https://nikverweel.github.io/dfr_webmap/
- Verweel, N. (2025b). MSc Thesis Digital Appendix - GitHub. <https://github.com/nikverweel/msc-thesis-appendix>
- Vizzarri, M., Pilli, R., Korosuo, A., Frate, L., & Grassi, G. (2021, November 24). *The role of forests in climate change mitigation: The eu context*. Springer, Cham. https://doi.org/10.1007/978-3-030-80767-2_15
- Wang, Y., Hyppä, J., Liang, X., Kaartinen, H., Yu, X., Lindberg, E., Holmgren, J., Qin, Y., Mallet, C., Ferraz, A., Torabzadeh, H., Morsdorf, F., Zhu, L., Liu, J., & Alho, P. (2016). International benchmarking of the individual tree detection methods for modeling 3-D canopy structure for silviculture and forest ecology using airborne laser scanning. *IEEE Transactions on Geoscience and Remote Sensing*, 54(9), 5011–5027. <https://doi.org/10.1109/tgrs.2016.2543225>
- White, J. C., Coops, N. C., Wulder, M. A., Vastaranta, M., Hilker, T., & Tompalski, P. (2016). Remote sensing Technologies for Enhancing Forest Inventories: a review. *Canadian Journal of Remote Sensing*, 42(5), 619–641. <https://doi.org/10.1080/07038992.2016.1207484>
- Wickham, H. (2016). *Ggplot2: Elegant graphics for data analysis*. Springer-Verlag New York. <https://ggplot2.tidyverse.org>
- Wielgosz, M., Puliti, S., Xiang, B., Schindler, K., & Astrup, R. (2024). Segmentanytree: A sensor and platform agnostic deep learning model for tree segmentation using laser scanning data. *Remote Sensing of Environment*, 313, 114367. <https://doi.org/10.1016/j.rse.2024.114367>
- Windrim, L., & Bryson, M. (2020). Detection, Segmentation, and Model Fitting of Individual Tree Stems from Airborne Laser Scanning of Forests Using Deep Learning. *Remote Sensing*, 12(9), 1469. <https://doi.org/10.3390/rs12091469>
- Wing, B. M., Ritchie, M. W., Boston, K., Cohen, W. B., Gitelman, A., & Olsen, M. J. (2012). Prediction of understory vegetation cover with airborne lidar in an interior ponderosa pine forest. *Remote Sensing of Environment*, 124, 730–741. <https://doi.org/10.1016/j.rse.2012.06.024>
- Wing, B. M., Ritchie, M. W., Boston, K., Cohen, W. B., & Olsen, M. J. (2015). Individual snag detection using neighborhood attribute filtered airborne lidar data. *Remote Sensing of Environment*, 163, 165–179. <https://doi.org/10.1016/j.rse.2015.03.013>
- Wohlin, C. (2014). Guidelines for snowballing in systematic literature studies and a replication in software engineering, 1–10. <https://doi.org/10.1145/2601248.2601268>

- Wu, Q., Zhong, R., Dong, P., Mo, Y., & Jin, Y. (2021). Airborne LIDAR intensity correction based on a new method for incidence angle correction for improving Land-Cover classification. *Remote Sensing*, 13(3), 511. <https://doi.org/10.3390/rs13030511>
- Yrttimaa, T., Luoma, V., Saarinen, N., Kankare, V., Junntila, S., Holopainen, M., Hyppä, J., & Vastaranta, M. (2020). Structural changes in boreal forests can be quantified using terrestrial laser scanning. *Remote Sensing*, 12(17), 2672. <https://doi.org/10.3390/rs12172672>
- Yu, Z., Wu, Y., Zhang, Z., Lu, C., Wang, H., Liu, Z., Zhang, X., Bao, L., Pan, J., Ou, G., & Luo, H. (2025). A precise estimation framework for individual tree AGB of *Pinus kesiya* var. *Langbianensis* utilizing point cloud registration Optimization. *International Journal of Applied Earth Observation and Geoinformation*, 140, 104612. <https://doi.org/10.1016/j.jag.2025.104612>
- Zaka, M. M., & Samat, A. (2024). Advances in remote sensing and machine learning methods for invasive plants study: A comprehensive review. *Remote Sensing*, 16(20), 3781. <https://doi.org/10.3390/rs16203781>
- Zhang, Y. (1996). A survey on evaluation methods for image segmentation. *Pattern Recognition*, 29(8), 1335–1346. [https://doi.org/10.1016/0031-3203\(95\)00169-7](https://doi.org/10.1016/0031-3203(95)00169-7)
- Zhong, L., Dai, Z., Fang, P., Cao, Y., & Wang, L. (2024). A review: Tree species classification based on remote sensing data and Classic Deep Learning-Based methods. *Forests*, 15(5), 852. <https://doi.org/10.3390/f15050852>
- Zhou, G., Li, H., Huang, J., Gao, E., Song, T., Han, X., Zhu, S., & Liu, J. (2024). Weighted Differential Gradient Method for Filling pits in Light Detection and Ranging (LIDAR) Canopy Height model. *Remote Sensing*, 16(7), 1304. <https://doi.org/10.3390/rs16071304>

Appendices

Appendix I

Table 9: Overview of the Dutch Forest Reserves, their forest type and size.

Reserve code	Reserve name	Forest type	Area (ha)
1	Starnumansbos	Mixed	54.35
2	Lheebroek	Mixed	37.41
3	Galgenberg	Mixed	42.57
4	Tussen de Goren	Coniferous	38.72
5	Vijlnerbos	Deciduous	20.72
6	Vechtlanden	Deciduous	11.79
7	Zeesserveld	Mixed	17.69
8	Meerdijk	Deciduous	18.45
9	Pijpebrandje	Mixed	36.49
10	Nieuw Milligen	Mixed	46.14
11	Drieduin 1	Mixed	22.05
12	Drieduin 2	Mixed	19.85
13	Drieduin 3	Mixed	27.48
14	Leesten	Mixed	40.78
15	Quin	Mixed	29.62
16	Sang	Deciduous	20.65
17	Grootvenbos	Deciduous	30.1
18	Schoonloerveld	Mixed	23.15
19	Oosteresch	Coniferous	30.67
20	Roodaam	Deciduous	36.34
21	Riemstruiken	Mixed	23.22
22	Zwarte Bulten	Mixed	46.72
23	Leenderbos	Mixed	29.98
24	Schone Grub	Deciduous	14.39
25	Dieverzand	Mixed	31.17
26	Keizersdijk	Deciduous	32.18
27	Kloosterkooi	Deciduous	29.63
28	Wilgenreservaat	Deciduous	63.63
29	Molenven	Mixed	43.64
30	Beerenplaat	Deciduous	23.19
31	Tongerense Hei	Mixed	43.76
32	Houtribbos	Mixed	15.55
33	Hollandse Hout	Deciduous	36.82
34	Kijfhoek	Deciduous	31.86
35	Geelders	Deciduous	14.38
36	Berkenvallei	NA	99.75
37	Slikken van Flakkee	NA	323.16
38	Pilotenbos	Deciduous	13.89
39	Duivelshof-Smoddebos	Mixed	15.43
40	Duursche Waarden	NA	112.21
41	Heul	Mixed	63.09
42	Bekendelle	NA	4.32
43	Liefstinghsbroek	Deciduous	17.26
44	Rot	Mixed	19.33
45	Kremboong	Deciduous	30.61
46	Norgerholt	Deciduous	25.54

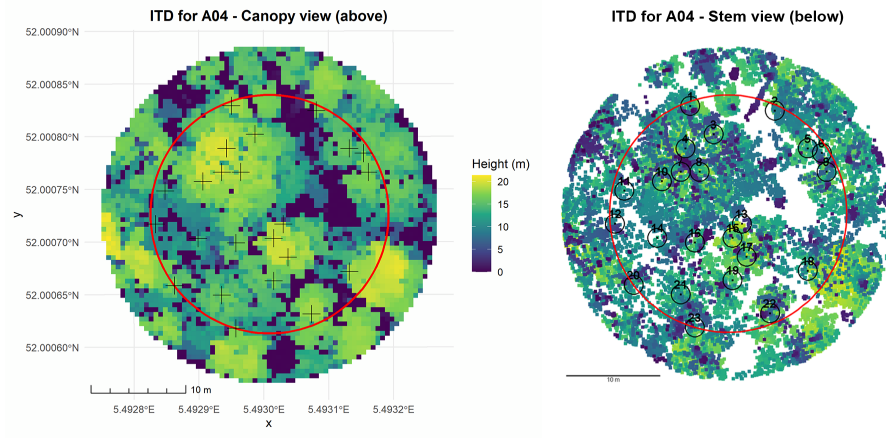
Reserve code	Reserve name	Forest type	Area (ha)
47	Stille Eenzaamheid	Mixed	87.52
48	Horsten	Deciduous	47.8
49	Kampina	Mixed	25.2
50	Smalbroeken	Mixed	42.1
51	Mattemburgh	Mixed	105.72
52	Herkenboscher Heide	Deciduous	70.73
53	Bunderbos	Deciduous	26.79
54	Heloma- en Bleekerspolder	NA	70.18
56	Imboschberg	Mixed	164.6
57	Grote Weiland	Deciduous	34.38
58	Oude Kat	NA	46.08
59	Achter de Voort	Deciduous	7.91
60	Ossenbos	Mixed	54.08

Appendix II

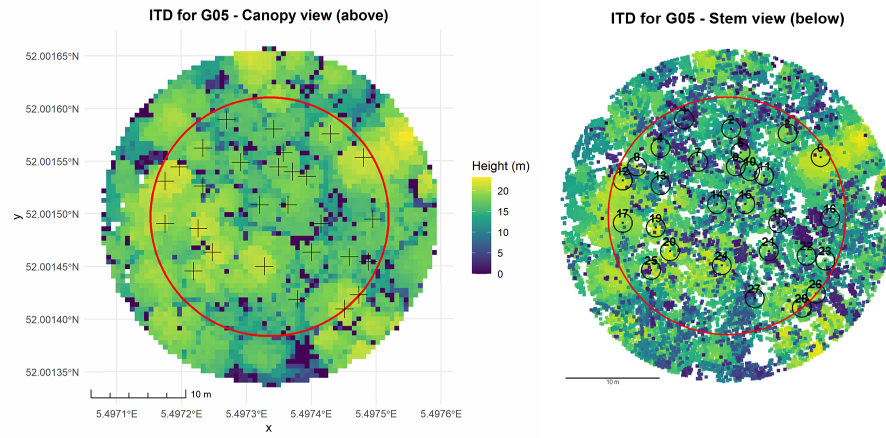
Table 10: Overview of considered seed articles and reasoning for inclusion or exclusion.

Article	Considered as seed article?	Reasoning
Sánchez-Chero et al. (2024)	Yes	Satisfies selection criteria
Marcello et al. (2024)	No	Focused on UAV data
Rodrigues et al. (2024)	Yes	Satisfies selection criteria
Kuang et al. (2024)	No	Focused on UAV data
Zaka and Samat (2024)	No	Not focused on forests
Roy et al. (2024)	No	Focused on mangrove forests
Goodbody et al. (2024)	Yes	Satisfies selection criteria
I. A. Brown et al. (2024)	No	Focused on UAV data
Khan et al. (2024)	Yes	Satisfies selection criteria
Ocón et al. (2024)	Yes	Satisfies selection criteria

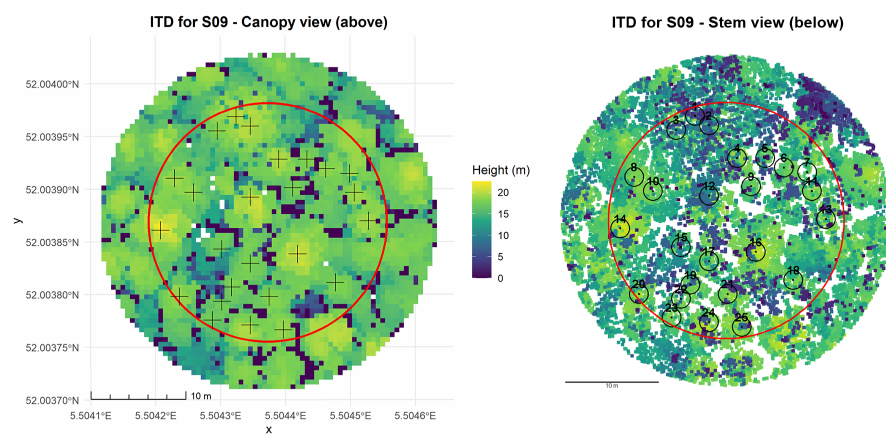
Appendix III



(a) Comparison between top and bottom view after ITD for sample plot A04 in forest reserve *Galgenberg* (RSV 3)

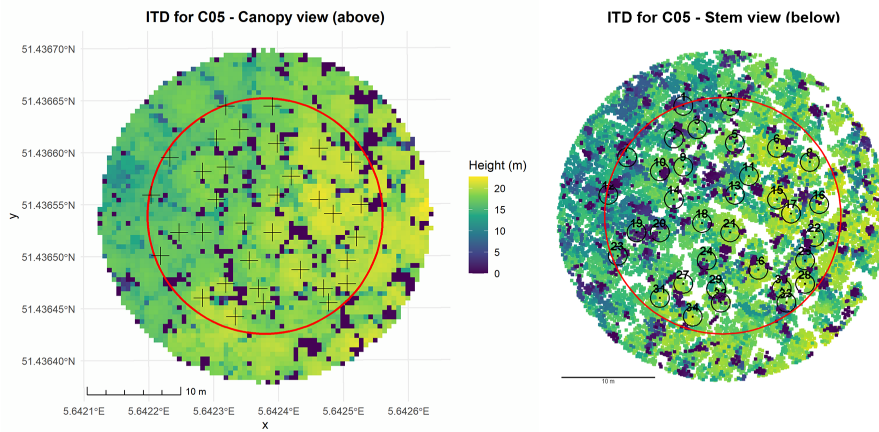


(b) Comparison between top and bottom view after ITD for sample plot G05 in forest reserve *Galgenberg* (RSV 3)

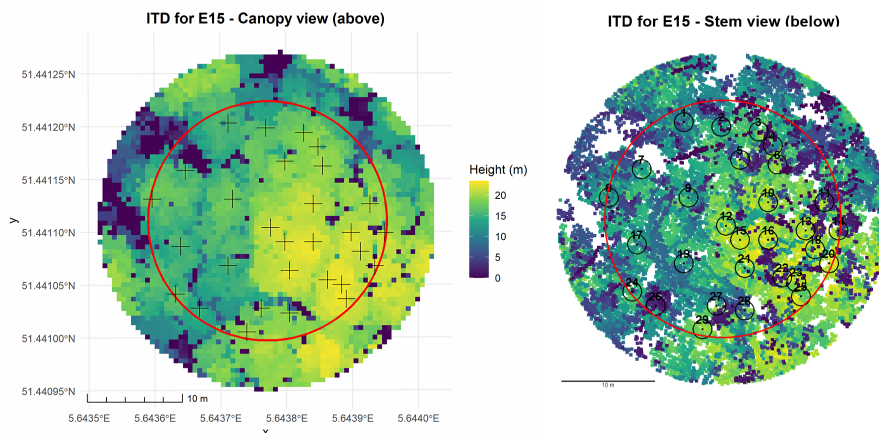


(c) Comparison between top and bottom view after ITD for sample plot S09 in forest reserve *Galgenberg* (RSV 3)

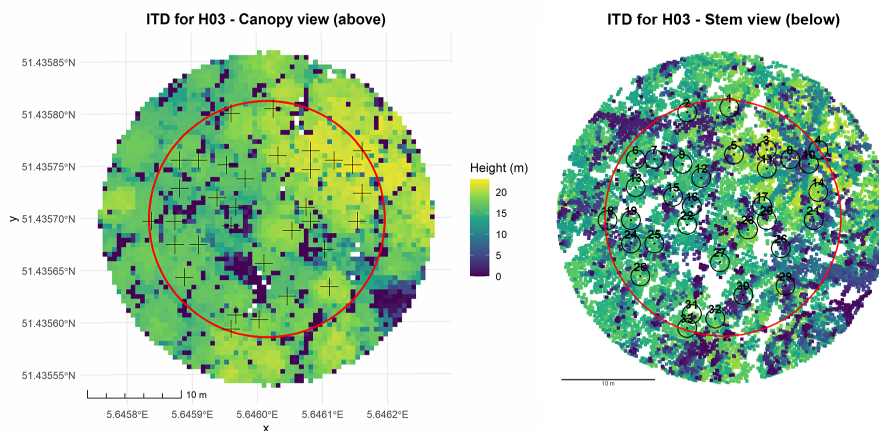
Figure 14: Comparison between canopy- and stem-down views after ITD for representative sample plots in reserves *Galgenberg* (RSV 3)



(a) Comparison between top and bottom view after ITD for sample plot C05 in forest reserve Sang (RSV 16)

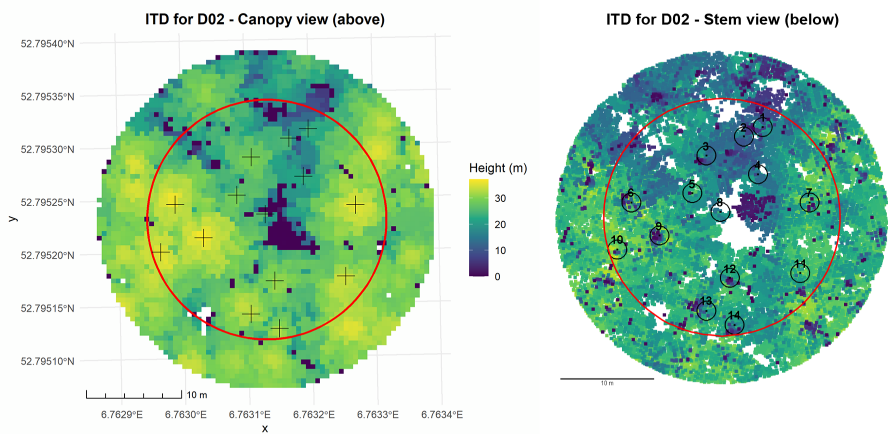


(b) Comparison between top and bottom view after ITD for sample plot E15 in forest reserve Sang (RSV 16)

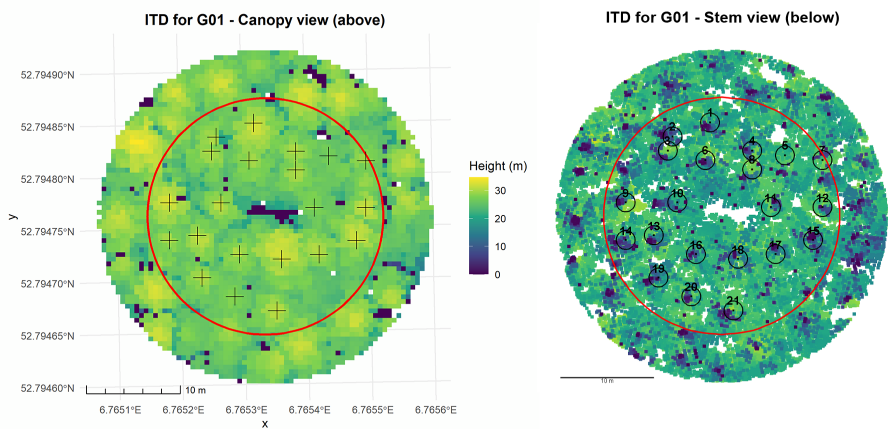


(c) Comparison between top and bottom view after ITD for sample plot H03 in forest reserve Sang (RSV 16)

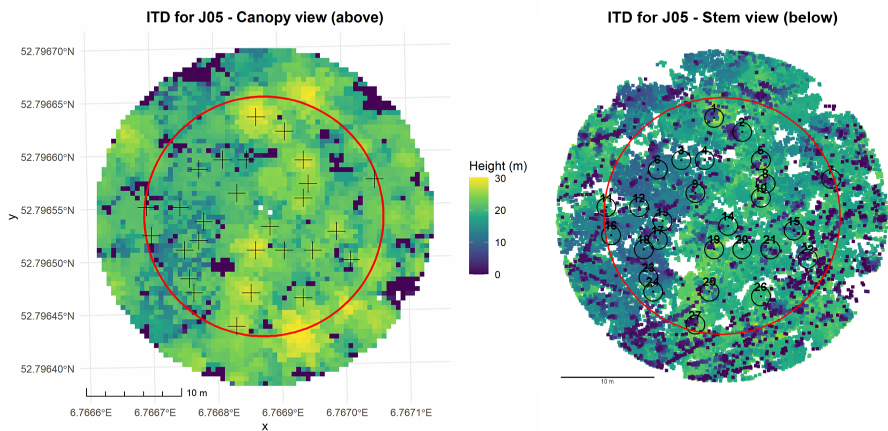
Figure 15: Comparison between canopy- and stem-down views after ITD for representative sample plots in reserves Sang (RSV 16)



(a) Comparison between top and bottom view after ITD for sample plot D02 in forest reserve *Oosteresch* (RSV 19)



(b) Comparison between top and bottom view after ITD for sample plot G01 in forest reserve *Oosteresch* (RSV 19)



(c) Comparison between top and bottom view after ITD for sample plot J05 in forest reserve *Oosteresch* (RSV 19)

Figure 16: Comparison between canopy- and stem-down views after ITD for representative sample plots in reserves *Oosteresch* (RSV 19)

Appendix IV

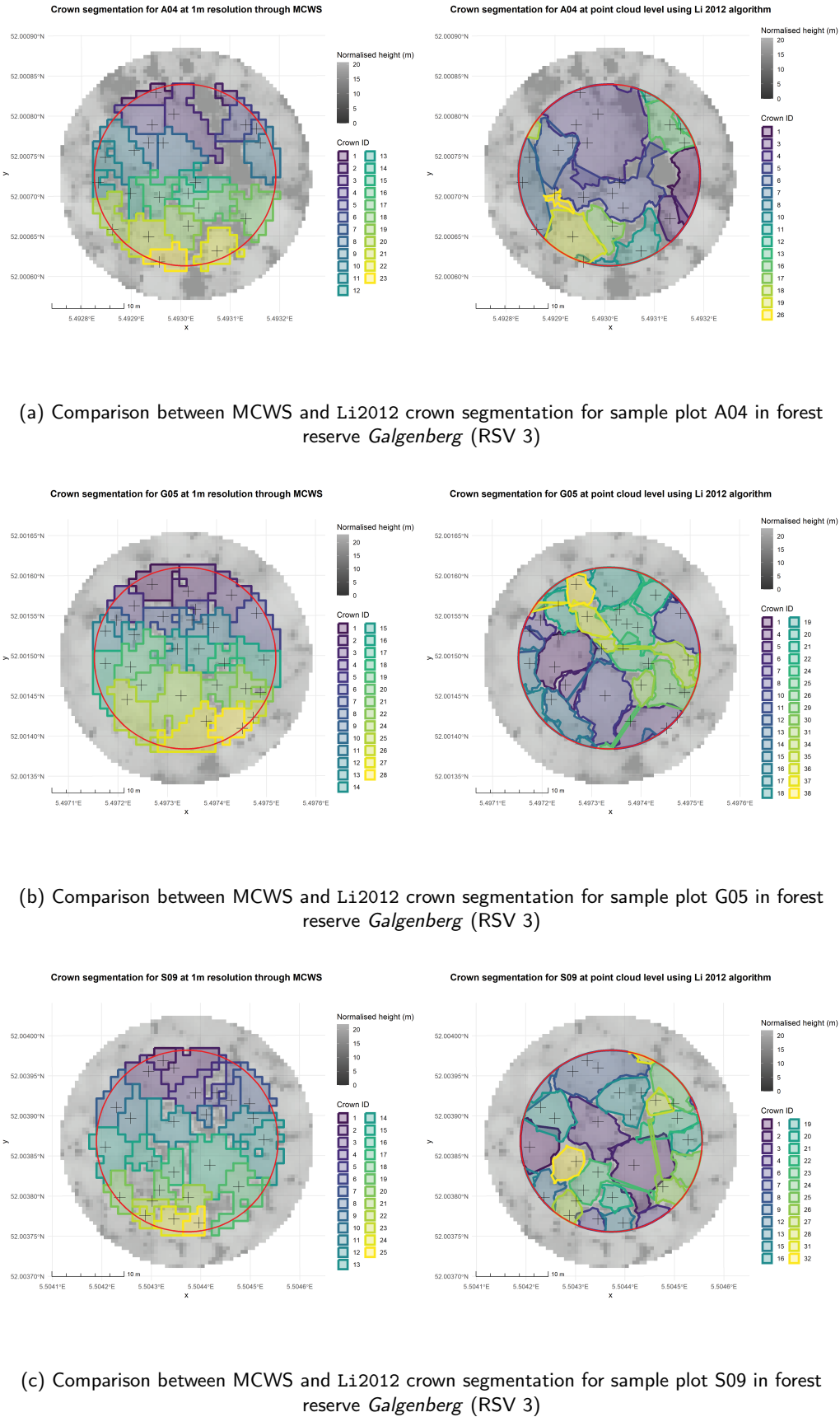
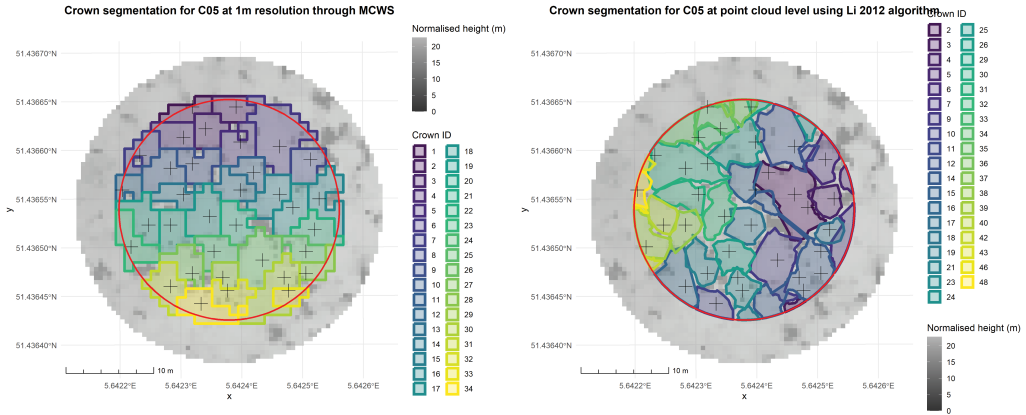
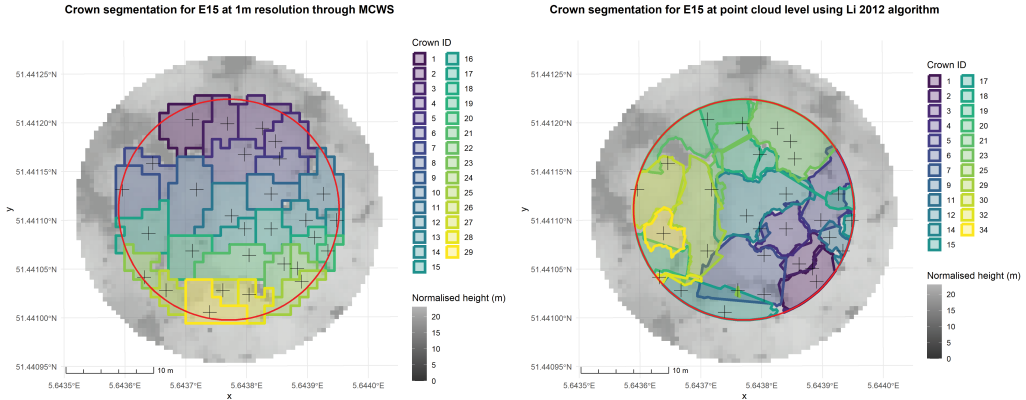


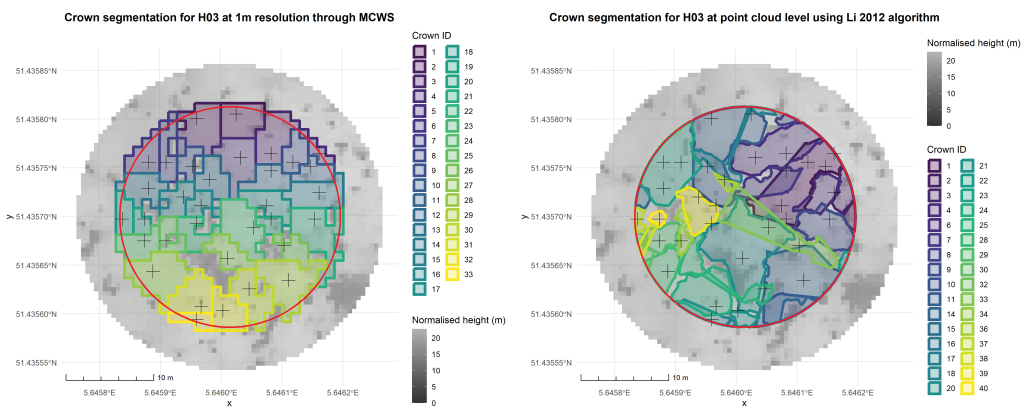
Figure 17: Comparison between MCWS and Li2012 crown segmentation for representative sample plots in reserves Galgenberg (RSV 3)



(a) Comparison between MCWS and Li2012 crown segmentation for sample plot C05 in forest reserve Sang (RSV 16)

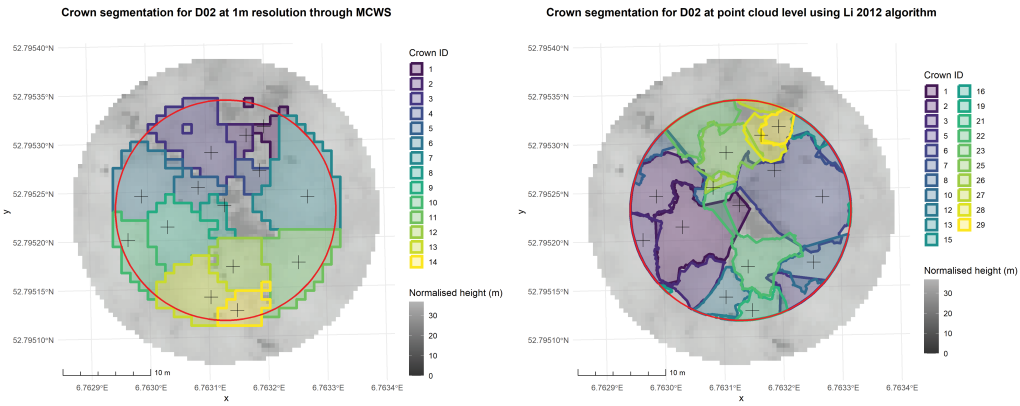


(b) Comparison between MCWS and Li2012 crown segmentation for sample plot E15 in forest reserve Sang (RSV 16)

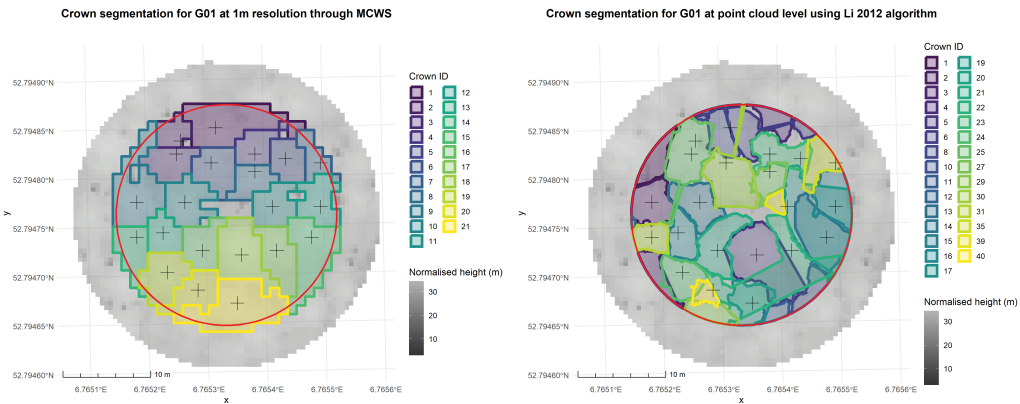


(c) Comparison between MCWS and Li2012 crown segmentation for sample plot H03 in forest reserve Sang (RSV 16)

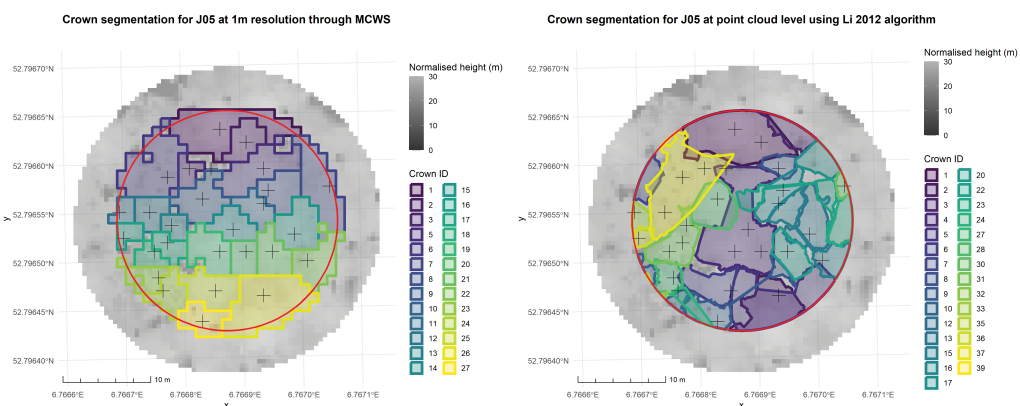
Figure 18: Comparison between MCWS and Li2012 crown segmentation for representative sample plots in reserves Sang (RSV 16)



(a) Comparison between MCWS and Li2012 crown segmentation for sample plot D02 in forest reserve *Oosteresch* (RSV 19)



(b) Comparison between MCWS and Li2012 crown segmentation for sample plot G01 in forest reserve *Oosteresch* (RSV 19)



(c) Comparison between MCWS and Li2012 crown segmentation for sample plot J05 in forest reserve *Oosteresch* (RSV 19)

Figure 19: Comparison between MCWS and Li2012 crown segmentation for representative sample plots in reserves *Oosteresch* (RSV 19)

Appendix V

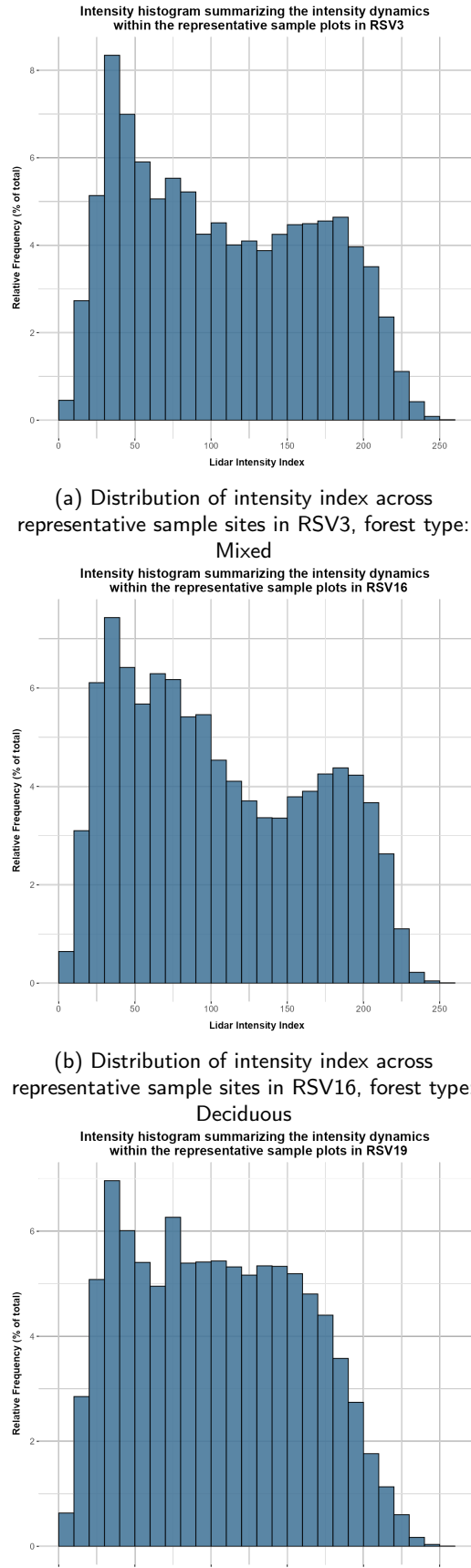


Figure 20: Distribution of intensity index across representative sample sites of different forest types